

## **General Disclaimer**

### **One or more of the Following Statements may affect this Document**

- This document has been reproduced from the best copy furnished by the organizational source. It is being released in the interest of making available as much information as possible.
- This document may contain data, which exceeds the sheet parameters. It was furnished in this condition by the organizational source and is the best copy available.
- This document may contain tone-on-tone or color graphs, charts and/or pictures, which have been reproduced in black and white.
- This document is paginated as submitted by the original source.
- Portions of this document are not fully legible due to the historical nature of some of the material. However, it is the best reproduction available from the original submission.

NASA CONTRACTOR  
REPORT

NASA CR-144348

(NASA-CR-144348) HIGH TORQUE DC MOTOR  
FABRICATION AND TEST PROGRAM Final Report  
(Bendix Corp.) 140 p HC \$6.00 CSCL 09A

N76-27476

G3/33 Unclass  
44612

HIGH TORQUE DC MOTOR FABRICATION AND TEST PROGRAM

By Paul Makus

The Gyroscopic Devices Laboratory  
Bendix Corporation  
Guidance Systems Division  
Teterboro, New Jersey 07608

Final Report

May 24, 1976

Prepared for

NASA - GEORGE C. MARSHALL SPACE FLIGHT CENTER  
Marshall Space Flight Center, Alabama 35812





1. REPORT NO. NASA CR-144348		2. GOVERNMENT ACCESSION NO.		3. RECIPIENT'S CATALOG NO.	
4. TITLE AND SUBTITLE  High Torque DC Motor Fabrication and Test Program				5. REPORT DATE 24 May 1976	
				6. PERFORMING ORGANIZATION CODE	
7. AUTHOR(S) Paul Makus				8. PERFORMING ORGANIZATION REPORT #	
9. PERFORMING ORGANIZATION NAME AND ADDRESS  The Gyroscopic Devices Laboratory Bendix Corporation Guidance Systems Division Teterboro, New Jersey 07608				10. WORK UNIT NO.	
				11. CONTRACT OR GRANT NO. NAS8-30970	
12. SPONSORING AGENCY NAME AND ADDRESS  National Aeronautics and Space Administration Washington, D. C. 20546				13. TYPE OF REPORT & PERIOD COVERED  CONTRACTOR Final Summary Report	
				14. SPONSORING AGENCY CODE	
15. SUPPLEMENTARY NOTES					
16. ABSTRACT  The testing of a standard iron and standard alnico permanent magnet two-phase, brushless DC spin motor for potential application to the Space Telescope (ST) has been concluded. The purpose of this study was to determine spin motor power losses, magnetic drag, efficiency and torque speed characteristics of a High Torque DC Motor. The motor was designed and built to fit an existing reaction wheel as a test vehicle and to use existing brass-board commutation and torque command electronics. The results of the tests are included in this report.					
17. KEY WORDS			18. DISTRIBUTION STATEMENT Unclass/Unlimited COR: <u>Paul T. Galle</u> <u>1. F. Brooks Moore</u> F. BROOKS MOORE Director, Electronics & Control Lab.		
19. SECURITY CLASSIF. (of this report) Uncl		20. SECURITY CLASSIF. (of this page) Uncl		21. NO. OF PAGES 104	22. PRICE NTIS

### PREFACE

This report is submitted in fulfillment of the requirements of Phase II of the Statement of Work for NASA Contract NAS-8-30970. The work performed herein is in accordance with the instructions of Supplemental Agreement Modification 4 dated 2 December 1975.

## TABLE OF CONTENTS

<u>SECTION</u>	<u>TITLE</u>	<u>PAGE</u>
1.0	INTRODUCTION	1-1
2.0	SUMMARY	2-1
3.0	CONCLUSIONS AND RECOMMENDATIONS	3-1
4.0	TEST RESULTS	4-1
4.1	TORQUE CHARACTERISTICS	4-3
4.2	POWER CHARACTERISTICS	4-10
4.3	EFFICIENCIES	4-13
4.4	TORQUE TRANSIENTS	4-19
4.5	CURRENT WAVEFORMS	4-20
5.0	BRUSHLESS DC MOTOR	5-1
5.1	DESCRIPTION AND HISTORY	5-1
5.2	DESIGN FEATURES	5-1
5.3	MOTOR TEST RESULTS	5-2
5.4	REACTION WHEEL TEST RESULTS	5-5
5.5	ANALYSIS	5-9
6.0	DRIVE ELECTRONICS ANALYSIS	6-1
7.0	TEST EQUIPMENT	7-1
8.0	TEST DATA	8-1
8.1	PERFORMANCE DATA	8-1
8.2	COMPUTER DATA ANALYSIS	8-2

## LIST OF ILLUSTRATIONS

<u>FIGURE</u>	<u>TITLE</u>	<u>PAGE</u>
1-1	BRUSHLESS DC MOTOR	1-2
1-2	50 FT-LB-SEC MWA AND WHEEL ASSEMBLY	1-4
1-3	BRUSHLESS DC MOTOR PWM DRIVE ELECTRONICS	1-5
1-4	PWM DRIVE ELECTRONICS H-BRIDGES	1-7
4-1	REACTION TORQUE VS SPEED AND TORQUE COMMAND	4-4
4-2	TORQUE SCALE FACTOR VS SPEED	4-6
4-3	COMPUTED BIAS TORQUE VS SPEED	4-8
4-4	DRAG TORQUE VS SPEED	4-9
4-5	MOTOR EFFICIENCY VS SPEED	4-15
4-6	SUBSYSTEM EFFICIENCY VS SPEED	4-16
4-7	ELECTRONICS EFFICIENCY VS SPEED	4-17
4-8	H BRIDGE EFFICIENCY VS SPEED	4-18
4-9 TO	MOTOR CURRENT WAVEFORMS	4-23 TO
4-17	MOTOR CURRENT WAVEFORMS	4-31
5-1	HIGH TORQUE BRUSHLESS DC MOTOR PARAMETERS	5-1
5-2 TO 5-3	HALL LOCATION TESTS	5-14 - 5-15
5-4	POWER FLOW DIAGRAMS AT 1250 RPM CW AND MAXIMUM TORQUE	5-16
5-5	BRUSHLESS DC MOTOR - NO ARMATURE REACTION	5-17
5-6	BRUSHLESS DC MOTOR - WITH ARMATURE REACTION	5-18
5-7	BRUSHLESS DC MOTOR - WITH ARMATURE REACTION AND HALL PLACEMENT ERROR	5-19
6-1	SPIN MOTOR DRIVE ELECTRONICS - BLOCK DIAGRAM	6-2
6-2	SPIN MOTOR DRIVE ELECTRONICS - SCALING DIAGRAM	6-4
6-3	FREQUENCY RESPONSE	6-6

# LIST OF ILLUSTRATIONS - (CONT.)

<u>FIGURE</u>	<u>TITLE</u>	<u>PAGE</u>
8-1	STABLE POWER	8-10
8-2	REACTION TORQUE VS SPEED	8-11
8-3	CW DRAG TORQUE	8-12
8-4	CCW DRAG TORQUE	8-13
8-5	CW LOW SPEED DRAG TORQUE	8-14
8-6	CCW LOW SPEED DRAG TORQUE	8-15
8-7	ZERO CROSSING TORQUE	8-16
8-8	CW AC MOTOR DRAG TORQUE	8-17
8-9	CCW AC MOTOR DRAG TORQUE	8-18
8-10	SUBSYSTEM POWER VS SPEED	8-19
8-11	COS MOTOR POWER VS SPEED	8-20
8-12	SIN MOTOR POWER VS SPEED	8-21
8-13	SUBSYSTEM POWER FOR 24 AND 32 VDC BUSS	8-22
8-14	COS MOTOR POWER FOR 24 AND 32 VDC BUSS	8-23
8-15	SIN MOTOR POWER FOR 24 AND 32 VDC BUSS	8-24
8-16 to 8-19	CW TORQUE TRANSIENTS FOR 0.5, 1.0, 2.5 AND 5.0 VOLT TORQUE COMMANDS	8-25 to 8-28
8-20 to 8-23	CCW TORQUE TRANSIENTS for 0.5, 1.0, 2.5 AND 5.0 VOLT TORQUE COMMANDS	8-29 to 8-32
8-24 to 8-27	ZERO SPEED TORQUE TRANSIENTS FOR 0.5, 1.0, 2.5 AND 5.0 VOLT TORQUE COMMANDS	8-33 to 8-38
8-28 to 8-35	CW DIGITAL TORQUE TRANSIENTS FOR 0.5, 1.0 2.5 AND 5.0 VOLT TORQUE COMMANDS	8-39 to 8-46
8-36 to 8-42	CCW DIGITAL TORQUE TRANSIENTS FOR 0.5, 1.0, 2.5 AND 5.0 VOLT TORQUE COMMANDS	8-47 to 8-52



# LIST OF ILLUSTRATIONS - (CONT.)

<u>TABLE NO.</u>	<u>TITLE</u>	<u>PAGE</u>
2-1	HIGH TORQUE DC MOTOR CHARACTERISTICS	2-2
4-1	CURRENT HARMONIC ANALYSIS	4-22
5-1	HIGH TORQUE BRUSHLESS DC MOTOR PARAMETERS	5-13
8-1	PERFORMANCE DATA	8-5
8-2	HIGH TORQUE DC MOTOR EFFICIENCY TABULATIONS	8-6
8-3	HIGH TORQUE DC MOTOR EFFICIENCY TABULATIONS	8-7
8-4	SCALE FACTOR	8-8
8-5	POWER DATA	8-9
8-6 to 8-16	HIGH TORQUE DC MOTOR COMPUTER DATA	8-53 to 8-63

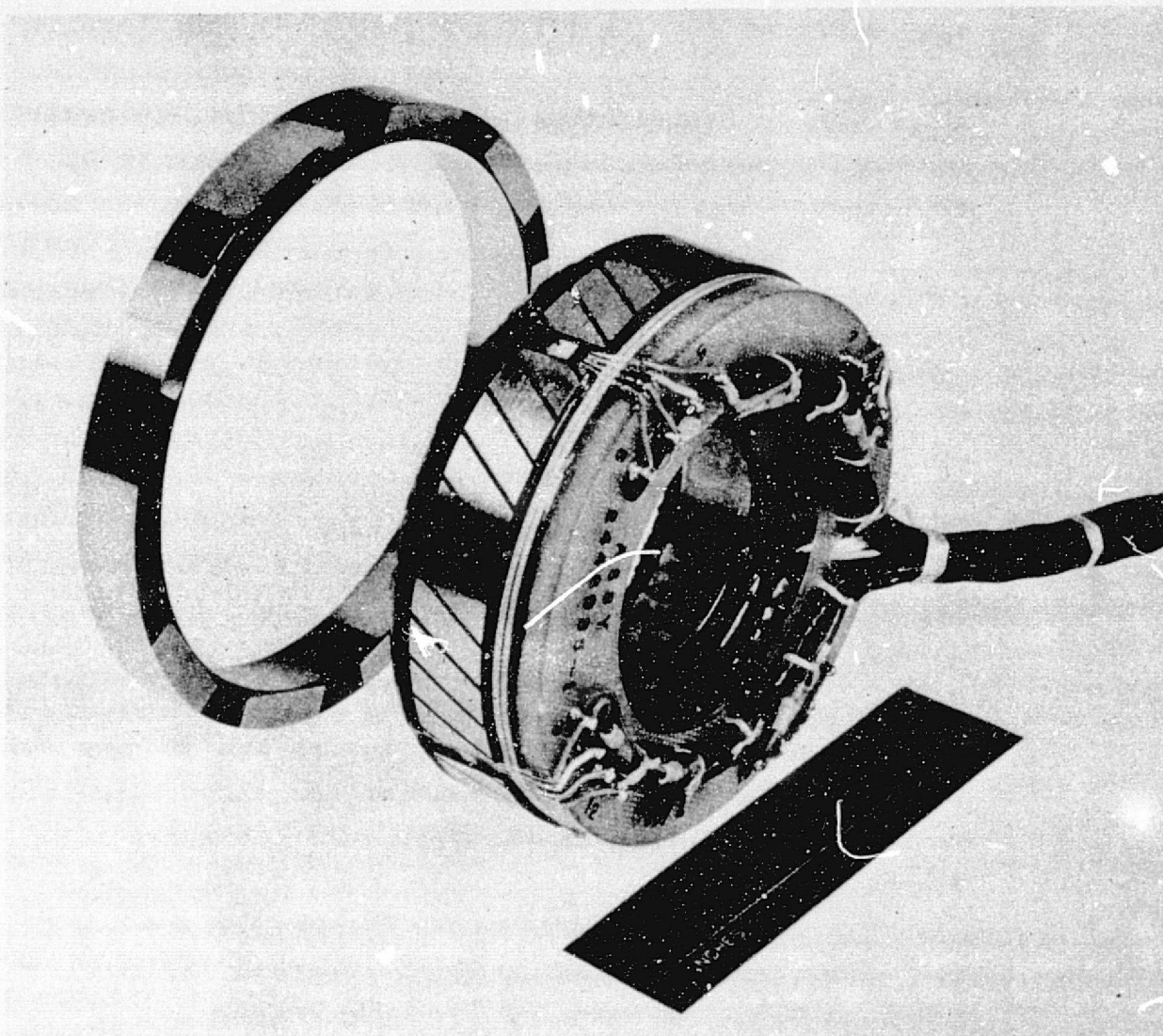
## 1.0

### INTRODUCTION

The Bendix Corporation, Guidance Systems Division (GSD) has concluded testing of a standard iron and standard alnico permanent magnet two phase, brushless DC spin motor for potential application to the Space Telescope (ST). The purpose of this study was to determine spin motor power losses, magnetic drag, efficiency and torque speed characteristics of a High Torque DC Motor. GSD designed and built this motor to fit an existing reaction wheel as a test vehicle and to use existing brass-board commutation and torque command electronics.

The spin motor was designed for a nominal torque output of 50 ounce inch (.35 NM) over a speed range of  $\pm 3000$  RPM. The motor rotor consists of 10 poles of alnico permanent magnets. The stator, located inside the rotor, consists of two phases of windings in quadrature. Hall elements are located on the outer periphery of the stator laminations so as to sense the rotor flux in the air gap and provide rotor position information for electronic commutation. A picture of the spin motor is shown in Figure 1-1.

The reaction wheel used as a test vehicle for the spin motor is a new 50 ft-lb-sec (68 N-M-sec) Momentum Wheel. This unit has been designed so that it can be used as a normal reaction wheel, a biased momentum wheel, or as the wheeled section of a low output torque, control moment gyro, either single or dual gimbal. The unit has an angular momentum potential between 50 and 150 ft-lb-sec.



BRUSHLESS DC MOTOR

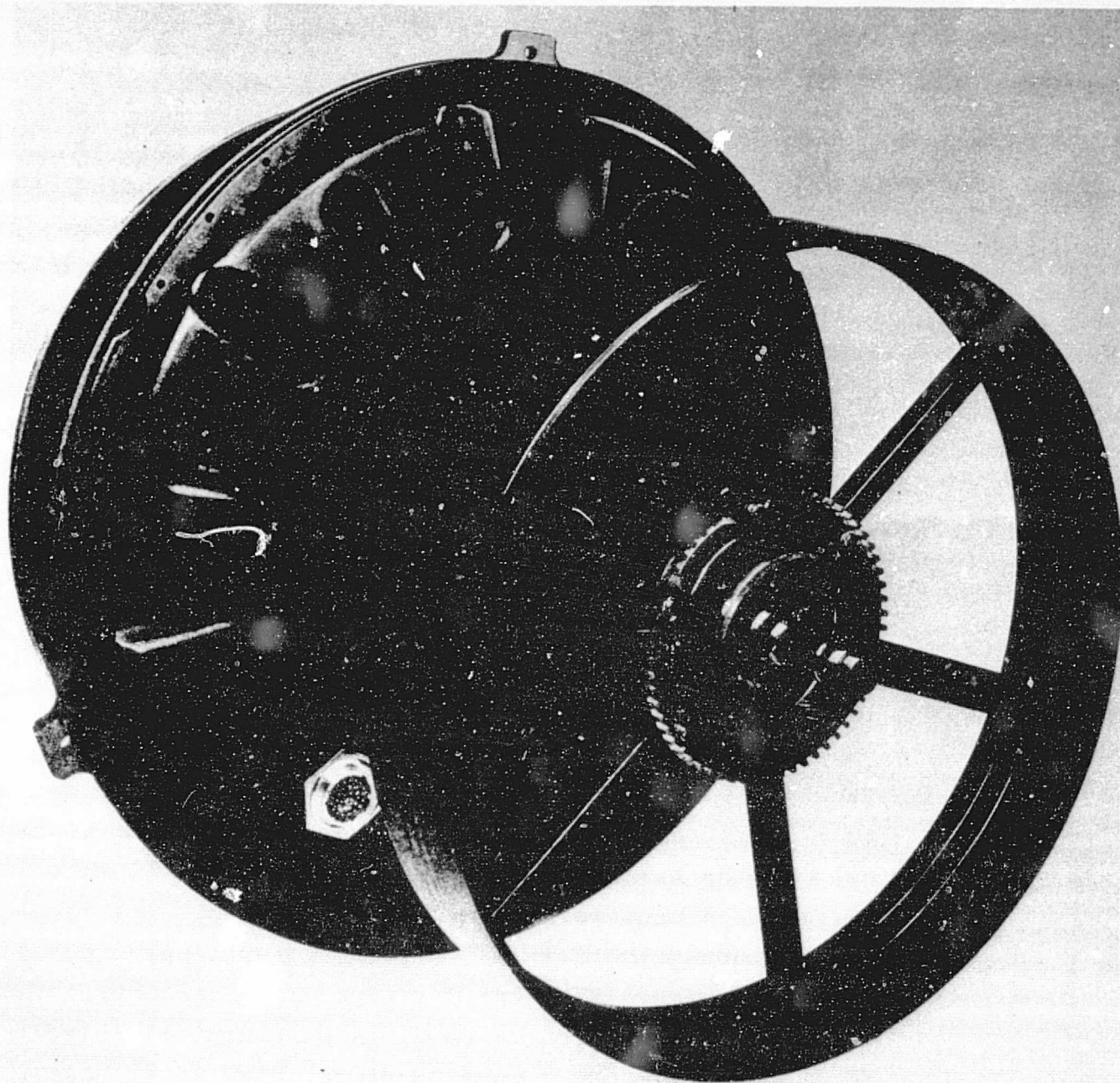
FIGURE 1-1

REPRODUCIBILITY OF THE  
ORIGINAL PAGE IS POOR

The reaction wheel consists of a spoked 16 inch (.406M) diameter wheel in a magnesium housing. A picture is shown in Figure 1-2. The assembly is about 16.5 inches (.42M) in diameter by 7.25 inches (.184M) high. It utilizes a three point mount and weighs 32 pounds (14.5KG). Single 104H angular contact ball bearings, with a 10 pound (.453KG) axial preload provided by a belleville spring are used in the reaction wheel configuration. The bearings used during test were lubricated with a fixed amount of SRG-40 mineral oil.

The reaction wheel has been previously tested with an AC induction motor installed to determine the units drag torque characteristics. The unit has been designed to operate in a low pressure or vacuum environment. All of the tests results presented were performed with the units internal pressure between 100 and 150 micros (0.1-0.15 Torr).

The spin motor drive electronics used for this study is a brassboard set similar to the one which was to be used on the Earth Limb Measurement Satellite (ELMS) program. A picture is shown in Figure 1-3. The electronics consists of an EMI filter, power supply, pulse width modulator (PWM) and H-bridge drive circuits. The input to the electronics consists of a nominal 28 volt DC buss and DC torque command signal of 0 to +5 volts. The output is a PWM current drive, modulated by the Hall commutators, to the spin motor windings. The current feedback stability circuitry was modified for higher speed operation (3000 RPM vs 880 RPM for ELMS).

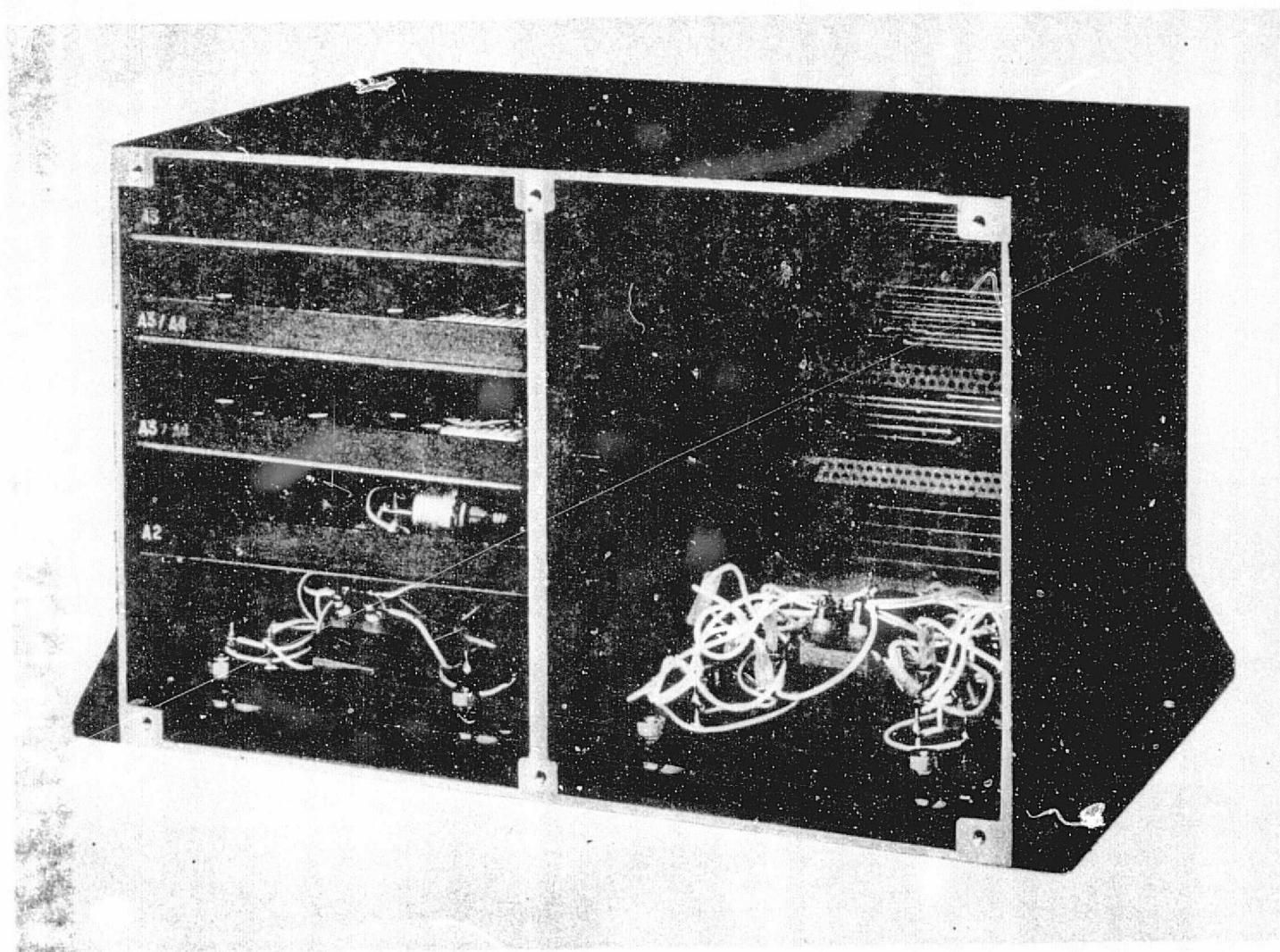


50 FT-LB-SEC MWA AND WHEEL ASSEMBLY

FIGURE 1-2

REPRODUCIBILITY OF THE  
ORIGINAL PAGE IS POOR

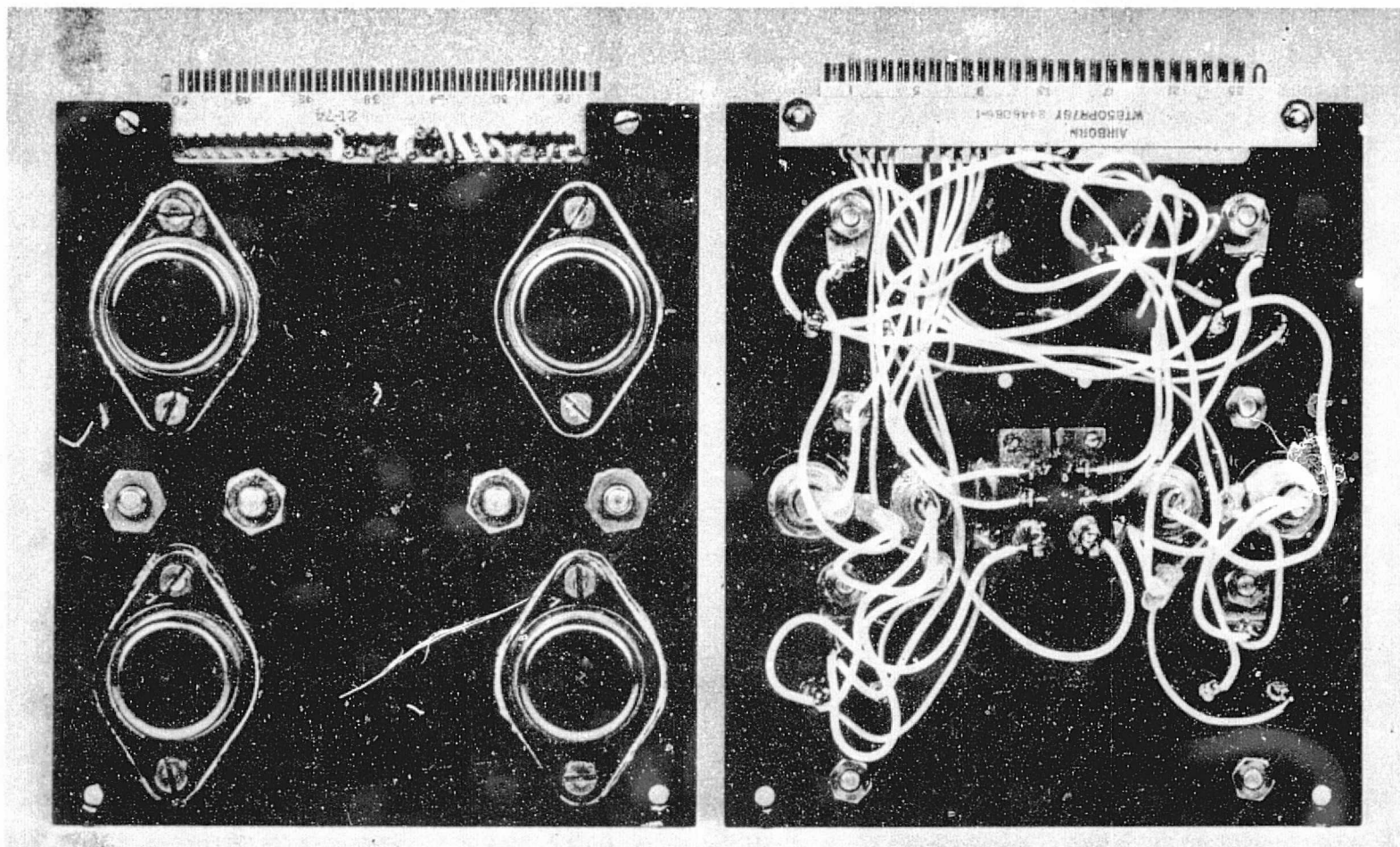




BRUSHLESS DC MOTOR PWM DRIVE ELECTRONICS

FIGURE 1-3

The power H-bridges, see Figure 1-4, were rebuilt to accommodate the approximately three times higher power levels required.



PWM DRIVE ELECTRONICS H-BRIDGES

FIGURE 1-4

REPRODUCIBILITY OF THE  
ORIGINAL PAGE IS POOR

## 2.0

### SUMMARY

A two phase, brushless high torque DC motor was designed and built to fit within the physical constraints of an existing 50 ft-lb-sec reaction wheel. The motor was sized to fit existing hardware and was therefore limited to a maximum torque of 50 ounce inches. The motor was also designed to operate with existing PWM drive electronics without modification. Unfortunately, during the course of integration of the motor and electronics, it was discovered that the existing H-bridge power transistors could not adequately handle the higher motor current and so new H-bridges had to be built.

The electronics were also modified with a double feedback circuit to extend the amplifier bandwidth from its former 73 Hertz bandwidth to a 250 Hertz bandwidth. The subsystem, consisting of motor, reaction wheel and drive electronics was then tested for its performance characteristics. Although the motor performed according to its design, an unexpected amount of sensitivity to armature fields was experienced. This "armature reaction" did tend to cause dissymetry in the data but did not seriously affect the test effort. The wheel speed was limited to a maximum of 2500 RPM rather than the desired 3000 RPM because the motor back EMF constant was erroneously calculated for square wave excitation rather than the actual sinusoidal current.

The results of this effort have been summarized in Tables 2-1 and 2-2. The functional test results, are shown and discussed in Section 4. The motor itself is discussed in Section 5. Section 6 contains a discussion of the frequency response of the drive electronics.

# HIGH TORQUE DC MOTOR CHARACTERISTICS

Motor Type	Rotor outside stator, brushless DC
Commutation	Hall elements on stator
No. Poles	12
No. Phases	2
Size	3.99" OD x 1.63" ID x 1.25" Length
Weight	21 ounces (.595Kg)
Magnet Mat'l	Alnico 9
Maximum Torque	54 oz-in
Torque Scale Factor (Max)	10.25 oz-in/pKamp (.072NM/pkamp)
	(Apparent) 9.6 oz-in/pKamp (.068NM/pKamp)
Maximum Speed (at 32V)	3000 RPM
Peak power at 2500 RPM and max torque	103 watts
Motor constant (Max)	16 oz-in/ $\sqrt{\text{watt}}$
Back EMF Constant	0.00758 volts pk/RPM
Motor Time Constant	2 milliseconds
DC Resistance (each phase)	0.41 ohms
Total AC Impedance (each phase)	0.65 ohms
Inductance (each phase)	0.8 millihenries
Drag Torque near zero speed	
(Bearing and windage)	0.6 oz-in
(Magnetic)	0.15 oz-in
Drag Torque at 3000 RPM	
(Bearing and windage)	1.5 oz-in
(Magnetic)	0.9 oz-in
Efficiency at 2500 RPM	
(Max Torque)	76%
(20% Torque)	87%

TABLE 2-1



### SUBSYSTEM CHARACTERISTICS

Input Power	28 $\pm$ 4 VDC
Torque Command Signal	0 to $\pm$ 5 VDC
Torque Command Scale Factor	10.8 oz-in/volt
	0.076 NM/volt
	9.6 oz-in/pk amp
Peak Power at 2500 RPM and max torque	187 watts
Quiescent power at zero speed at constant 3000 RPM	8.5 watts
	13.5 watts
Efficiency at 2500 RPM (Max)	59%
(Min)	52%
PWM Frequency	4.8 KHz
Type	Brassboard

### 3.0

#### CONCLUSIONS AND RECOMMENDATIONS

The High Torque DC Motor tested for this report showed a definite advantage over an AC motor for meeting ST satellite requirements. The DC motor inherently has much higher torque and is much more efficient for use in a reaction wheel. The DC motor also tends to be much more efficient at low torque levels than high torque levels indicating even higher efficiency when operated at low duty cycles. The biggest disadvantage of this motor is the drag torque of the rotor magnets on the stator iron. The magnetic drag amounts to 50% of the bearing and windage drag at maximum speed and 20% near zero speed.

The magnetic drag of the brushless DC motor can be eliminated by using an ironless stator. This type of motor construction would also run more efficient since the stator core losses would be reduced. The stator core losses of the standard motor are significant at high torque levels since they are proportional to the square of motor current. The ironless stator brushless DC motor would be the next logical step of investigation if it is desired to have increased performance over the standard brushless DC motor.

There were several areas of the motor design which requires improvement. The first is the stator iron. The stator core losses, although negligible at low torque levels, proved to be significant at high torque levels. These may be reduced by increasing the amount of iron in the stator. The Hall sensors were located

on the stator laminations. Although this location is satisfactory at low torque levels, the amount of stator flux pickup became significant at high torque levels leading to current waveform distortion.

For future designs, the Hall sensors should be moved out of the stator field. An obvious solution is an external (to the motor) position resolver. This would require additional cost however and a better method would be to place the Hall sensors at the sides of the rotor magnets. This would require that axial wheel motion be limited so as not to affect the scale factor. Perhaps the best method would be to extend the rotor magnets axially so as to overlap the stator winding end turns and place the Hall sensors in this location. No matter which method is chosen it is desirable to have the position sensors mounted so as to allow peaking and balancing of the motor torque under dynamic test conditions.

The armature reaction effect will be small for an iron-less stator motor due to the large air gap. Therefore, this type of motor would be able to operate satisfactorily with Hall elements located on the stator.

#### 4.0

#### TEST RESULTS

The High Torque DC Motor was tested as part of a subsystem which included a Pulse Width Modulated (PWM) Drive Electronics and a 50 foot-pound-second Reaction Wheel Assembly (RWA). The primary parameters of interest were reaction torque and power. The motor's reaction torque was measured by suspending the RWA from a strain gage torque cell with the spin axis vertical. The natural resonance of the suspended spring mass system was 4.14 Hertz. This necessitated filtering of the torque indicators output with a 0.1 Hertz low pass filter. Since the RWA takes six minutes to change direction of maximum speed at maximum torque, this filtering was not considered detrimental.

Power measurements were made with a wattmeter which obtains a wattage reading by electronically multiplying the current signal by the voltage signal. Subsystem power measurements are easily measured since they are basically DC levels. The motor power measurements, however, posed a problem in that the voltage across the motor is pulse width modulated at a frequency of 4.8 kilohertz. Although the rated frequency response of the wattmeter is 2 kilohertz, it is believed that the wattmeter was responding with reasonable accuracy for these tests.

The RWA Drive Electronics was controlled by a speed controller modified to use the RWAs spare set of Hall resolvers as a tachometer. The speed controller put out a torque command voltage adjustable

from 0 to +5 volts. The 5 volt torque command corresponds to maximum motor torque.

The RWA could not be operated above 2600 RPM at full torque and 28 volts DC buss voltage because of the motor back emf being higher than planned (see motor discussion). Although the motor could be run at 3000 RPM with either an increased DC buss voltage or lower torque command, it was decided not to run the motor past 2600 RPM for these tests.

The peak motor current was limited to 6 amperes thus limiting the maximum torque level to 50 ounce inches. Although the motor and drive electronics were capable of being operated at a higher current (torque) level, the "armature reaction effect" on the Hall position resolvers was too great at higher levels for satisfactory operation (see motor discussion).

The reaction wheel was operated in vacuum with a wheel cavity pressure of 100 to 150 microns maintained throughout all tests to keep windage losses constant.

In addition, a repeatable bearing preload from unit build to unit build was accomplished using Belleville washers (springs) which were captured in special adjusting nuts, threaded into the Beryllium bearing support housings. These preload nut assemblies (two per unit), are adjusted so that the spring is approximately .005 inches from flat bottom. Once this deflection is achieved, a



thrust load of approximately 9.0 pounds, based on the spring's spring rate, is applied to each bearing outer race in the spin axis horizontal position.

Since each preload washer still has .005 inch before the flat bottom position is reached, the flywheel has a total axial end share of .010 inch. Therefore, a repeatable preload of approximately 9 pounds is achieved by always adjusting the preload nut assemblies to yield an axial end shape of .010 inches.

#### 4.1 TORQUE CHARACTERISTICS

The reaction torque characteristics of the subsystem are shown in Figure 4-1. The subsystem was operated at nominal buss voltage (28 VDC) and with five different torque command levels through four quadrants (modes of operation) arbitrarily designated.

- I - Counterclockwise Acceleration
- II - Clockwise Deceleration
- III - Clockwise Acceleration
- IV - Counterclockwise Deceleration

Quadrants I and II correspond to positive reaction torque output whereas quadrants III and IV correspond to negative reaction torque output.

The reaction torque values for the five torque commands in each quadrant were read from the curves every 250 RPM. A least squares straight line was then fitted to each set of data at each speed to determine the torque command scale factor. The coefficient of correlation was deter-

REACTOR TORQUE IN SPEED  
AND LOADABLE COMMANDS  
HIGH TORQUE DC MOTOR

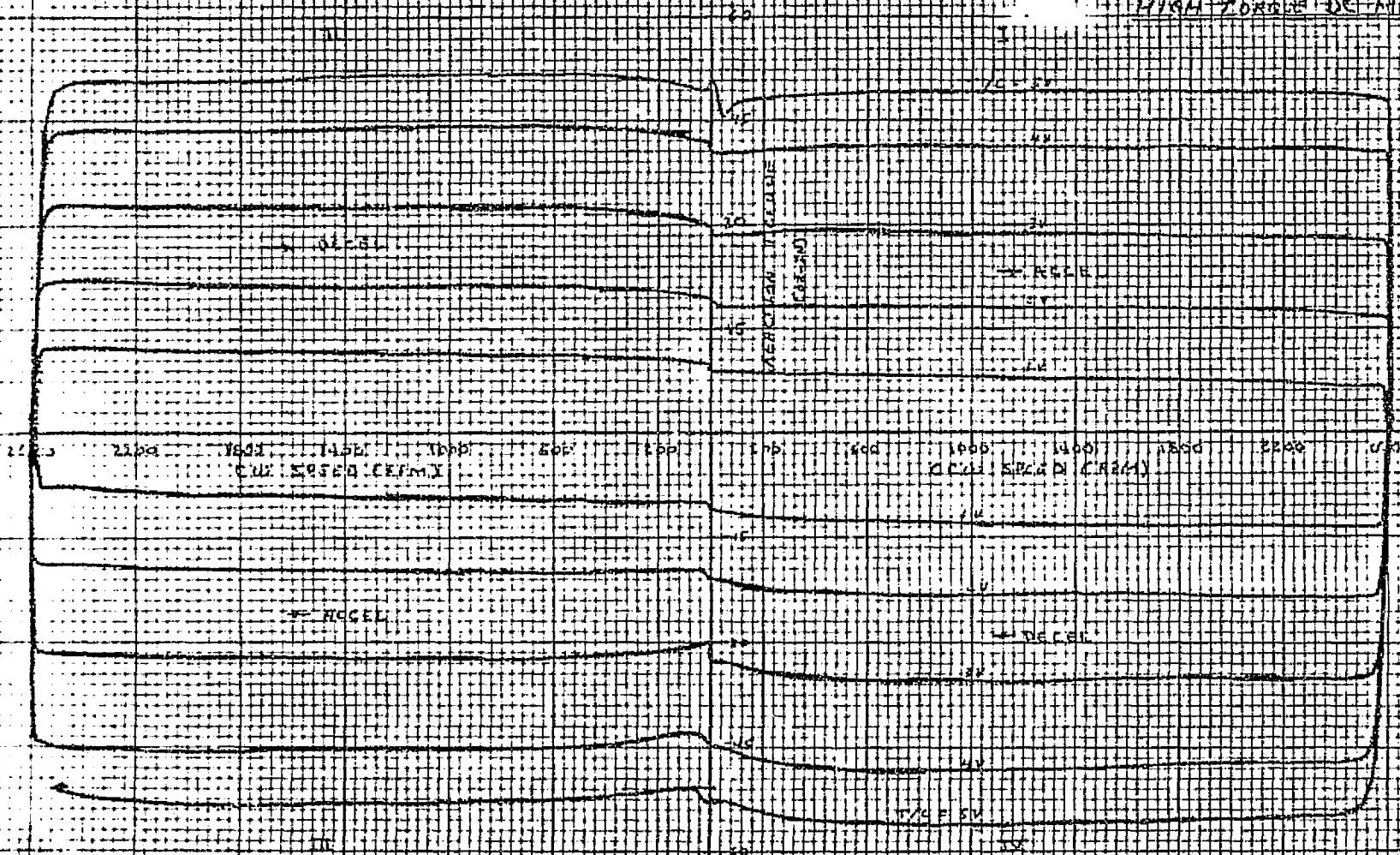


FIGURE 4-1

4-4

REPRODUCIBILITY OF THE  
ORIGINAL PAGE IS POOR

mined for each regression line with the lowest correlation being 0.995. The results of these computations are shown graphically in Figure 4-2 and are tabulated in Section 8.0. Immediately apparent is the different scale factors between positive and negative torque commands of about 7%. This is due primarily to the armature reaction effect of the Hall resolvers. Also apparent in the graph is the primarily positive slope during speed acceleration and the primarily negative slope during deceleration. This effect is due to the change of the motor from acting as a motor during acceleration to a generator during deceleration. The total torque scale factor for all conditions is 10.7 ounce inch per volt  $\pm 13\%$  ( $3\sigma$ ). The scale factors for positive and negative torques, respectively, are

(+) 10.34 ounce inch/volt  $\pm 8\%$  ( $3\sigma$ )

(-) 11.08 ounce inch/volt  $\pm 8\%$  ( $3\sigma$ )

The above scale factors were determined from the reaction torque curves of Figure 4-1.. The torque scale factors were also computed from the motor power curves (see Section 4.2) and are listed here to show concurrence of data.

(+) 10.71 ounce inch/volt

(-) 11.47 ounce inch/volt

It can be seen that there is less than 4% discrepancy between the two methods.

# HIGH TORQUE DC MOTOR TORQUE SCALE FACTOR VS SPEED

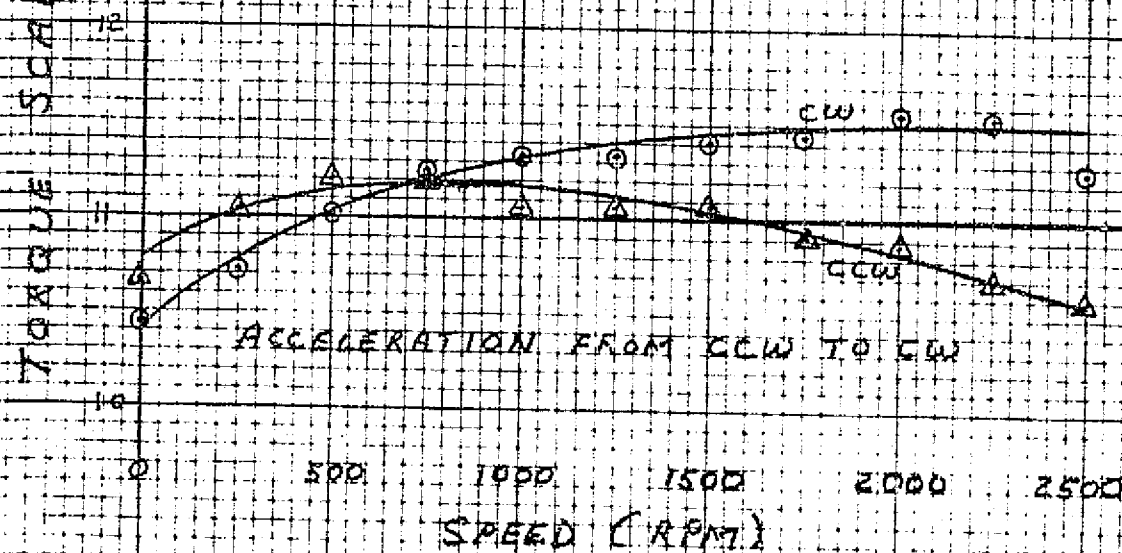
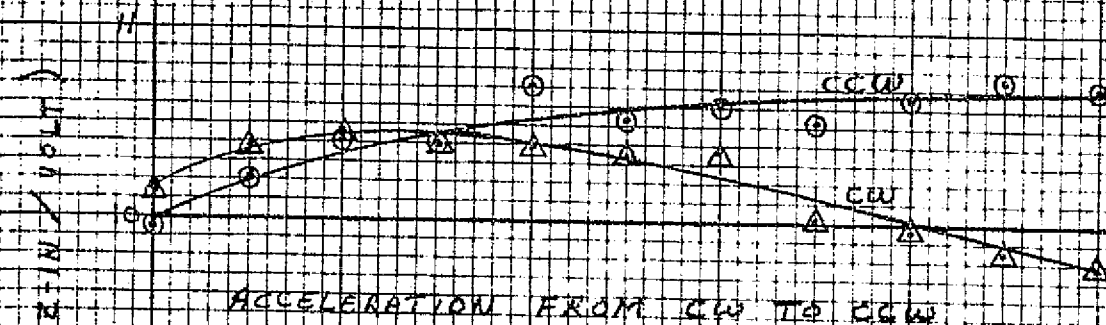


FIGURE 4-2

The drag torque of the RWA with the AC motor installed was measured and approximated by a straight line of

$$T_{AC} = 0.34 \times S + 0.45 \text{ ounce inch}$$

where  $T_{AC}$  = drag torque with AC motor  
S = motor speed in KRPM

Using the same method (measuring rundown reaction torque with motor windings open) and with the same bearing preload and wheel cavity pressure, the drag torque for the High Torque DC Motor was determined to be

$$T_{DC} = 0.60 \times S + 0.60$$

Thus, the DC motor, assuming no error in setting bearing preload, has about 0.15 ounce inch additional zero crossing torque. The magnetic drag of the rotor magnets on the stator iron amounts to 0.26 ounce inch per 1000 RPM or an additional 0.78 ounce inch of torque at 3000 RPM.

The torque scale factor was computed by fitting a least squares straight line to five points of torque command voltage vs reaction torque at given speeds. The slope of this line is the torque scale factor and the intercept or bias should be the drag torque given a linear system. These biases were plotted and are shown in Figure 4-3. These torque curves represent what may be called "dynamic" drag torques and when averaged together yield a dynamic drag torque of

$$T_{DYN} = 0.99 \times S + 0.74$$

# HIGH TORQUE DC MOTOR COMPUTED BIAS TORQUE VS SPEED

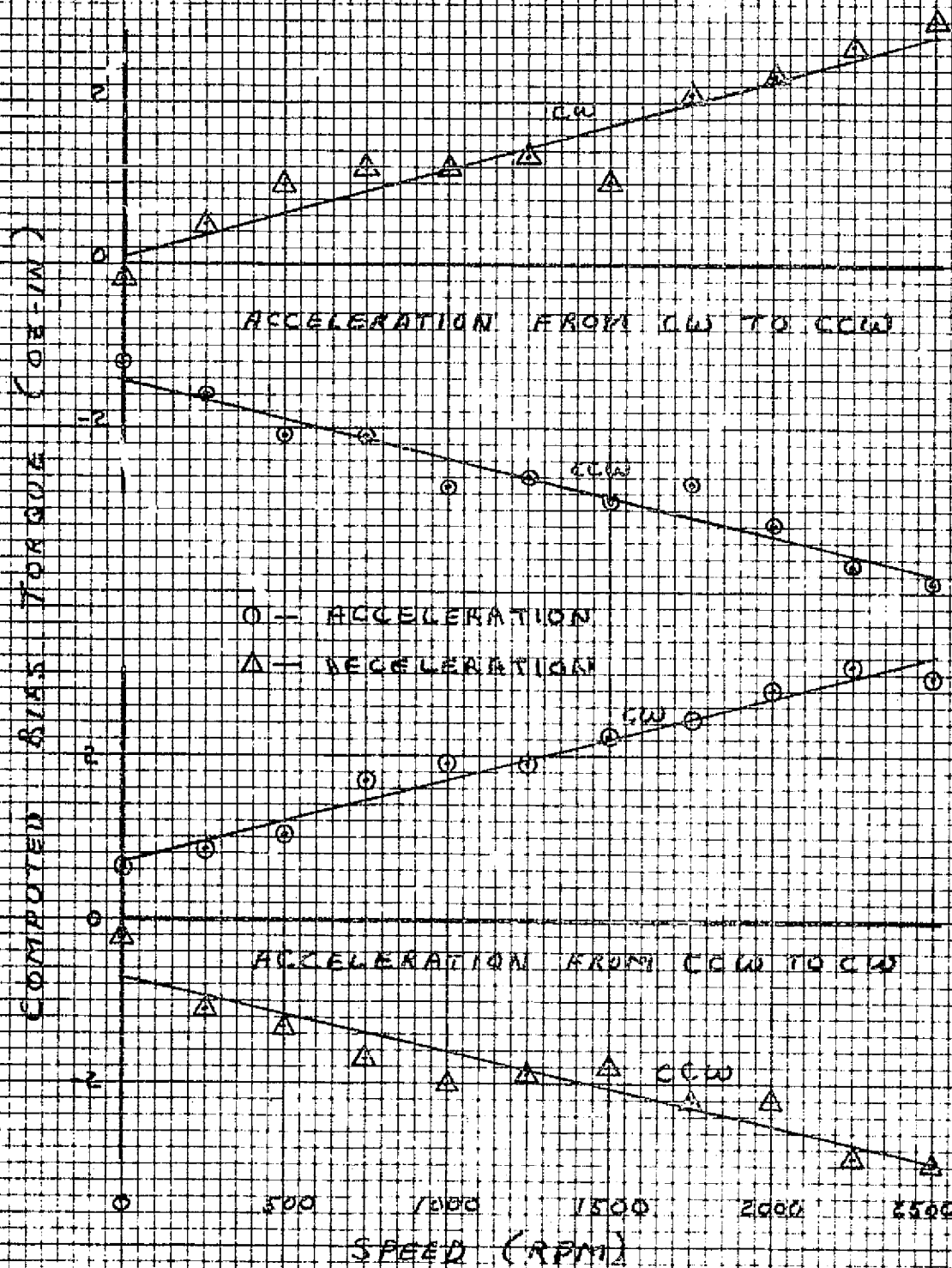


FIGURE 4-3

# HIGH TORQUE DC MOTOR DRAG TORQUE VS SPEED

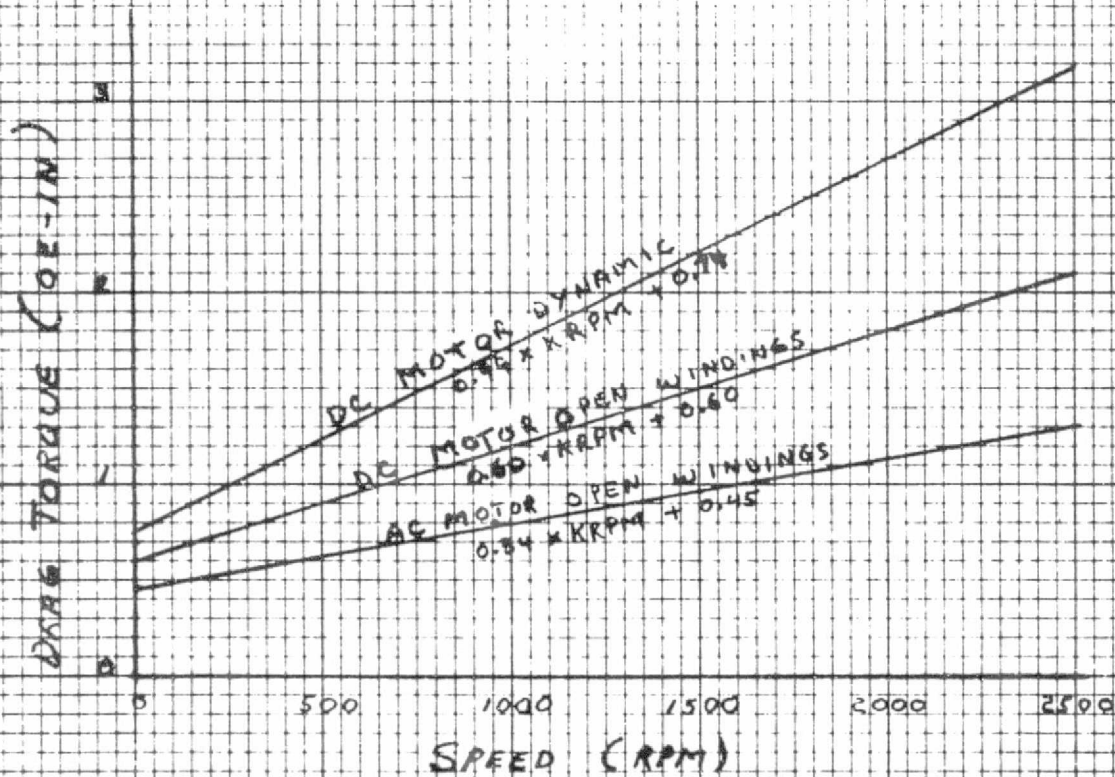


FIGURE 4-4

This dynamic drag torque may represent additional drag due to hysteresis and eddy current losses, electronics losses or simply non-linearity in computation. There is still speculation at this time about the nature of this curve. Data presented in the next section supports the open motor drag torque curve and therefore is the one purported to be the true motor drag torque. All three curves are presented graphically in Figure 4-4.

#### 4.2 POWER CHARACTERISTICS

The sine and cosine motor phase powers were plotted against speed in the same manner as the reaction torque of section 4.1. The data was also summarized in a similar fashion for computer analysis. (See section 8 for curves and tabulations.) Least squares straight lines were fitted to the total motor power vs speed curve at each torque command level and for positive and negative reaction torques. The slopes of these lines were assumed to be directly proportional to the torque scale factor and another least squares straight line was fitted to the slope vs torque command data. The line was forced through the origin and the resultant slope represented the torque scale factor. Following are the scale factors for positive and negative torques, respectively:

(+) 10.71 ounce inch/volt

(-) 11.47 ounce inch/volt

Since the torque command voltage is proportional to motor current (this is not entirely true because the



armature reaction effect on the Hall position sensors causes not only distortion of the current waveform proportional to current, but also some positive feedback effects), the intercepts of power vs speed curves are proportional to the  $I^2R$  losses of the motor and wiring. Thus by setting the intercepts proportional to the torque command voltage squared and fitting a straight line through these points and the origin, the  $I^2R$  constant can be computed. The RMS current as shown in the pictures of section 4.5 is approximately 0.8 amps RMS per volt of torque command. Using the average  $I^2R$  constant of 1.2 watts/volt<sup>2</sup> and 0.8 amps/volt, the effective resistance of the motor is computed to be 1.88 ohms or 0.94 ohms per phase. The measured DC resistance was 0.62 ohms. The measured DC resistance was 0.41 ohms plus 0.2 ohms wiring and an additional 0.24 ohms of AC losses at 100 Hz.

The steady state power of the subsystem was measured at zero speed and  $\pm 3000$  RPM. The speed control circuit was used to keep the speed constant while the measurements were made. The buss supply voltage was then varied  $\pm 4$  volts DC.

<u>Speed</u>	<u>Subsystem Power</u>		
	<u>24V</u>	<u>28V</u>	<u>32V</u>
0	6.0	8.5	10.8
CW 3000	11.6	13.7	15.4
CCW 3000	11.4	13.2	15.1
0	5.8	7.4	9.4 (motor open)

<u>Spin Motor Power</u>			
<u>Speed</u>	<u>24V</u>	<u>28V</u>	<u>32V</u>
0	0.3	0.6	0.9
CW 3000	6.5	6.5	6.8
CCW 3000	5.3	5.4	5.5

For the subsystem power at zero speed, the quiescent power is clearly proportional to the voltage squared thus representing  $I^2R$  losses in the electronics. The difference between zero speed and maximum speed subsystem powers should represent the spin motor power required at maximum speed. The measured spin motor powers, however, are higher by an amount partially accounted for by the  $I^2R$  losses of the 4.8 KHz PWM ripple current in the motor circuit. This is evident by comparing the subsystem power at zero speed with the motor in and out of the circuit.

The stable spin motor power is also representative of drag torque at constant speed. Using the spin motor powers at  $\pm 3000$  RPM and the motor torque constant developed earlier, the drag torque at 3000 RPM is computed to be 2.2 ounce inch which agrees closely with the measured drag torque.

The effect of the supply voltage buss change from 24 volts to 32 volts was generally less than 10% throughout the speed range. Interestingly, the subsystem required less power at 32V during motor acceleration. The effect on the motor power was negligible and small differences observed were attributed to the electronics operation.

### 4.3

#### EFFICIENCIES

The reaction torque vs speed, drag torque, motor power and subsystem power curves mentioned in the previous sections were also used to compute various efficiencies. The motor efficiency was computed from the ratio of Required Power over Measured Power. The required motor power is computed from

$$P_R = \frac{T_M S}{1352}$$

where  $T_M$  = Motor Torque = Reaction Torque + Drag Torque  
S = Speed IN RPM

The motor efficiency is

$$E_M = 100 \frac{P_R}{P_M} \%$$

The efficiencies were computed for each Torque Command Voltage from 1 to 5 volts every 250 RPM. The range of efficiencies was then plotted vs speed as shown in Figure 4-5. The motor efficiency is obviously zero at zero speed and is a function of speed. It is also a function of torque with the highest efficiency occurring at the lowest torque level. Thus, it can be seen that the motor is approaching 90% efficiency at maximum speed and low torque levels and 75% efficiency at maximum torque.

The subsystem efficiency was computed from

$$E_S = 100 \frac{P_R}{P_T} \%$$

where  $P_T$  = Total Subsystem Power

As above, the subsystem efficiency was plotted vs speed and is shown in Figure 4-6. The efficiency is again zero at zero speed and is about 55% at 2500 RPM. The tendency is for maximum efficiency at about 1/2 torque. The range of efficiencies with torque command is lower than the motor being generally less than  $\pm 4\%$ .

The electronics efficiency was computed from

$$E_E = 100 \frac{P_M}{P_T} \%$$

and is shown in Figure 4-7. The efficiency tends to dip down to about 36% at zero speed and rises to about 65%  $\pm 5\%$  at 2500 RPM. It should be noted, however, that the electronics are breadboard and were not designed to permit highest efficiency.

The quiescent power ( $P_Q$ ) of the subsystem at zero speed was measured as 8.5 watts and this power was used to compute the effective efficiency of the H-Bridge or

$$E_H = 100 \frac{P_M}{(P_T - P_Q)} \%$$

The results are shown in Figure 4-8. The H-Bridge efficiency appears to be generally about 70% over most of the range and rising to 75%  $\pm 5\%$  at 2500 RPM. As with the motor, the H-Bridge efficiency tends to be higher at low torque levels and lower at high torque levels.

# HIGH TORQUE DC MOTOR

## MOTOR EFFICIENCY

VS SPEED

FOR 20 TO 100 % TORQUE RANGE

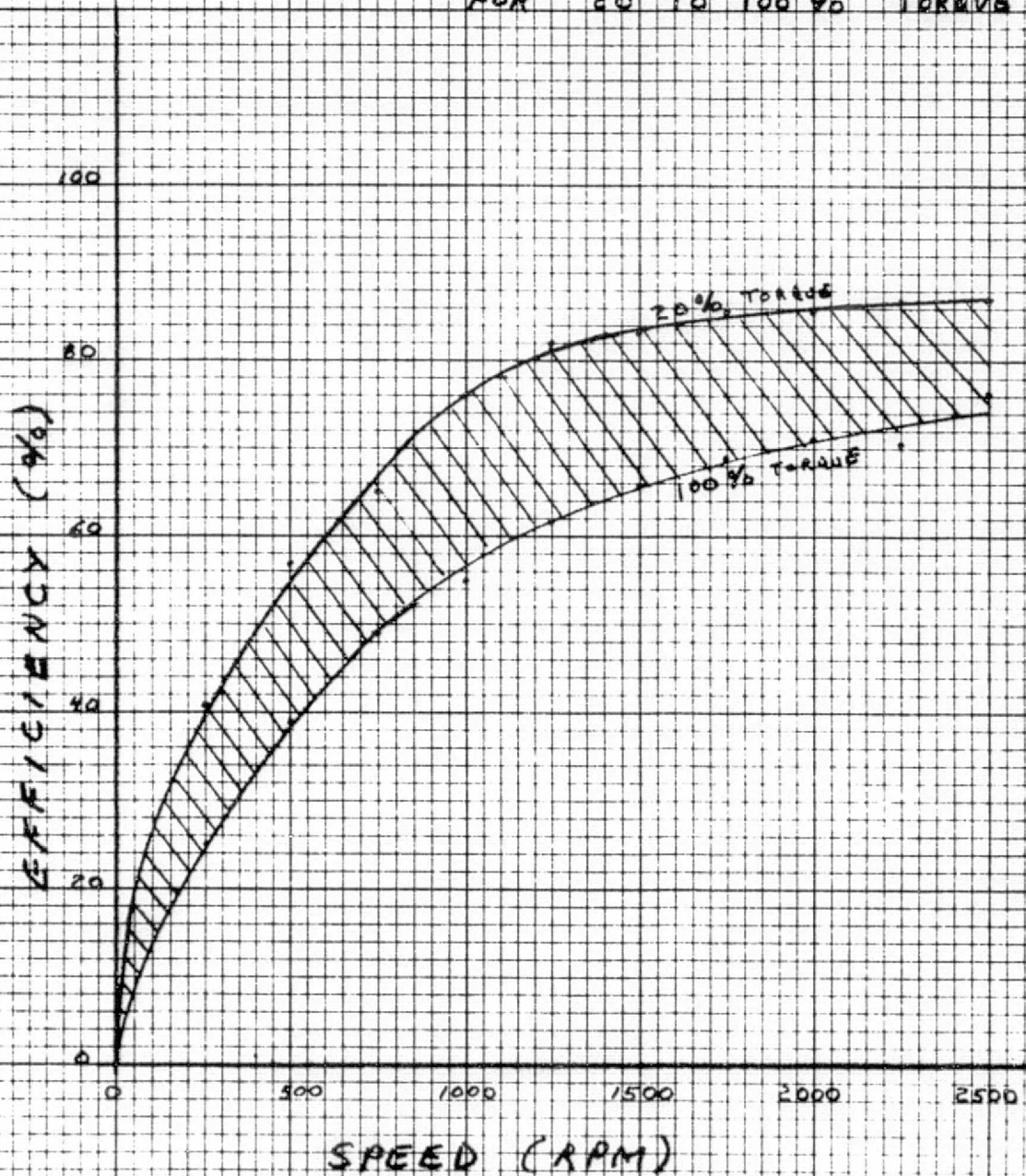


FIGURE 4-5



HIGH TORQUE DC MOTOR  
SUBSYSTEM EFFICIENCY  
VS SPEED

FOR 20 TO 100 % TORQUE RANGE

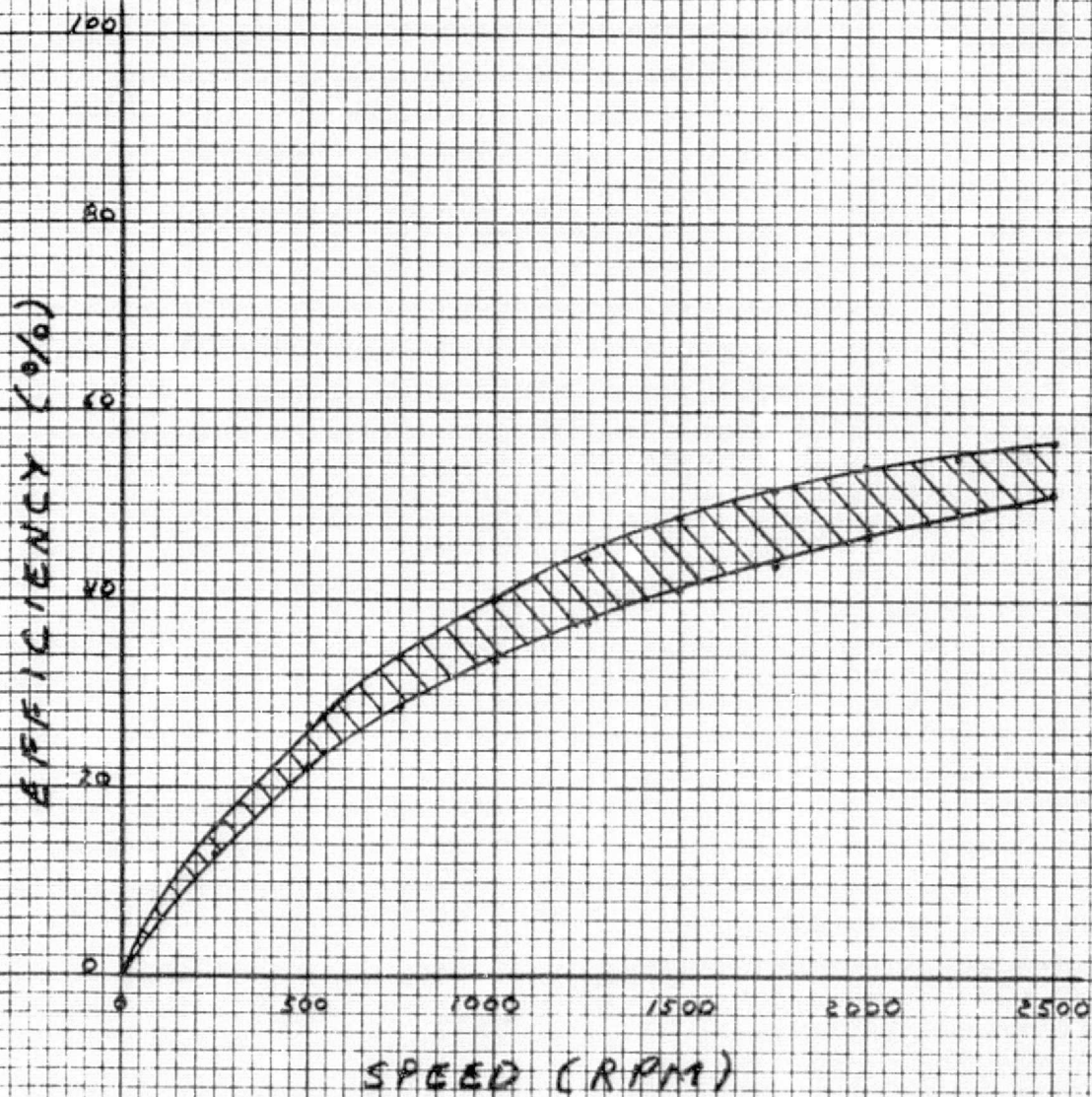


FIGURE 4-6

# HIGH TORQUE DC MOTOR ELECTRONICS EFFICIENCY VS SPEED

FOR 20 TO 100% TORQUE RANGE

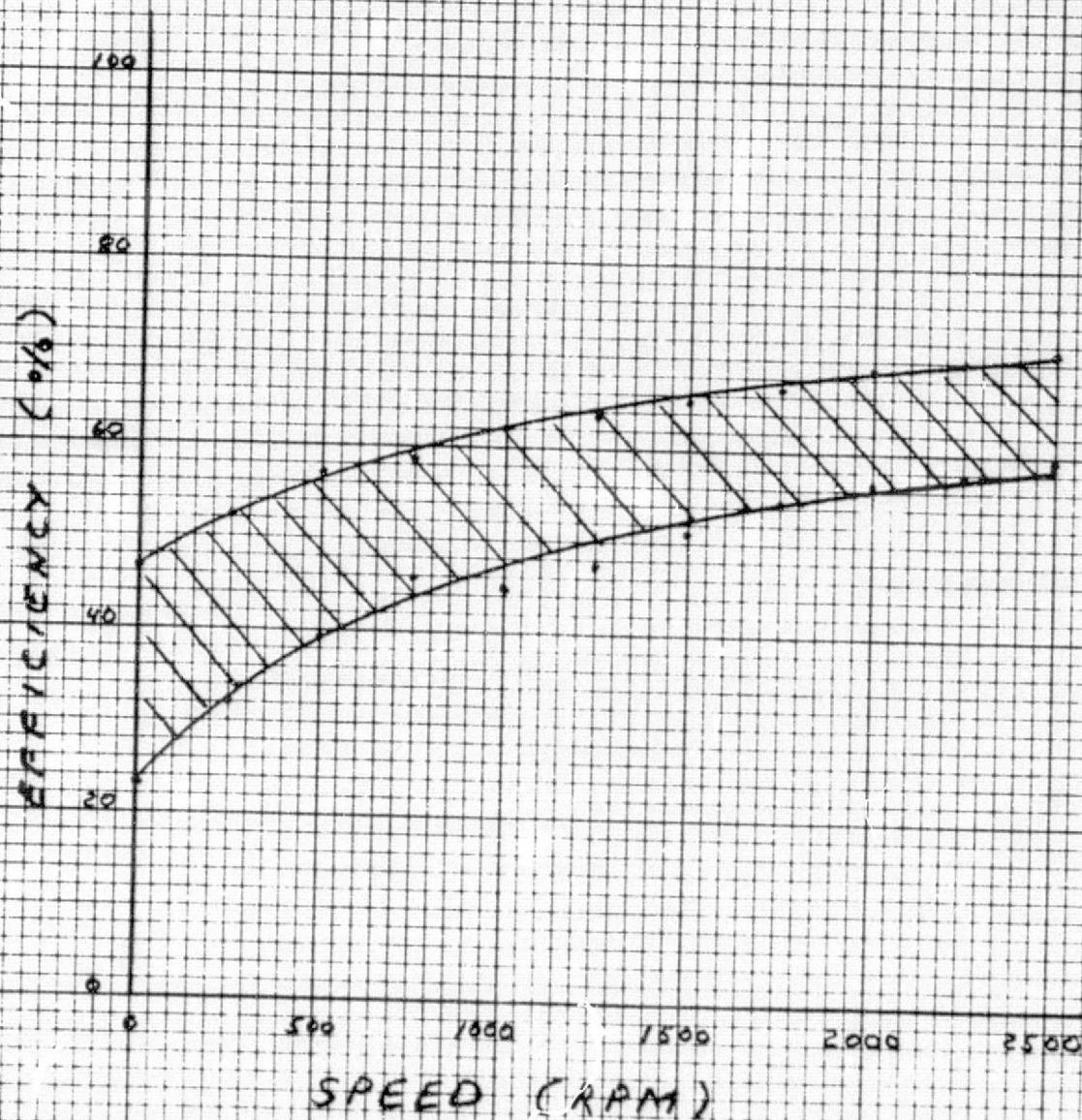


FIGURE 4-7



# HIGH TORQUE DC MOTOR H BRIDGE EFFICIENCY VS SPEED FOR 40 TO 100 % TORQUE RANGE

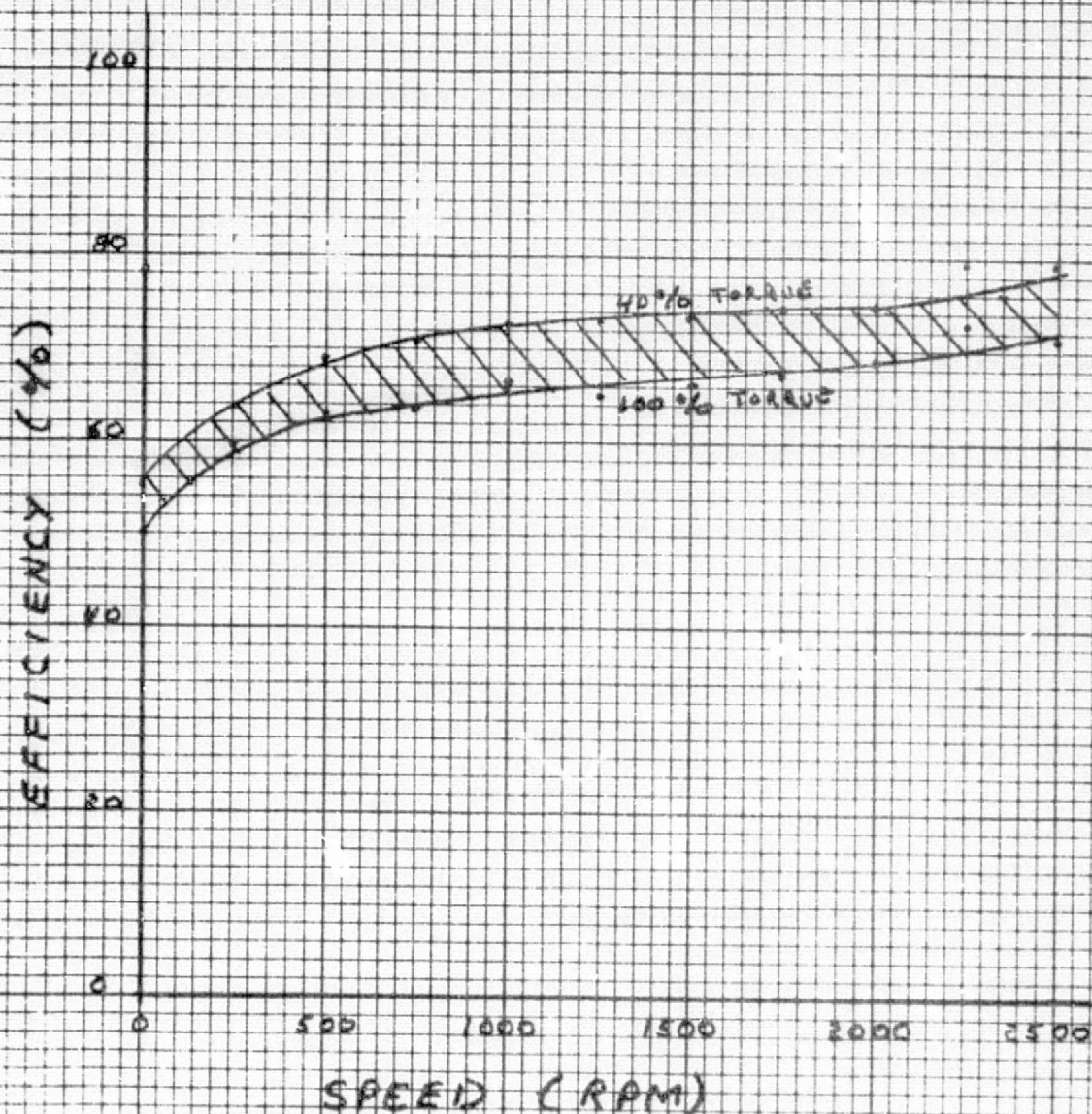


FIGURE 4-8



The efficiencies of the electronics must not be taken too strongly since no attempt was made during circuit modifications at reducing power consumption. This was because the main object of this study was the motor characteristics. Future circuits would naturally employ optimization techniques for increasing electronics power efficiency.

#### 4.4 TORQUE TRANSIENTS

The RWA was tested for torque transients with step torque commands of  $\pm 10\%$ ,  $\pm 20\%$ ,  $\pm 50\%$  and  $\pm 100\%$  of maximum at CW 2600, CCW 2600 and zero RPM. The filter across the output of the torque indicator was removed for these tests. The resultant torque graphs are shown in Section 8, Figures 8-16 to 8-27. The 4 Hertz oscillation frequency of the spring mass system is apparent in these graphs. Also the slew rate (15 inches/second) of the plotter is evident. However, an observable time constant of about 1/2 second can be seen in the graphs with maximum torque command. This time constant did not seem reasonable so a preset counter and digital printer were used to time wheel revolutions during the transient. The digital measurement system was able to time every third revolution or about 70 milliseconds between prints at 2600 RPM. These readings were converted to speeds and plotted by computer as shown in section 8, Figures 8-28 to 8-42. It appears from these graphs that the step torque commands resulted in constant speed-time slopes or constant torque levels with no time constants in the 500 millisecond range.

The apparent time constant in the reaction torque graphs are therefore attributed to limitations of the test equipment and not to the RWA subsystem.

#### 4.5 CURRENT WAVEFORMS

Pictures were taken of the High Torque DC Motor currents to show the effect of armature reaction on the Hall resolvers. The RWA was operated at CW 1250 RPM with torque commands of  $\pm 20\%$ ,  $\pm 50\%$  and  $\pm 100\%$  of full torque. The RWA was also run at CCW 1250 RPM and  $\pm 100\%$  of full torque. Figures 4-9 and 4-10 show the effect of armature reaction on the sensitivity of the Hall rotor position resolvers to the stator electromagnetic field. The clipping (flat topping) of the current waveforms is due to electronic current limiting but the remainder of the distortion is due to armature reaction. This is evident by comparing Figures 4-11 through 4-16 where conditions were the same except for motor current. The low current pictures show much less distortion than those at high current.

The motor currents of Figures 4-11 and 4-12 were subjected to a Fourier harmonic analysis to determine the amount of distortion in the waveform. The results shown in Table 4-1 indicate that for accelerating torque at 1250 RPM, the harmonic power loss was 3.5% and 8.9% for decelerating. The average torque producing currents were 4.14 amps RMS accelerating and 3.77 amps RMS decelerating, a difference of 9%. These differences are attributed to armature reaction effects on the Hall resolvers.

The effect of the back EMF of the motor on the current at maximum speed can be seen in Figure 4-17. The peaking of the current at maximum is a result of insufficient buss voltage to supply the demanded current. At higher buss voltage this effect disappears and likewise at lower back EMF's.

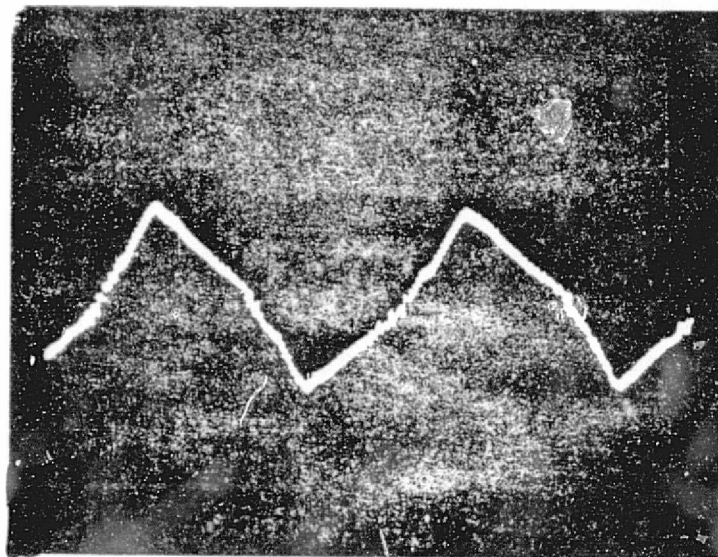
CURRENT HARMONIC ANALYSIS  
1250 RPM CW ACCELERATING

	CURRENT-AMPS-PEAK		RATIO TO POSITIVE SEQUENCE CURRENT		POWER COMPONENT	
	SIN PHASE	COS PHASE	SIN PHASE	COS PHASE	SIN PHASE	COS PHASE
FUNDAMENTAL	6.2477	5.4694	1.06642	.93357	---	---
+1	5.8586	5.8586	1.00000	1.00000	.500000	.500000
-1	.3891	.3891	.06642	.06642	.002206	.002206
2	.7024	.0644	.11990	.01099	.007188	.000060
3	.3950	.8269	.0674	.14115	.002273	.009962
5	.6144	.0578	.10488	.00986	.005500	.000049
7	.1677	.0742	.02863	.01267	.000410	.000080
9		.0709		.01211		.000073
4.8KHz	.4000	.4000	.06828	.06828	<u>.002331</u>	<u>.002331</u>
TOTAL HARMONIC POWER PER PHASE					.019907	.014761
TOTAL HARMONIC POWER					.034668	
TOTAL POSITIVE SEQUENCE POWER					1.000000	

1250 RPM CW DECELERATING

FUNDAMENTAL	4.1567	6.5080	.77953	1.22047	---	---
+1	5.3323	5.3323	1.00000	1.00000	.500000	.500000
-1	1.1756	1.1756	.22047	.22047	.024304	.029304
2	.2012	.5952	.03774	.11163	.000712	.006231
3	.9154	.6905	.17168	.12949	.014739	.008384
5	.1993	.2790	.03737	.05232	.000698	.001369
7	.1529	.1955	.02867	.03667	.000411	.000672
9	.2454	.0735	.04603	.01379	.001059	.000095
4.8 KHz	.4000	.4000	.07501	.07501	<u>.002814</u>	<u>.002814</u>
TOTAL HARMONIC POWER PER PHASE					.044735	.043868
TOTAL HARMONIC POWER					.088603	
TOTAL POSITIVE SEQUENCE POWER					1.000000	

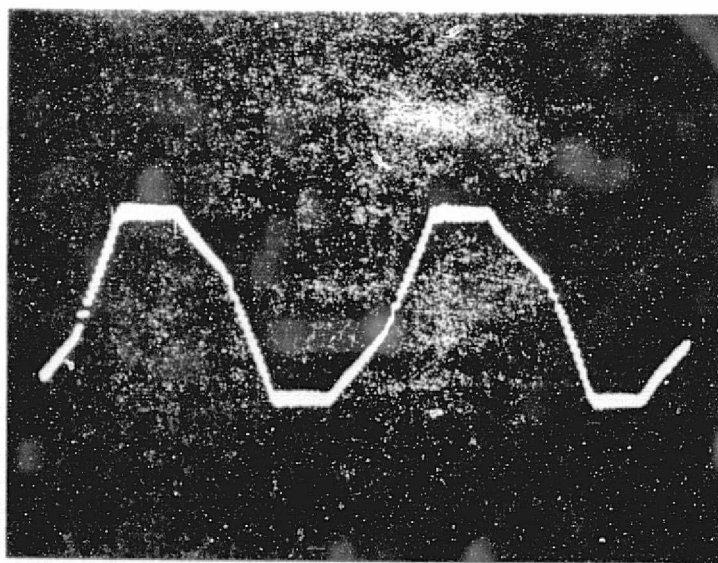
TABLE 4-1



SIN  
PHASE

2 MS/CM

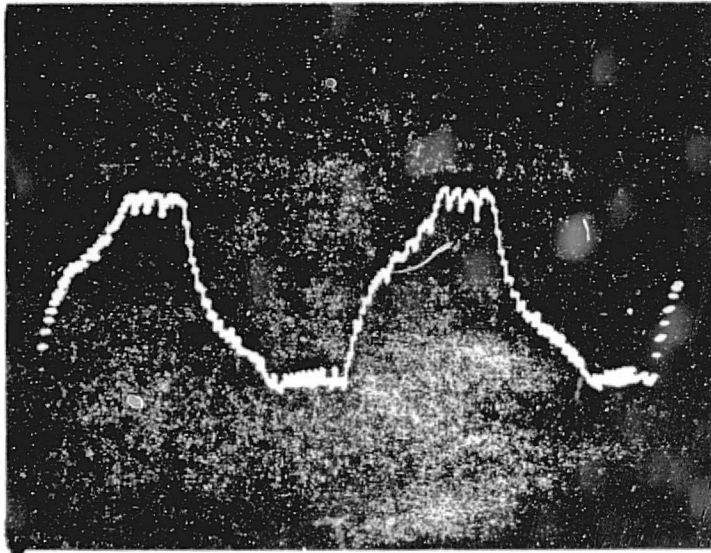
4 AMP/CM



COS  
PHASE

CCW ROTATION ACCELERATING  
5V TORQUE COMMAND

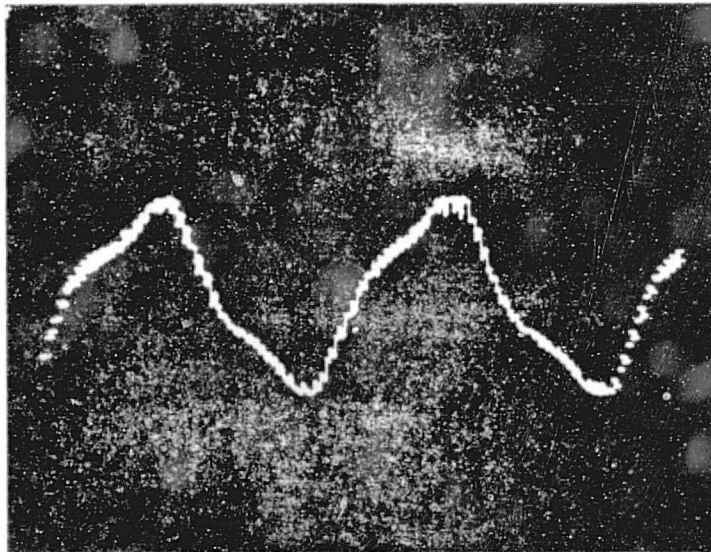
MOTOR CURRENT WAVEFORMS  
FIGURE 4-9



SIN  
PHASE

2 MS/CM

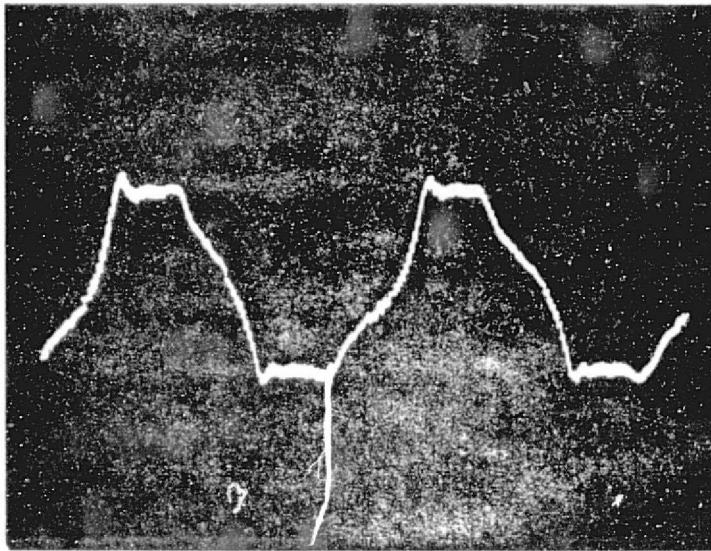
4 AMP/CM



COS  
PHASE

CCW ROTATION DECELERATING  
5V TORQUE COMMAND

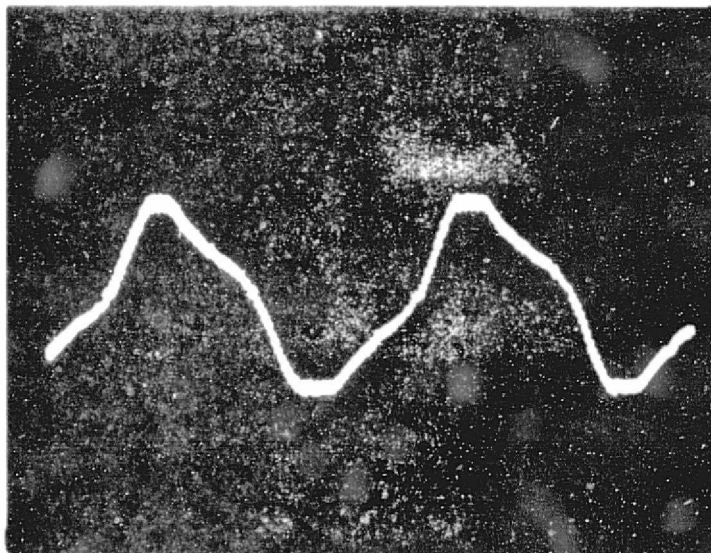
MOTOR CURRENT WAVEFORMS  
FIGURE 4-10



SIN  
PHASE

2 MS/CM

4 AMP/CM

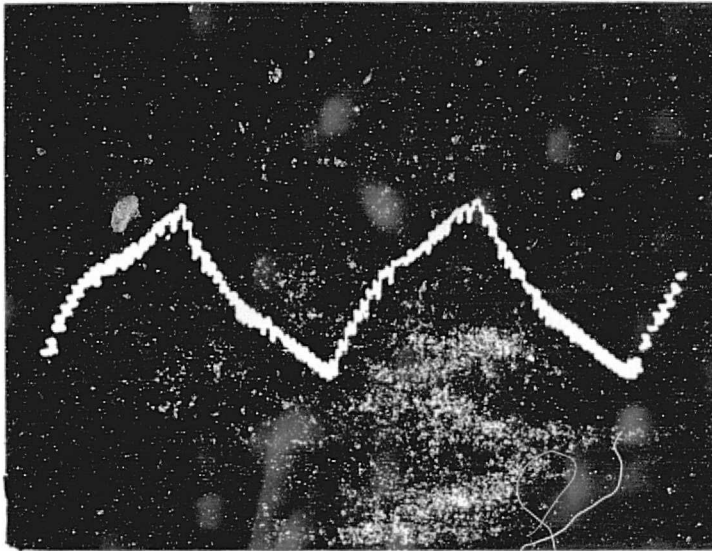


COS  
PHASE

CW ROTATION ACCELERATING  
5V TORQUE COMMAND

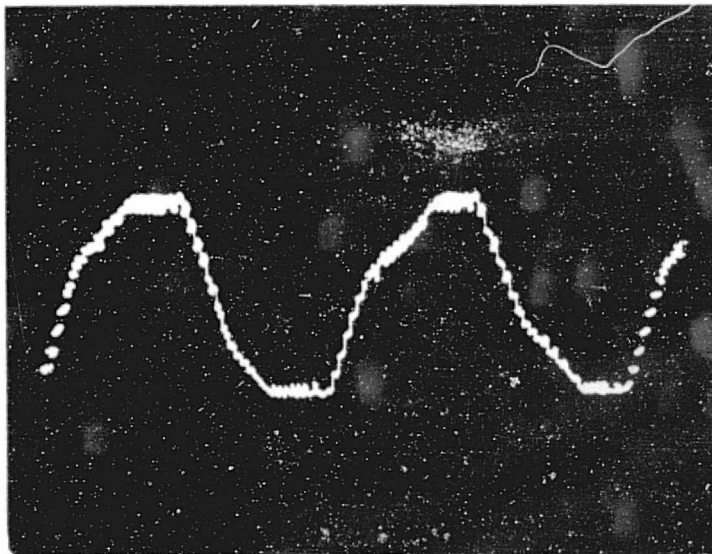
MOTOR CURRENT WAVEFORMS

FIGURE 4-11



SIN  
PHASE

2 MS/CM  
4 AMP/CM

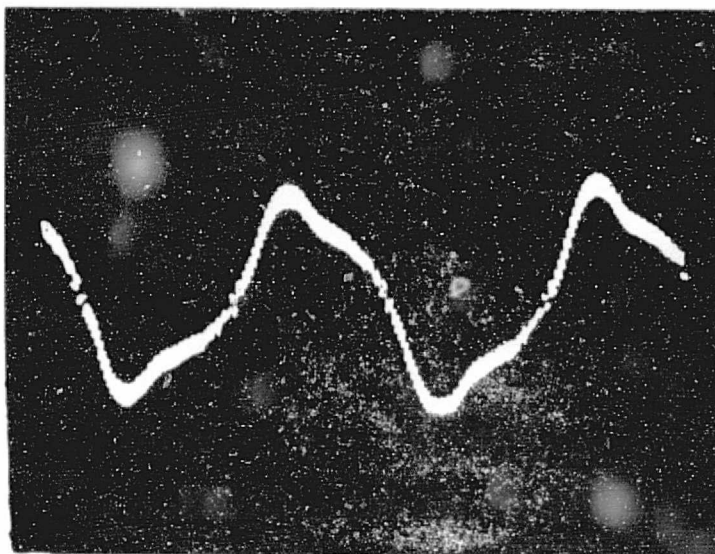


COS  
PHASE

CW ROTATION DECELERATING  
5V TORQUE COMMAND

MOTOR CURRENT WAVEFORMS  
FIGURE 4-12

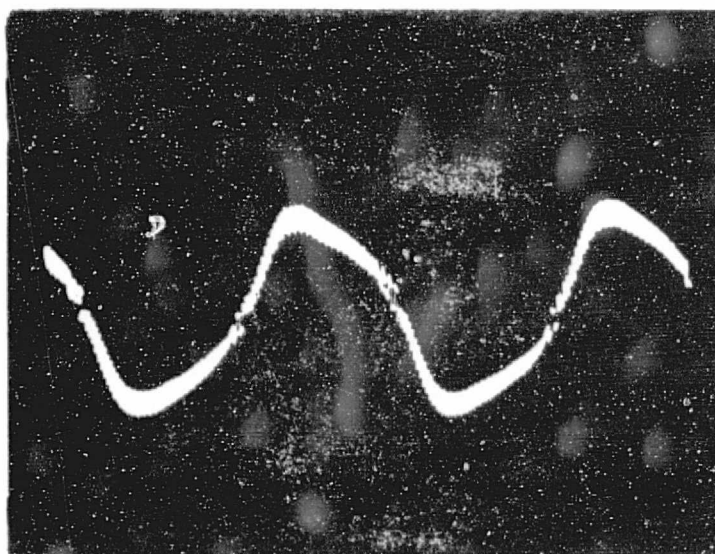




SIN  
PHASE

2 MS/CM

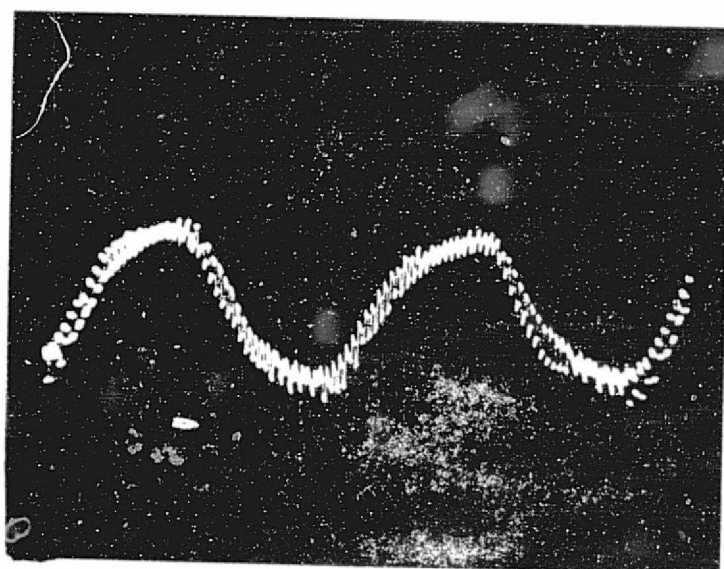
2 AMP/CM



COS  
PHASE

CW ROTATION ACCELERATING  
2.5V TORQUE COMMAND

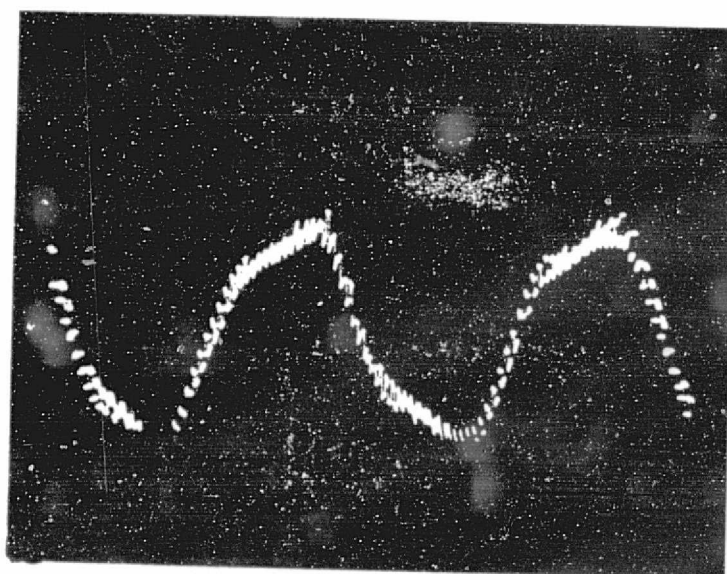
MOTOR CURRENT WAVEFORMS  
FIGURE 4-13



SIN  
PHASE

2 MS/CM

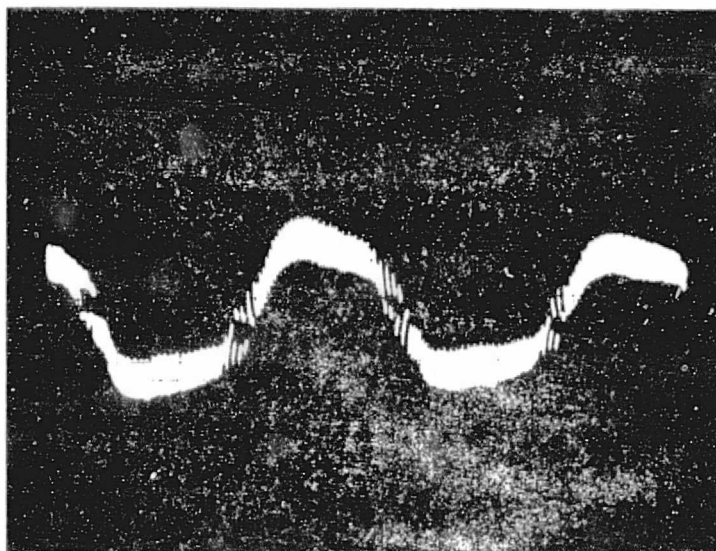
2 AMP/CM



COS  
PHASE

CW ROTATION DECELERATING  
2.5V TORQUE COMMAND

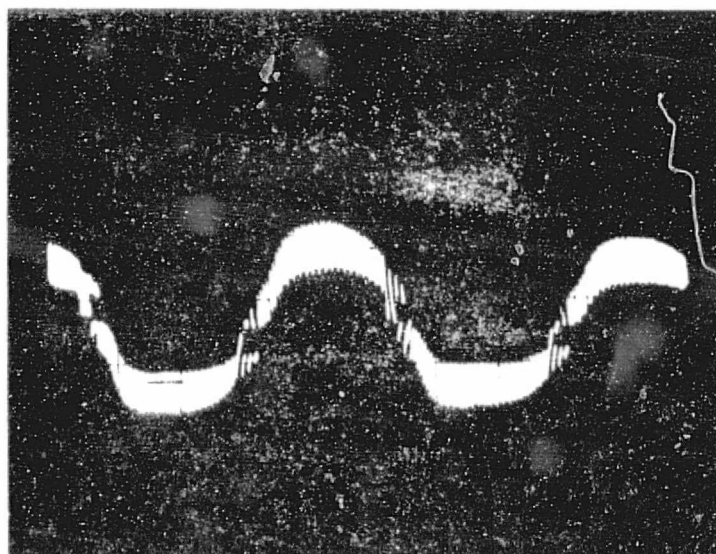
MOTOR CURRENT WAVEFORMS  
FIGURE 4-14



SIN  
PHASE

2 MS/CM

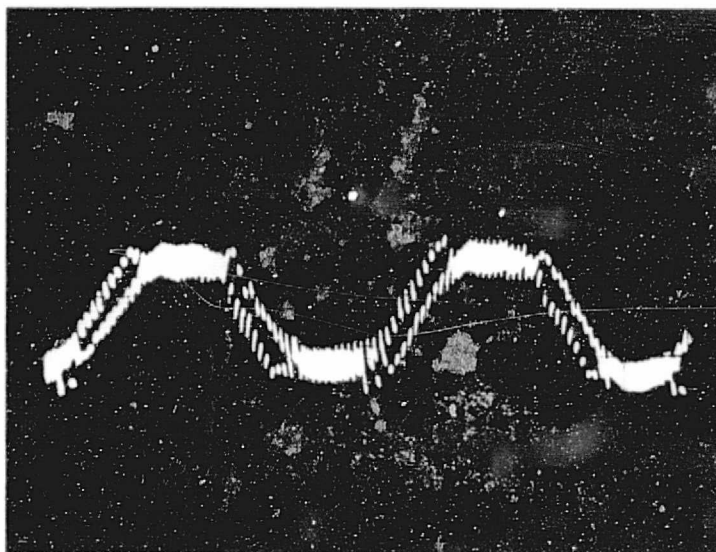
1 AMP/CM



COS  
PHASE

CW ROTATION ACCELERATING  
1V TORQUE COMMAND

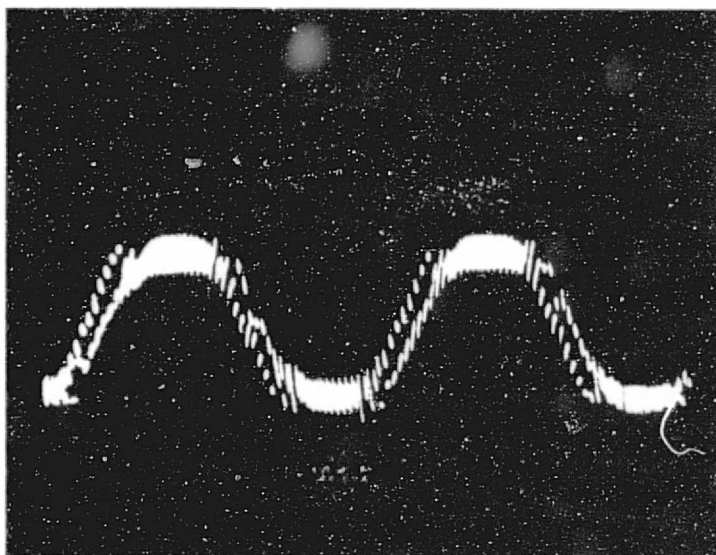
MOTOR CURRENT WAVEFORMS  
FIGURE 4-15



SIN  
PHASE

2 MS/CM

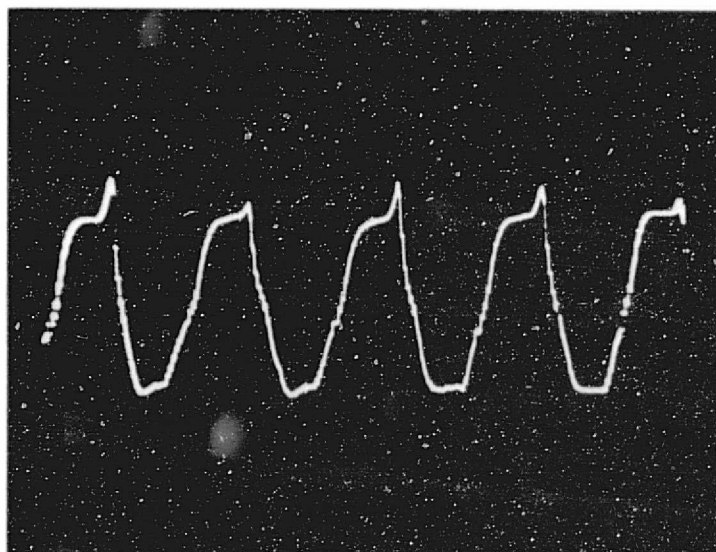
1 AMP/CM



COS  
PHASE

CW ROTATION DECELERATING  
1V TORQUE COMMAND

MOTOR CURRENT WAVEFORMS  
FIGURE 4-16



SIN  
PHASE

2 MS/CM  
4 AMP/CM

CW ROTATION ACCELERATING  
5V TORQUE COMMAND

MOTOR CURRENT WAVEFORM  
FIGURE 4-17

## 5.0 BRUSHLESS DC MOTOR

### 5.1 DESCRIPTION AND HISTORY

The high torque DC motor consists of a permanent magnet rotor located outside of a two phase wound stator. This type of construction employs a rotor comprised of ten alnico 9 permanent magnet segments positioned and embedded circumferentially in a soft iron pole structure. A photograph of this type of motor is shown in Figure 1-1. The multipolar design insures a high torque and minimizes space and weight. This machine is designed to develop up to 50 oz-in of torque. The stator is wound for two phase operation with two pairs (for redundancy) of Hall elements located in the motor air gap for rotor position sensing.

This type of motor has been built successfully and tested for the Roll Reaction Wheel which was to be used on the Earth Limbs Measurements Satellite before the program was cancelled.

### 5.2 DESIGN FEATURES

#### 5.2.1 Winding Placement

After tests were performed on the ELMS motor it was discovered that the Hall devices which were assembled in grooves placed into the stator at the motor air gap were not properly located. After much analysis the conclusion was reached that the cause for the shift must be due to the fact that the coils were lap wound into the stator. The lap winding places one half of

the coil in the bottom of a slot and the other half at the top of a slot. Since the slots are long and narrow, the axis of the coil is considerably shifted off the radial direction. The theory is that the stator flux pattern does not faithfully follow the teeth but tends to flow perpendicular to the coils.

In order to avoid this undesirable error, the winding for the high torque motor was modified to insure that the coils are all perpendicular to the teeth. This was accomplished by placing the individual coils either totally in the bottom of slots or totally in the top of slots.

#### 5.2.2 Winding Determination

The windings were designed to give full torque of 50 oz-in at 3000 rpm when operated from a 20 volt zero to peak square wave. This is equivalent to  $(4/\pi)(20) = 25.5$  volts peak sinusoidal excitation. The back EMF was calculated to be 0.00744 volts peak/rpm and actually tested 0.00758 volts peak/rpm. The correlation was good but, unfortunately, the excitation differed from the square wave assumed. The actual excitation is a pulse width modulated wave of 0 to 20 volts which makes it a 20.0 volt peak sinusoidal wave. For this reason the back EMF was high and the high speeds were not attained.

#### 5.3 MOTOR TEST RESULTS

Refer to Figure 5-1 for a listing of pertinent motor parameters discussed in the following paragraphs.

### 5.3.1 Back EMF Constant

The motor was placed in a test fixture and the shaft driven by an external motor. The voltages generated by the windings at various speeds were recorded. The back EMF was then calculated to be 0.00758 volts peak/rpm. The maximum torque constant is calculated to be 1352 times the back EMF constant. For this machine it is 10.25 oz-in/amp peak. This torque constant is attainable if the commutation angle is exactly at 90 degrees.

### 5.3.2 Hall Location Tests

After the reaction wheel was assembled some simple tests were run to determine the accuracy of the Hall placements. These tests are described pictorially in Figures 5-2 and 5-3. The tests were run in numerical sequence. One set of Hall elements were series input connected and set to 40 milliamps and the millivolt outputs were recorded for different rotor positions. Test 1 indicated that with 2.5 amps flowing through the A winding a field was established attracting a S pole (assumed polarity) of the rotor. With this set of conditions the A Hall element generated 23 mv and the B Hall elements generated 72 mv. After the excitation to winding A was removed Test 2 gave the Hall outputs for the same rotor position. Note that the diagrams show only two poles when in reality the machine has 10 poles and the rotor had a possibility of five distinct positions where it could line up.



Test 3 was run with the B winding excited and the rotor turned 90 degrees electrically from Tests 1 & 2. Test 5 was run with both windings excited giving the rotor a 45 degree electrical position. Similar tests were run with reversed stator currents as shown in Figure 5-3.

The question arises if the Hall locations are accurate. Tests 2, 4 and 8 indicate that they are fairly well located, where one element reads at a high level and the other at a null. But test 10 indicates considerable error.

Comparison of test 6 to Tests 2 and 4 indicate that the wave shape is not sinusoidal. One would expect that the Hall outputs of test 6 to be  $\sin 45^\circ$  or 70.7% of the "maximum" outputs of tests 2 & 4. They are instead:

$$\text{Hall A } \frac{64}{76} = 84.2\%$$

$$\text{Hall B } \frac{60}{63} = 95.2\%$$

Comparison of test 12 to test 8 indicates similar distortion.

The odd numbered tests give an indication of distortion of the air gap flux field due to stator flux. These tests do not represent actual running conditions of the motor since the rotor should never be line up with the stator field but should be in electrical quadrature. Regardless of that fact, one would expect Hall A of test 1 to be at a low null value. It measured 23 mv indicating distortion of air gap flux.

## 5.4 REACTION WHEEL TEST RESULTS

### 5.4.1 Current Wave Analysis

In order to verify the motor design and try to explain its losses it proved necessary to analyze the current wave shapes of the motor windings. The currents for clockwise rotation both accelerating and decelerating at 1250 rpm and 5 volts command are given in Figures 4-11 & 4-12. These photographs were analyzed by Fourier series and the results are given in Table 4-1.

The useful current into the brushless DC machine is the balanced two phase current that will produce a constant magnitude 10 pole magneto-motive force wave in the air gap of the machine. This is called the positive sequence (+1) current system. Since the fundamental currents of the two phases are not equal, there will be a negative sequence (-1) current system which will not produce any useful torque but will consume power. Similarly, all the harmonics of current will not produce useful torques but will consume power. Table 4-1 shows the magnitudes of the harmonics, the relative magnitude to the positive sequence, and the heating value of these components. For the clockwise accelerating mode at 1250 rpm the useful current is 5.86 amps peak per phase and the total harmonic power into the motor plus leads is 3.47% of the conventional copper losses. For the decelerating mode the useful current is -5.33 amps peak per phase and the harmonic power adds 8.86% to the conventional copper losses.

#### 5.4.2 Power Flow Diagrams

Using the current wave analyses, reaction wheel measurements, and motor measurements a power flow diagram can be constructed to explain the power flow to the motor and reaction wheel.

Figure 5-4 shows the power flow diagrams for 1250 rpm cw accelerating and decelerating at maximum torque. In each case, it can be explained from right to left. For the accelerating case the reaction wheel torque was taken from the plotted curves (Figure 8-2) at full command voltage of 5 volts accelerating in the clockwise direction. The power output is simply the reaction torque times the speed divided by 1352 (or  $53.25 \times 1250 / 1325 = 49.23$  watts). The friction and windage is given by the rundown test of the AC motor shown in Figure 4-4. The AC motor curve gives the required information because the friction and windage conditions are identical to the High Torque DC Motor case with the additional feature that no magnetic field is present in the motor.

The input to the reaction wheel or output of the idealized brushless DC motor, 50.04 watts, is the reaction wheel output power plus the friction and windage power.

The motor rotor experiences a magnetic drag with rotation due to the varying magnetic flux that it produces in the stator. This is also given in Figure 4-4 and is the friction and windage portion (AC motor curve) subtracted from the DC motor open winding curve.

The copper loss of the stator, 14.08 watts, of the idealized machine is the positive sequence peak current squared times the winding resistance of 0.41 ohms.

The stator core loss was determined by making impedance measurements of the motor. The effective resistance at 104.2 Hertz which corresponds to 1250 rpm was measured and the DC resistance subtracted to give the portion of resistance attributable to core loss. This has a value of 0.24 ohms per phase. The stator core loss then is simply  $(5.86 \text{ amps})^2 \times 0.24 \text{ ohms}$  or 8.24 watts.

Summing the motor output power and the three types of motor losses gives the idealized motor input of 72.80 watts.

The wiring external to the motor was measured at 0.20 ohms. This dissipates 6.87 watts at 5.86 amps peak positive sequence current.

The harmonic analysis of the current resulted in 3.47% additional copper losses due to the wave shape distortions and imbalance. This amounts to 0.73 watts additional to the motor and wiring copper losses and is shown as harmonic losses.

The total accountable power input to the motor and reaction wheel is 80.40 watts leaving 0.60 watt of miscellaneous power or error to account for making the total measured value of 81.0 watts.

The decelerating case is calculated in a similar fashion except that the power flow is running from the reaction wheel through the motor and into the supply lines. In reality, the brushless DC machine is acting as a generator.

For this case the current is -5.33 amps peak for the positive sequence and the harmonics account for 8.86% additional copper loss due to wave shape distortions and imbalance.

Assuming the measured value of 23.0 watts of generated electrical power as being accurate, there results an error of 1.96 watts of unexplained additional power generation.

#### 5.4.3 Torque Constant and Power Angle

Referring to the power flow diagrams of Figure 5-4 one can derive the apparent torque constant for the motor in the two modes of operation. The torque constant is defined as the air gap torque divided by the positive sequence current. The air gap torque is the output torque of the motor plus the magnetic drag torque. For the generator, the air gap torque is minus the output torque plus the magnetic drag torque. For this case the current is also negative resulting in a positive torque constant.

Figure 5-1 lists the apparent torque constants 9.317 oz-in/amp peak for accelerating and 9.483 oz-in/amp peak for decelerating. The maximum torque constant is

10.25 oz-in/amp peak as determined from the back EMF constant.

The torque angle is the electrical displacement of the rotor flux wave and the stator flux wave. This is ideally set for  $90^{\circ}$  but, shifts due to armature reaction affecting the Hall outputs. The angle is calculated as the sine of the ratio of the apparent torque constant to the maximum torque constant and is given in Figure 5-1 as 114.64 and 112.31 electrical degrees.

## 5.5 ANALYSIS

At this point it would be helpful to study briefly the operation of the brushless DC machine with Hall devices in the air gap.

### 5.5.1 Brushless DC Motor - No Armature Reaction

Figure 5-5 gives a simplified representation of a two pole brushless DC machine. The rotor is represented by a bar magnet and the stator is represented by two Hall elements and their corresponding windings. Hall element A senses the vertical flux that passes through it and Hall element B senses the horizontal flux that passes through it. Winding A produces a flux along its axis which is horizontal and winding B produces a vertical flux.

This diagram shows the ideal operation of the machine where the Hall devices sense only the rotor flux and produce currents in the windings which in turn produce stator flux in quadrature to rotor flux. At the rotor

position shown Hall A is at a maximum and winding A is drawing maximum current. The B circuit is at zero. As the rotor turns clockwise (upper diagram) the flux vector system follows synchronously so that a uniform torque is developed for all positions. The torque is proportional to the product of rotor flux,  $\phi_R$ , stator flux,  $\phi_S$ , and the sine of the angle between them. The convention for the torque direction is that the rotor flux vector tries to align with the stator flux vector.

The lower diagram shows the motor operation for counter clockwise torque.

#### 5.5.2 Brushless DC Motor - with armature reaction

Figure 5-6 represents the more realistic vector diagram for the flux vectors of the brushless DC machine with Hall devices in the air gap. The actual flux that passes through the Hall resolvers is not just the rotor component as assumed in the previous paragraph but the total flux,  $\phi_T$ , which is the vectorial sum of  $\phi_R$  and  $\phi_S$  in the air gap of the machine. This flux is sensed and a stator field is produced in quadrature to it. This effect is called armature reaction. The torque is proportional to the product of  $\phi_R$ ,  $\phi_S$ , and the sine of the angle between them (torque angle) as stated before. Figure 5-1 gives the torque angle that was determined under a set of conditions,  $114.64^\circ$  accelerating and  $112.31^\circ$  decelerating. These can be considered close enough to be the same.

By comparing the clockwise torque (upper) to the counter clockwise torque (lower) vector diagrams of Figure 5-6 one notices that there is the symmetry of torque magnitude and angle with direction of rotation. The conclusion one reaches at this point in the analysis is that the Hall devices are properly located.

#### 5.5.3 Brushless DC Motor - with armature reaction and Hall placement error

Suppose the Hall elements are both displaced relative to the windings by an angle,  $\theta$ , instead of  $90^\circ$  as they should be. Then the machine will appear as shown in Figure 5-7. Now the Hall devices sense the total flux,  $\phi_T$ , and the stator field is located at  $180^\circ - \theta$  or  $\theta$  depending on the torque direction. Also, the magnitudes of the stator fields,  $\phi_S$ , are not the same since the magnitudes of  $\phi_T$  sensed in each direction are not equal.

Note the dissimilar vector diagrams for the two torque directions. The winding currents and the torque for the lower diagram are higher than the corresponding values for the upper diagram.

From the data on the High Torque Motor it appears that this type of misplacement of Hall elements does not exist, but this is not positively proven. For instance, the Hall placement tests of Par. 5.3.2 left some doubt as to the accuracy of placement.



Another source of information that may produce some doubt as to the accuracy of the Hall placement are the current waveforms of Figures 4-11 and 4-12. The distortions of the wave shapes plus the fact that the waves were electronically clipped could be hiding the fact that the Hall elements are not ideally located but are being compensated by circuitry.

#### 5.5.4 Distortion at Air Gap and Skew

One undisputable source of error for this type of machine is the flux wave distortion that takes place in the air gap of the machine. Since the Hall devices sense the total air gap flux which is not necessarily sinusoidal and these in turn are amplified and fed to the windings, there is a compounding of distortions. If the machine has a large air gap, the distortions will be reduced and the stator flux portion will be minimized.

Another source of flux distortion is caused by the stator skew. The flux in the air gap tends to concentrate axially as well as circumferentially in the areas of rotor to stator attraction. The flux takes the least reluctance paths available by following the skew of the stator.

## HIGH TORQUE BRUSHLESS DC MOTOR PARAMETERS

### GENERAL

Number of Phases	2
Number of Poles	10
Outside Diameter	3.990 In.
Inside Diameter	1.627 In.
Overall Length	1.25 In.
Weight	21 Oz.

### MOTOR MEASUREMENTS

Back emf constant	0.00758 Volts Peak/RPM
Maximum torque constant	10.25 Oz-in/amp peak
DC Resistance per phase	0.41 Ohm
AC component of resistance per phase at 104.2 Hz	0.24 Ohms
Inductance per phase	0.80 Millihenry

### REACTION WHEEL MEASUREMENTS AT 1250 RPM $\hat{e}$ MAX. TORQUE

	<u>Accelerating</u>	<u>Decelerating</u>
Apparent torque constant (oz-in/amp peak)	9.317	9.483
Torque angle (degrees electrical)	114.64	112.31
Torque angle (degrees mechanical)	22.92	22.46

FIGURE 5-1

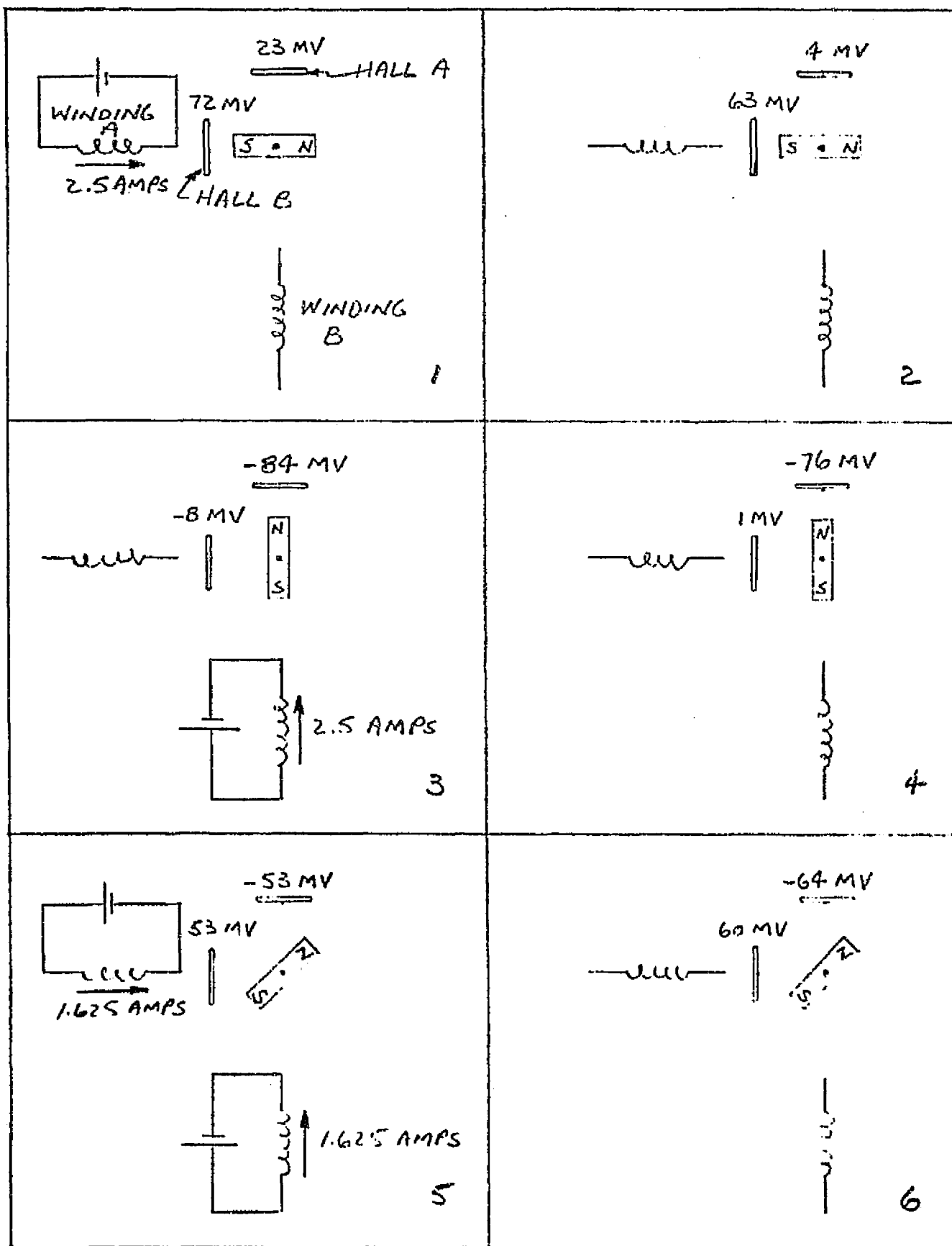


FIGURE 5-2 HALL LOCATION TESTS 1 THROUGH 6

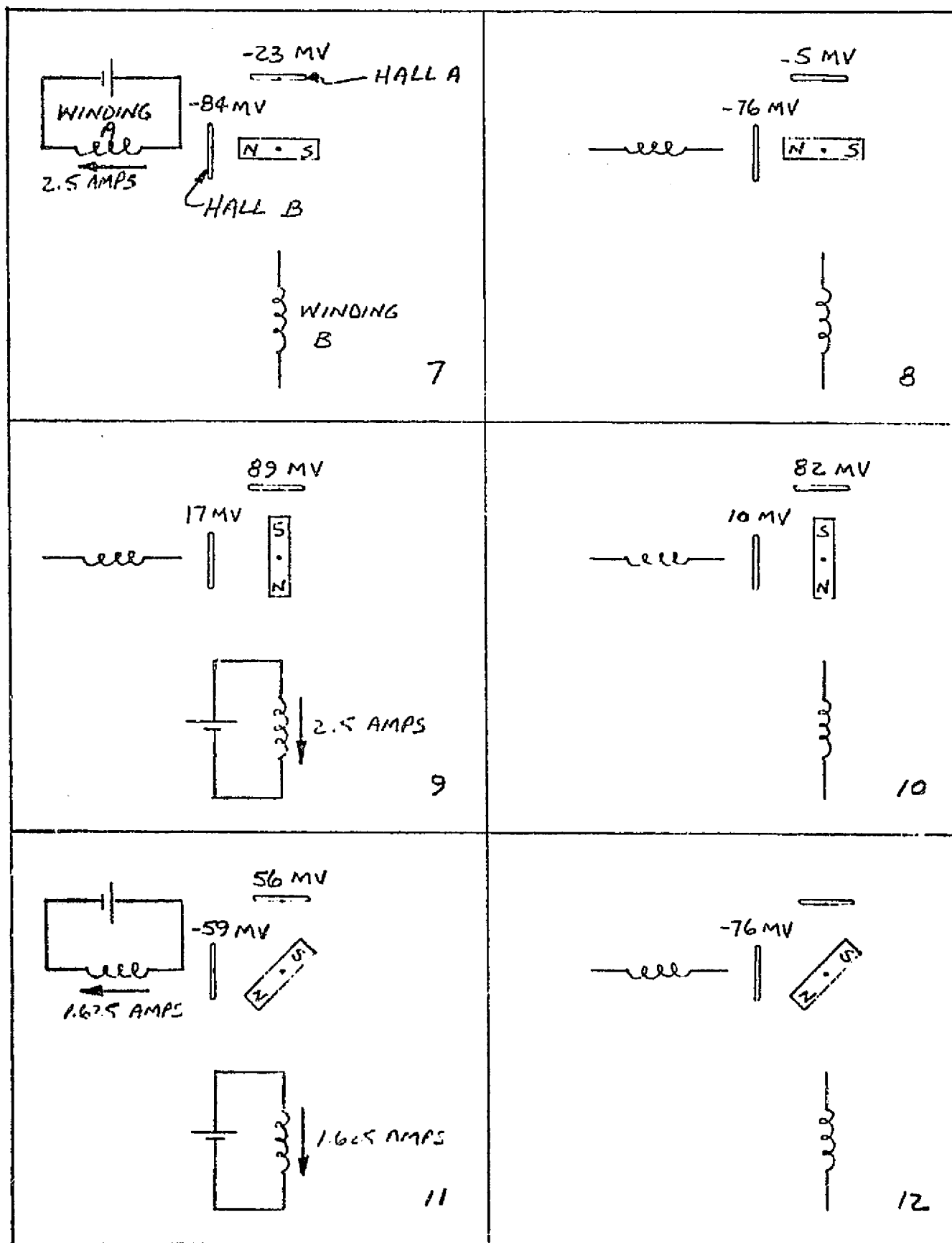
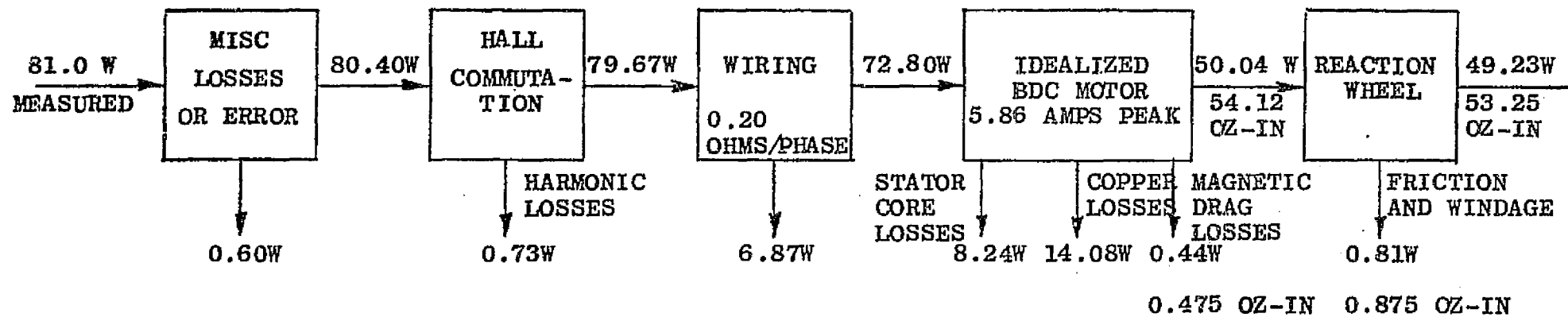


FIGURE 5-3 HALL LOCATION TESTS 7 THROUGH 12

# ACCELERATING



# DECELERATING

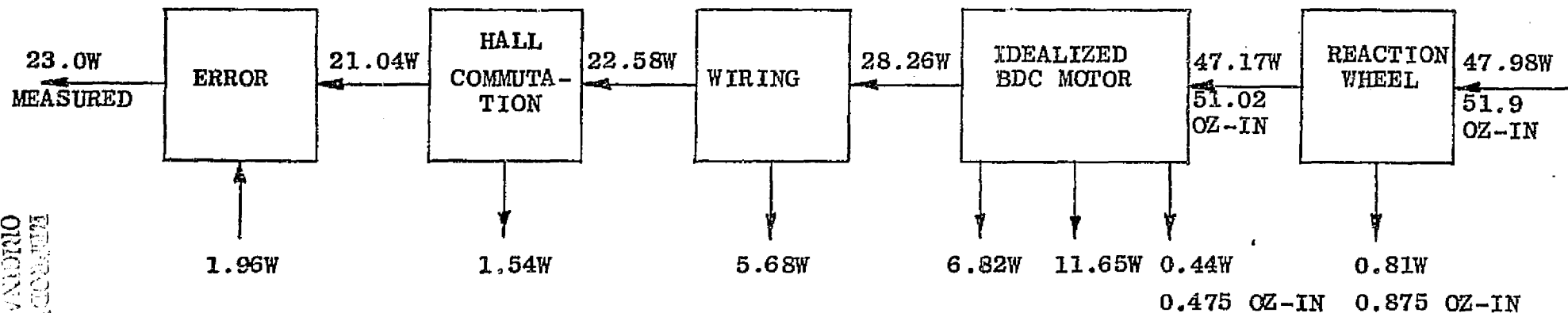


FIGURE 5-4

POWER FLOW DIAGRAMS AT 1250 RPM CW AND MAXIMUM TORQUE

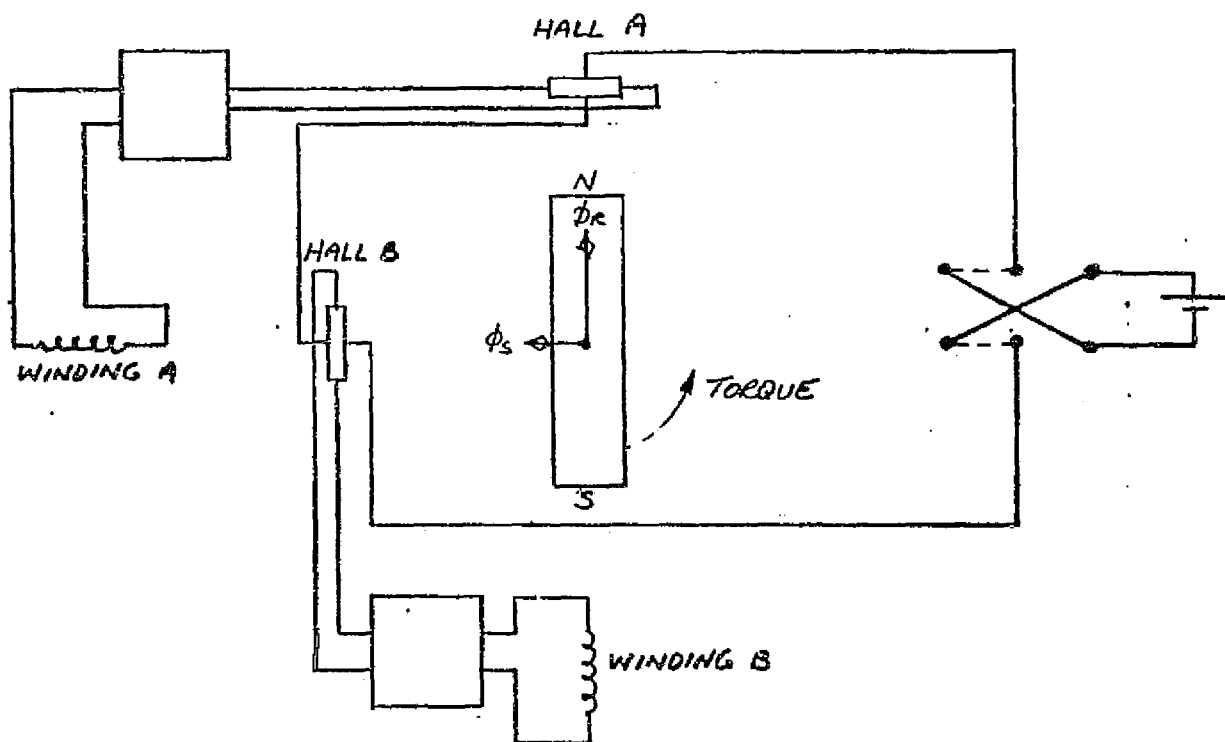
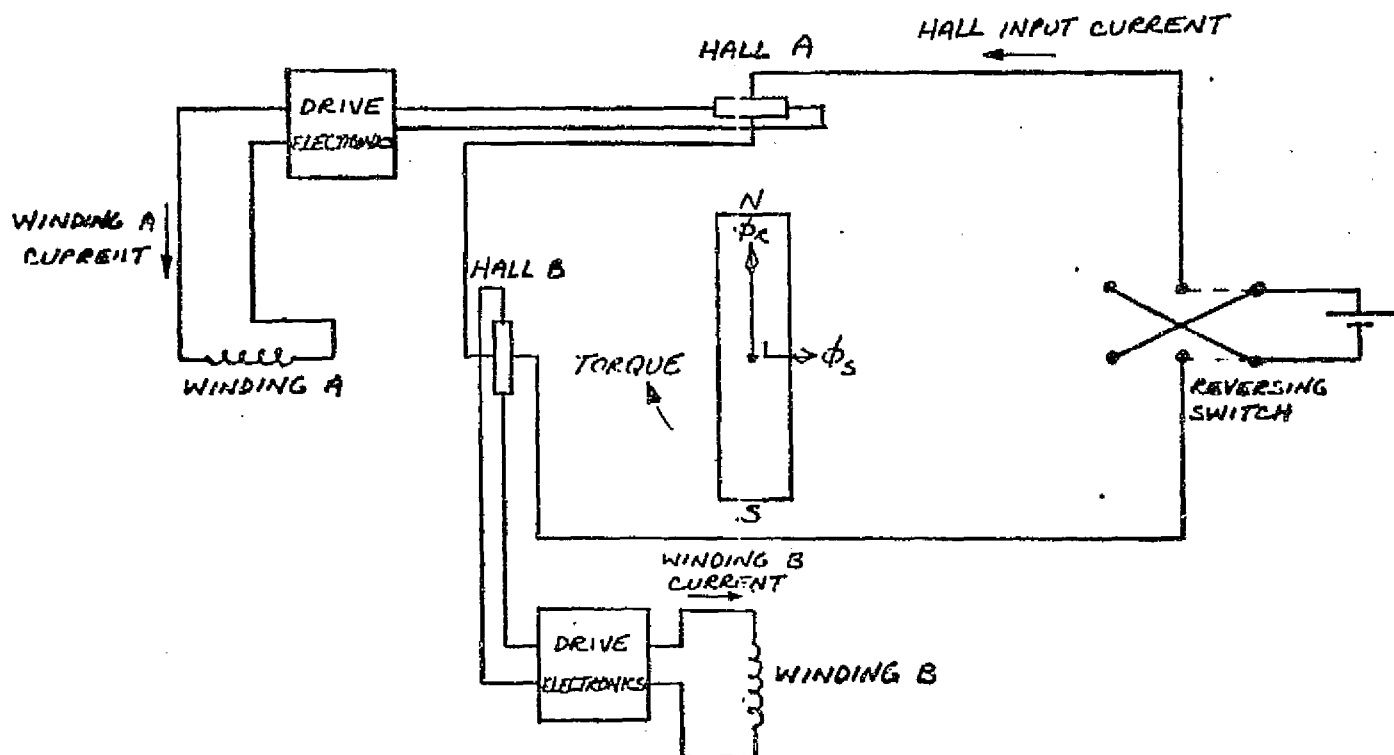


FIGURE 5-5 BRUSHLESS DC MOTOR - NO ARMATURE REACTION  
5-17

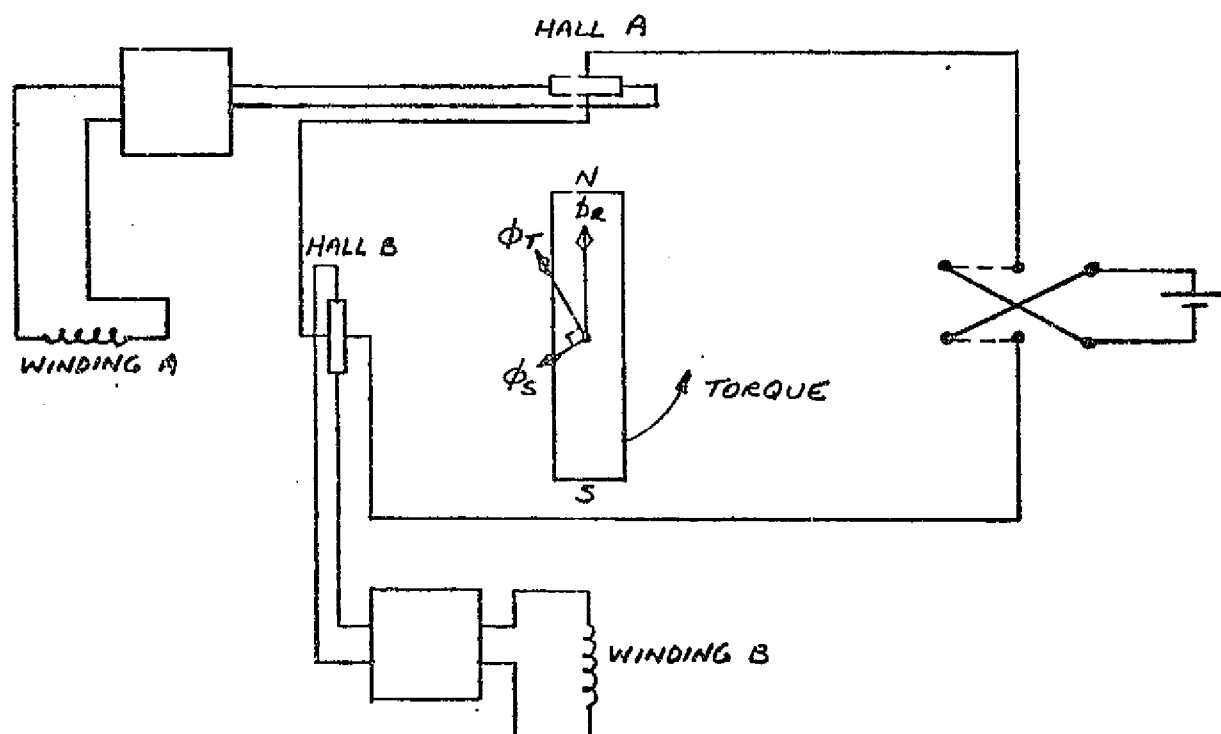
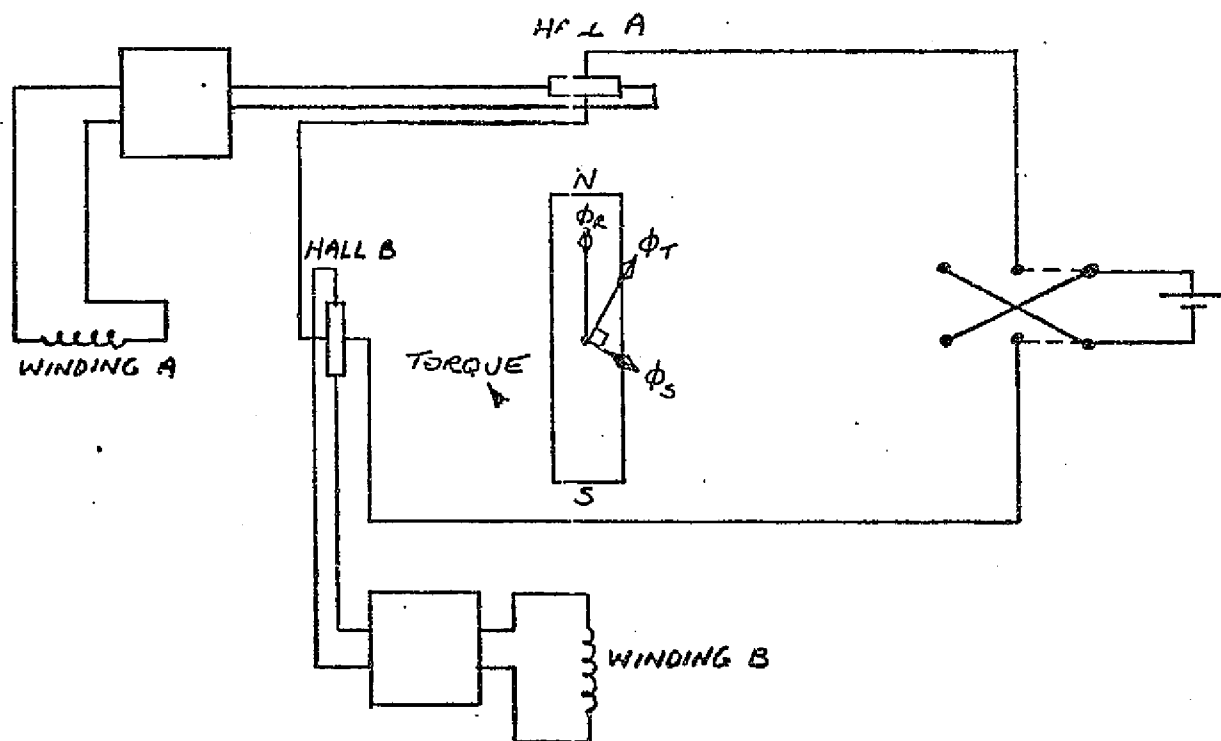


FIGURE 5-3 BRUSHLESS DC MOTOR - WITH ARMATURE REACTION

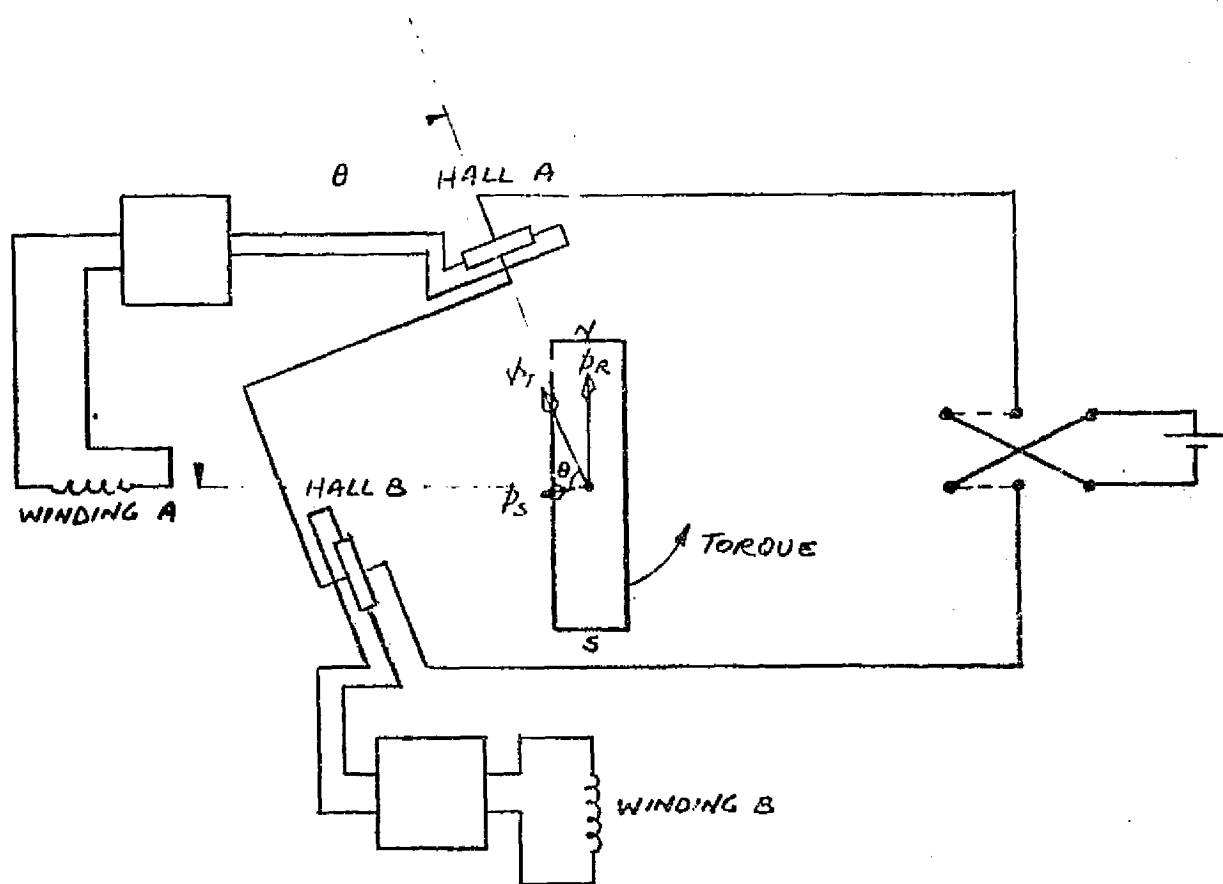
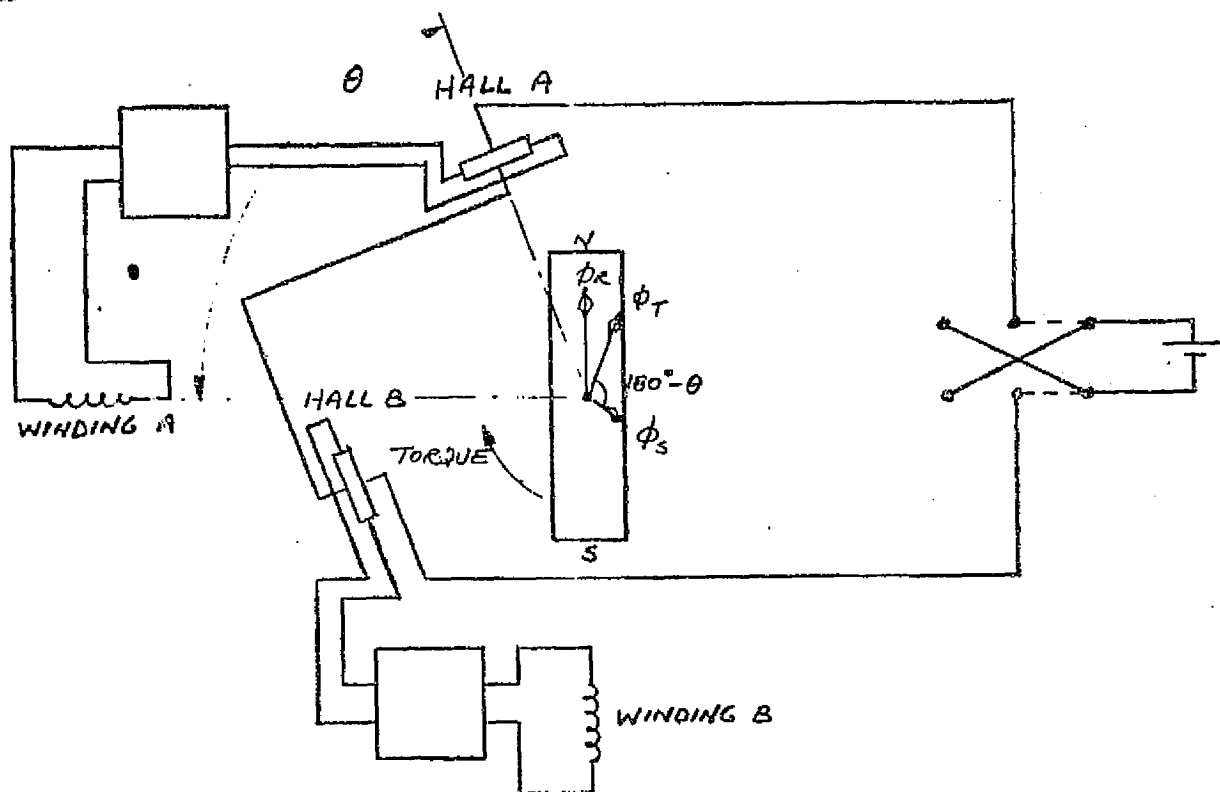


FIGURE 5-7 BRUSHLESS DC MOTOR - WITH ARMATURE REACTION  
AND HALL PLACEMENT ERROR 5-19



## 6.0

### DRIVE ELECTRONICS ANALYSIS

To obtain proper motor torque at all speeds, the motor current must follow the Hall voltage, in both amplitude and phase, at all frequencies up to maximum speed. A block diagram of the spin motor drive system is shown in Figure 6-1 where:

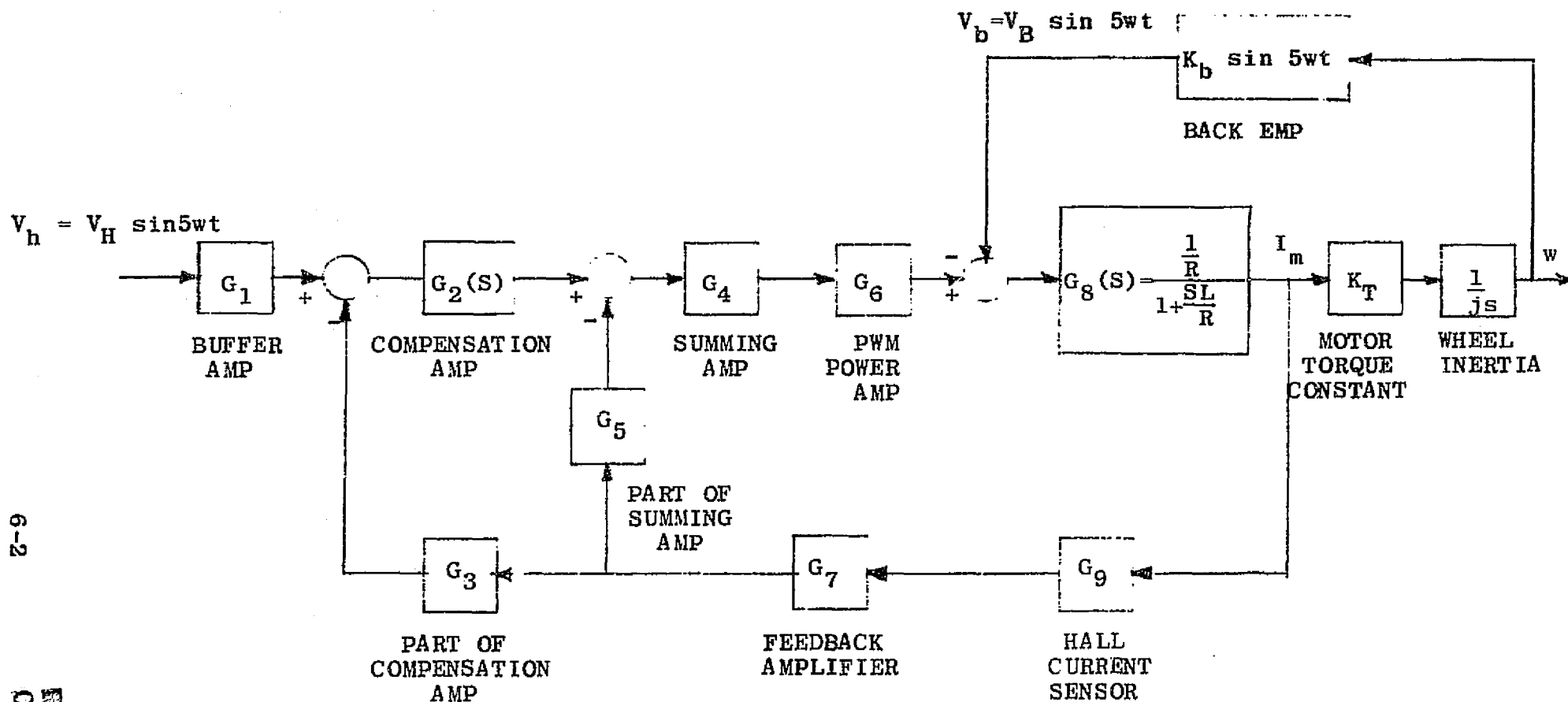
$$L = \text{Motor inductance} + \text{Hall current sensor inductance} \\ = 0.82\text{mH}$$

$$R = \text{Motor resistance} + \text{PWM power stage resistance} + \\ \text{Hall current sensor resistance} = 1.0 \text{ ohm}$$

$$K_T = \text{Motor torque constant} = 10.3 \text{ oz-in/amp}$$

$$K_b = \text{Motor back emf constant} = .00758 \text{ volts/rpm}$$

Note that the Hall output voltage is assumed to be in phase with the motor back emf. Since it is required that the motor current ( $I_M$ ) follow the Hall voltage ( $V_h$ ) at all frequencies up to maximum speed, the drive electronics must be designed to minimize the motor current generated by the back emf ( $V_b$ ). This problem is the conventional servo problem of minimizing an unwanted disturbance, which means maximizing the values of  $G_2$ ,  $G_4$  and  $G_6$  at all frequencies of interest. As the values of  $G_2$ ,  $G_4$  and  $G_6$  increase, however, the amplifier bandwidth increases. From a stability viewpoint, the maximum allowable bandwidth is set by the PWM power stage, which contributes a sampled-data-type phase lag. The PWM design used in the present system has a 9.6KHz effective sampling frequency, and the electronics are designed to produce a loop crossover frequency of 2500Hz, or about  $\frac{1}{4}$  of the pulse-width-modulation sampling rate.



SPIN MOTOR DRIVE ELECTRONICS - BLOCK DIAGRAM

FIGURE 6-1

As a result, referring to Figure 6-1,

$$G_1 = 10 \text{ V/V}$$

$$G_2(S) = 40 \frac{1 + \frac{S}{2\pi 1625}}{1 + \frac{S}{2\pi 12.7}} \text{ V/V}$$

$$G_3 = 0.5$$

$$G_4 = 5.23 \text{ V/V}$$

$$G_5 = .178$$

$$G_6 = 26 \text{ V/V (for } B^+ = 28\text{VDC)}$$

$$G_7 = 10 \text{ V/V}$$

$$G_8(S) = \frac{1 \text{ A/V}}{1 + \frac{S}{2\pi 194}}$$

$$G_9 = .03 \text{ V/A}$$

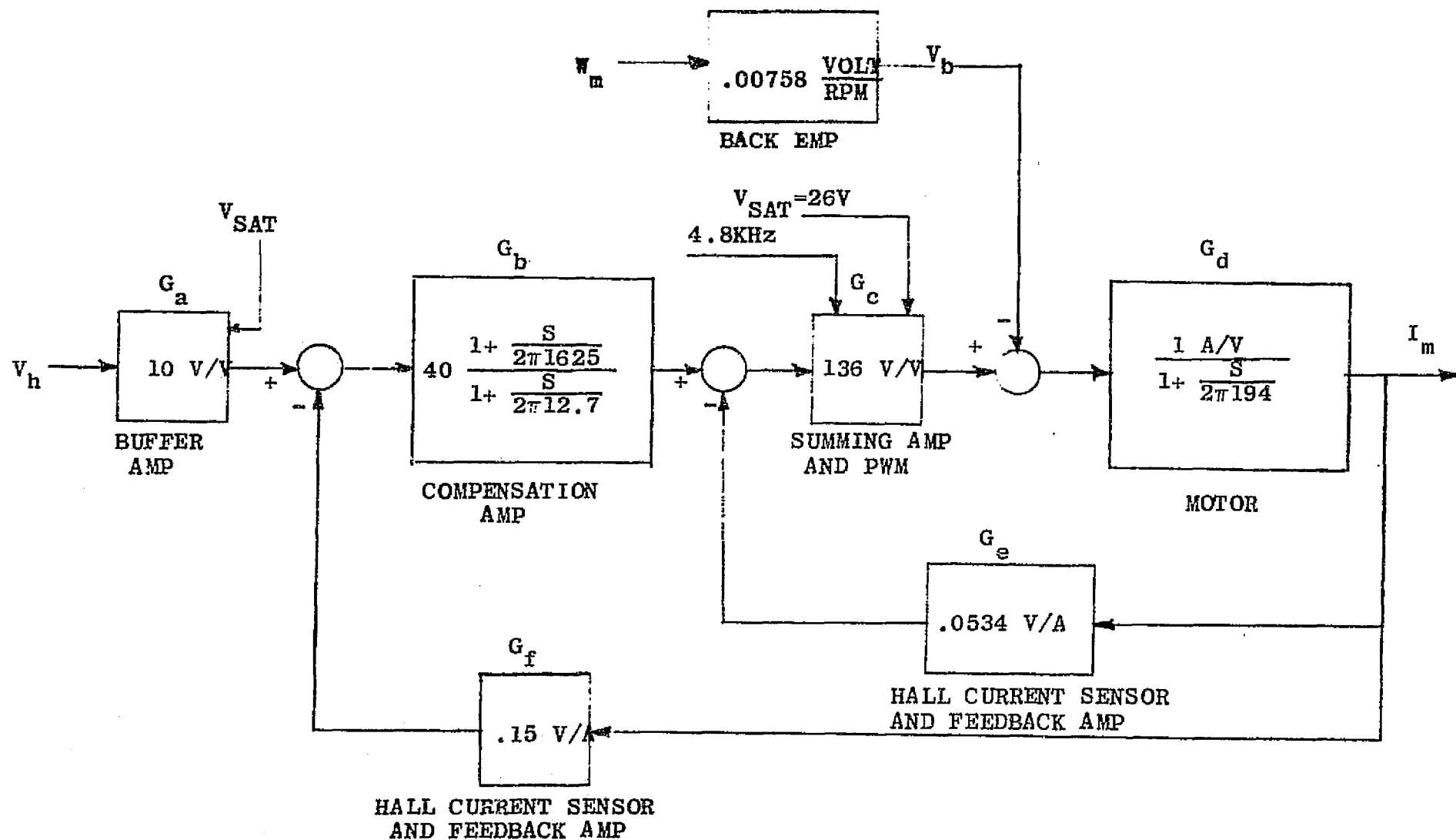
Using these values, the scaled block diagram of Figure 6-2 may be drawn. The open-loop transfer function,  $A(S)$ , of the loop (for stability verification only) is

$$A(S) = (G_e + G_f G_b) G_c G_{de} e^{-\frac{ST}{2}}, \quad T = 1/9600 \text{ sec}$$

where the transport lag approximates the dynamics of the pulse-width modulator.

Numerically,

$$A(S) = 823 \frac{1 + \frac{S}{2\pi 767}}{(1 + \frac{S}{2\pi 12.7})(1 + \frac{S}{2\pi 194})} e^{-\frac{S}{19,200}}$$



SPIN MOTOR DRIVE ELECTRONICS - SCALING DIAGRAM  
FIGURE 6-2

An asymptotic sketch of  $A(S)$  is shown in Figure 6-3. The crossover frequency is 2500 Hz and the phase margin is 30 degrees.

The transfer function relating motor current to Hall voltage and motor back emf is

$$I_m = \frac{G_a G_b G_c G_d V_h - G_d V_b}{1 + G_c G_d G_e + G_b G_c G_d G_f}$$

$$= \frac{66.0 V_h (1 + \frac{S}{2\pi 1625}) - 1.21 \times 10^{-3} V_b (1 + \frac{S}{2\pi 12.7})}{(1 + \frac{S}{2\pi 1369}) (1 + \frac{S}{2\pi 1483})}$$

Since the developed motor torque is proportional to the magnitude of the component of  $I_m$  in phase with  $V_h$  and  $V_b$  (i.e. the real part of  $I_m$ ), this last equation may be used for calculating torque roll off as a function of frequency at 250 Hz (which corresponds to 3000 rpm) the motor back emf equals 22.75 volts. With a Hall voltage of .0736V (corresponding to the maximum torque output of 50 oz/in)

$$R_e I_m = 4.690 \text{ amps}$$

At zero frequency, with  $V_h = .0736V$ ,

$$R_e I_m = 4.858 \text{ amps.}$$

Thus, the torque reduction due to frequency effects is 3.4% (-.3 dB) at 250 Hz, and the amplifier frequency response is adequate.

A(S)  
in dB

9-9

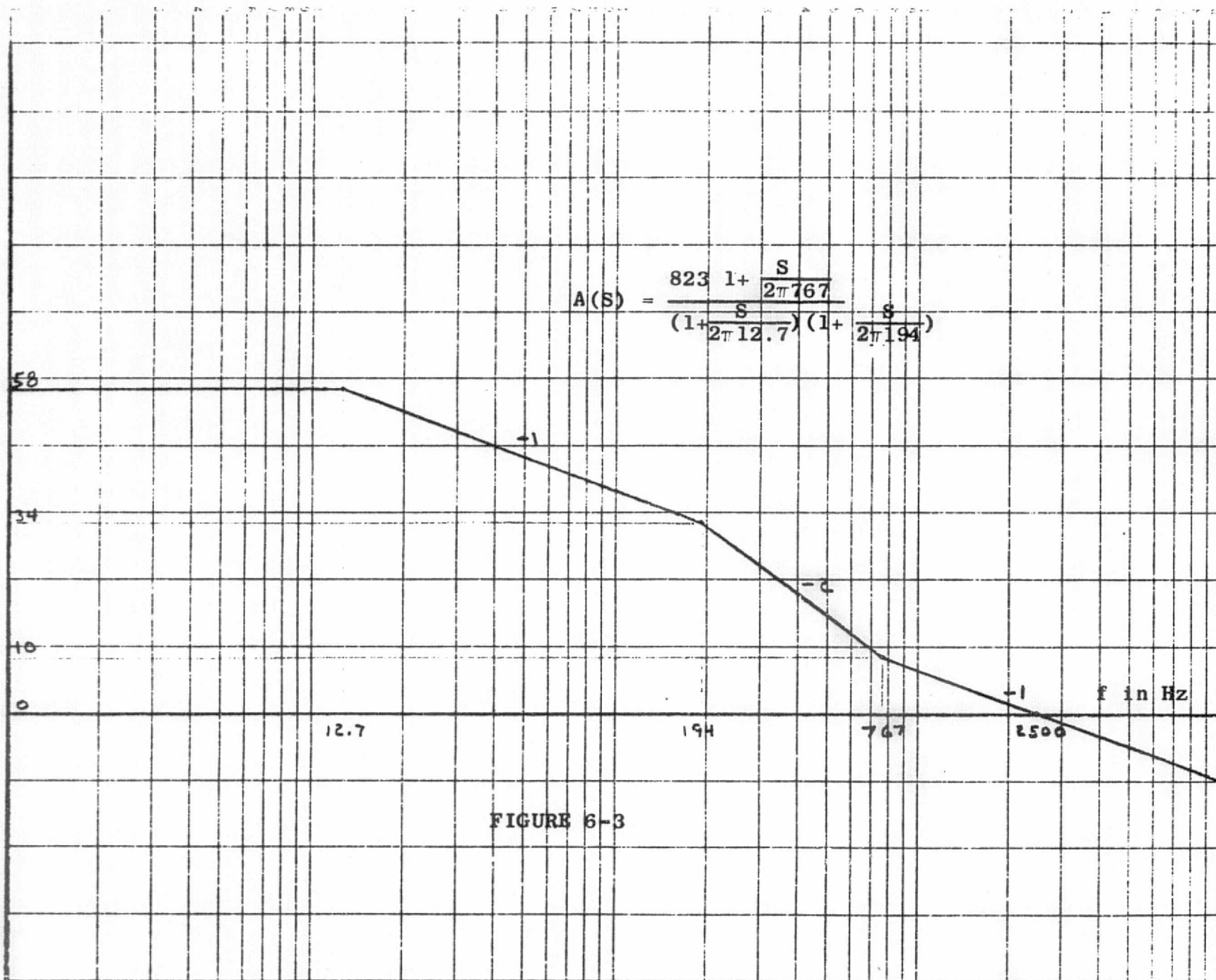


FIGURE 6-3

Up to this point it has been assumed that sufficient battery voltage is available to both overcome motor back emf and supply the current required to produce the commanded torque. The required battery voltage is given by the expression:

$$V_B = V_A + I_R + K_b W$$

where:

$V_B$  = required battery voltage

$V_A$  = constant voltage drop in drive amplifier = 2V max

$I$  = peak value of commanded drive current = 5.13 amp max

$R$  = motor resistance + drive amplifier resistance +  
Hall current sensor resistance = 1.0 ohm

$K_b$  = motor back emf coefficient = .00758 volts pk/rpm

$W$  = motor speed = 3000 rpm max

Thus, for the condition of maximum current (i.e. maximum torque) and maximum speed, the required battery voltage = 29.9V. For  $V_B = 28V$ , the maximum speed at which maximum torque can be achieved is 2750 rpm. For  $V_B = 24V$ , the maximum speed at which the maximum torque can be achieved is 2230 rpm.

If system requirements dictate that maximum torque be achievable at 3000 rpm, with the present motor design, a battery voltage of 30 volts must be provided. If this is not practical, the impedance of the motor can be lowered (by a winding change) permitting operation at higher current and lower operation.

## 7.0 TEST EQUIPMENT

The following equipment was used for testing the High Torque DC Motor and RWA.

<u>Description</u>	<u>Manufacturer</u>	<u>Model No.</u>	<u>Accuracy</u>
Torque Cell	Lebow	2105-100	0.1% Linearity
Torque Indicator	Lebow	7521	0.1%, 0-400 Hz
X-Y Plotter	Hewlett Packard	7046A	0.2%
Wattmeter	Industrial Test Eq.	5125	2%, 0 to 2 KHz
Current Probe	Tektronix	P6042	3%
Oscilloscope	Tektronix	545A	3%
Multimeter	Fluke	8375A	0.02% DC, 0.7% AC 0.01% Ohms
Preset Counter	Hewlett Packard	5330B	5 PPM
Digital Recorder	Hewlett Packard	5050B	Absolute
Power Supply	Power Designs	36250A	
Speed Control	Bendix		



## 8.0 TEST DATA

This section contains all of the performance test data taken during subsystem tests of the High Torque DC Motor in the 50 ft-lb-sec Reaction Wheel Assembly.

### 8.1 PERFORMANCE DATA

The performance data consists almost entirely of X-Y plotter curves with the exception of stable power measurements at constant speeds and digital torque transient data. All the curves consist of either torque vs speed, torque vs time, power vs speed or speed vs time (digital) data. A list of this data is found in Table 8-1 and the data itself follows Table 8-5.

The digital transient torque data consists of single wheel revolution times for every third wheel revolution. The revolution time period was converted to speed by

$$S_i = \frac{60}{P_i} \text{ (RPM)}$$

where  $P_i$  = Time period for  $i$ th revolution

The data points were converted to a time vs speed curve by the following

$$T_0 = 0$$

$$T_i = T_{i-1} + 3 P_i$$

$$S_0 = 60/P_0$$

$$S_i = 60/P_i - S_0$$

A least squares straight line was fitted to the points

indicated on the computer sheet and the torque computed from this is

$$TRQ = I K m \text{ (oz-in)}$$

where

$I = 30.24 = \text{Rotor Inertia in (oz-in-sec}^2\text{)}$

$m = \text{slope of least squares line in (RPM/sec)}$

$$K = \frac{2\pi}{60} \frac{(\text{RAD/SEC})}{\text{RPM}}$$

The sign of the torque in the result represents only accelerating or decelerating torque and is not in relation to reaction torque.

## 8.2 COMPUTER DATA ANALYSIS

A computer was employed for the purpose of determining the High Torque DC Motor characteristics from the data curves. Four of the curves were used in this analysis:

Figure 8-2 Reaction Torque vs Speed

Figure 8-10 Subsystem Power vs Speed

Figure 8-11 Motor Cos Phase Power vs Speed

Figure 8-12 Motor Sin Phase Power vs Speed

Vertical lines were drawn through the curves every 250 RPM and the values of intercepts with each curve coded for computer analysis.

The first data reduction consisted of fitting regression lines to the Reaction Torque vs Torque Command Voltage at each speed and each quadrant of operation (positive and negative torques and positive and negative wheel rotation). The motor torque was computed for each reaction torque with the equation:

$$T_M = T_R \pm T_D$$

where

$$T_D = \text{Drag Torque} = 0.0006S + 0.6$$

S = Speed in RPM

The required motor power was computed for each reaction torque from

$$P_R = \frac{T_M S}{1352} \text{ (watts)}$$

The resultant efficiencies for each point were computed from the following

$$E_M = 100 \frac{P_R}{(P_{SIN} + P_{COS})} \% = \text{Motor Eff.}$$

$$E_E = 100 \frac{(P_{SIN} + P_{COS})}{P_{TOTAL}} \% = \text{Elec. Eff.}$$

$$E_H = 100 \frac{(P_{SIN} + P_{COS})}{(P_{TOTAL} - P_Q)} \% = \text{H-Bridge Eff.}$$

$$E_S = 100 \frac{P_R}{P_{TOTAL}} \% = \text{Subsystem Eff.}$$

where

$P_{SIN}$  = Sin Motor Phase Power

$P_{COS}$  = Cos Motor Phase Power

$P_{TOTAL}$  = Subsystem Power

$P_Q$  = Quiescent Power = 8.5 watts

The efficiency data was then summarized in Tables 8-2 and 8-3. The data computed from the regression lines of Reaction Torque vs Torque Command Voltage at constant speed

was summarized in Table 8-4. In addition, a regression line was fitted to the intercepts of these regression lines. Also, an average and standard deviation were taken of the slopes.

The total motor power was summarized in Table 8-5. Regression lines were fitted to the Power vs Speed data points for each Torque Command Voltage and both positive and negative torques. The slopes of the regression lines vs torque command voltage were fitted to a least squares straight line through the origin. The intercepts of the straight lines vs torque command voltage squared were also fitted to a least squares straight line through the origin.

The computer printout containing the original data follows the analog data after Figure 8-42.

PERFORMANCE DATA

<u>FIGURE</u>	<u>TITLE</u>
8-1	STABLE POWERS
8-2	REACTION TORQUE VS SPEED
8-3	CW DRAG TORQUE
8-4	CCW DRAG TORQUE
8-5	CW LOW SPEED DRAG TORQUE
8-6	CCW LOW SPEED DRAG TORQUE
8-7	ZERO CROSSING TORQUE
8-8	CW AC MOTOR DRAG TORQUE
8-9	CCW AC MOTOR DRAG TORQUE
8-10	SUBSYSTEM POWER VS SPEED
8-11	COS MOTOR POWER VS SPEED
8-12	SIN MOTOR POWER VS SPEED
8-13	SUBSYSTEM POWER FOR 24 AND 32 VDC BUSS
8-14	COS MOTOR POWER FOR 24 AND 32 VDC BUSS
8-15	SIN MOTOR POWER FOR 24 AND 32 VDC BUSS
8-16 to 8-19	CW TORQUE TRANSIENTS FOR 0.5, 1.0, 2.5 AND 5.0 VOLT TORQUE COMMANDS
8-20 to 8-23	CCW TORQUE TRANSIENTS FOR 0.5, 1.0, 2.5 AND 5.0 VOLT TORQUE COMMANDS
8-24 to 8-27	ZERO SPEED TORQUE TRANSIENTS FOR 0.5, 1.0, 2.5 AND 5.0 VOLT TORQUE COMMANDS
8-28 to 8-35	CW DIGITAL TORQUE TRANSIENTS FOR 0.5, 1.0, 2.5 AND 5.0 VOLT TORQUE COMMANDS
8-36 to 8-42	CCW DIGITAL TORQUE TRANSIENTS FOR 0.5, 1.0, 2.5 AND 5.0 VOLT TORQUE COMMANDS

TABLE 8-1

# HIGH TORQUE DC MOTOR EFFICIENCY

SPEED 0. 250. 500. 750. 1000. 1250. 1500. 1750. 2000. 2250. 2500.

TC

## MOTOR

1	0.00	47.88	56.61	64.61	76.18	82.08	83.25	85.67	85.64	86.72	87.29
2	0.00	39.76	54.43	64.93	71.65	75.79	78.87	81.23	83.57	83.27	85.34
3	0.00	32.73	48.03	58.31	65.20	69.83	72.23	75.40	77.24	80.17	81.10
4	0.00	27.28	41.84	51.88	58.58	64.03	67.87	70.71	73.39	75.86	78.13
5	0.00	25.14	39.22	49.15	55.20	61.87	65.95	68.91	71.11	70.65	76.15

## ELECTRONICS

1	22.91	32.14	39.43	45.97	44.31	46.87	50.95	54.46	56.66	57.81	59.69
2	28.75	38.54	48.24	52.27	55.99	58.22	61.81	63.71	64.85	68.20	68.88
3	38.39	48.57	55.07	58.12	60.87	63.39	65.30	66.66	68.90	69.14	70.93
4	44.38	52.20	56.55	58.33	60.52	62.08	63.46	65.34	67.39	68.70	69.99
5	46.49	52.45	57.00	58.17	62.08	60.64	62.24	63.64	65.47	69.99	67.97

## H BRIDGE

1	78.57	81.81	81.56	85.21	72.22	72.58	75.71	78.20	79.06	78.72	79.99
2	50.00	59.67	68.76	70.40	72.40	72.77	75.64	76.45	76.58	79.68	79.54
3	55.12	63.53	68.26	69.50	71.03	72.62	73.67	74.35	76.14	75.83	77.35
4	54.86	61.55	64.57	65.19	66.86	67.66	68.55	70.11	71.93	73.02	74.17
5	54.63	59.59	63.30	63.52	67.04	64.91	66.18	67.31	68.91	73.50	71.21

## SUPSYSTEM

1	0.00	13.14	22.37	29.75	33.78	38.52	42.45	46.69	48.57	50.18	52.12
2	0.00	15.33	26.26	33.95	40.12	44.14	48.77	51.75	54.22	56.80	58.79
3	0.00	15.89	26.45	33.89	39.69	44.27	47.17	50.27	53.19	55.42	57.52
4	0.00	14.24	23.66	30.26	35.45	39.75	43.03	46.20	49.46	52.11	54.67
5	0.00	13.19	22.35	28.59	34.21	37.52	41.05	43.86	46.52	49.36	51.76

TABLE 8-2

# HIGH TORQUE DC MOTOR EFFICIENCY

		SPEED	0.	250.	500.	750.	1000.	1250.	1500.	1750.	2000.	2250.	2500.
TC		MOTOR											
1	CC ACC	0.00	38.42	52.34	61.02	73.96	77.74	80.22	82.40	83.37	83.67	84.39	
2	CC ACC	0.00	36.34	52.97	63.46	70.71	74.54	77.26	80.74	81.99	82.14	84.40	
3	CC ACC	0.00	33.22	47.91	58.29	65.48	69.91	72.35	75.94	78.63	80.43	81.52	
4	CC ACC	0.00	27.50	41.77	51.71	58.75	64.03	68.17	70.61	73.44	76.67	79.16	
5	CC ACC	0.00	25.24	39.34	49.23	58.05	61.37	66.17	68.78	71.03	67.69	76.21	
1	CA ACC	0.00	43.35	60.87	68.19	78.40	86.42	86.29	88.93	87.91	89.77	90.20	
2	CA ACC	0.00	40.16	56.00	66.40	72.58	77.04	80.48	81.71	85.15	84.41	86.29	
3	CA ACC	0.00	32.73	48.14	58.33	64.93	69.75	72.11	75.76	75.85	79.90	80.68	
4	CA ACC	0.00	27.06	41.91	52.05	58.41	64.03	67.57	70.91	73.34	75.04	77.10	
5	CA ACC	0.00	25.04	39.10	49.06	52.35	62.37	65.72	69.05	71.18	73.61	76.09	
		ELECTRONICS											
1	CC ACC	20.83	32.14	38.23	44.73	43.13	45.83	50.00	53.57	55.00	56.25	59.09	
2	CC ACC	27.50	37.50	48.21	51.51	55.40	57.14	60.86	63.00	63.63	67.24	68.54	
3	CC ACC	37.50	47.14	53.48	57.00	59.64	62.50	64.78	66.66	67.05	68.47	69.89	
4	CC ACC	44.44	50.90	56.06	58.44	60.22	62.24	63.30	65.54	67.18	67.88	69.09	
5	CC ACC	45.61	52.17	56.62	58.24	60.00	61.29	62.40	64.09	65.43	72.96	68.23	
1	CA ACC	25.00	32.14	40.62	47.22	45.45	47.91	51.92	55.35	58.33	59.37	60.29	
2	CA ACC	30.00	38.58	48.27	53.03	56.57	59.30	62.76	64.42	66.07	69.16	69.23	
3	CA ACC	39.28	50.00	56.66	59.25	62.09	64.28	65.82	66.66	70.74	69.80	71.96	
4	CA ACC	44.31	53.50	57.04	58.23	60.82	61.92	63.63	65.15	67.60	69.52	70.88	
5	CA ACC	47.36	52.73	57.38	58.09	64.16	60.00	62.08	63.19	65.42	67.02	67.70	
		H BRIDGE											
1	CC ACC	71.42	81.81	76.47	80.95	70.37	70.96	74.28	76.92	76.74	76.59	79.59	
2	CC ACC	47.82	59.06	69.23	69.33	71.92	71.64	74.66	75.90	75.26	78.78	79.43	
3	CC ACC	53.84	62.26	66.66	68.67	70.10	72.07	73.60	74.32	74.50	75.44	76.53	
4	CC ACC	54.79	60.71	64.34	65.69	66.56	68.15	68.65	70.58	71.96	72.37	73.43	
5	CC ACC	53.60	59.50	63.09	63.84	65.02	65.80	66.53	67.97	69.05	70.75	71.59	
1	CA ACC	85.71	81.81	86.66	89.47	74.07	74.19	77.14	79.48	81.39	80.85	80.39	
2	CA ACC	52.17	61.29	68.29	71.42	72.88	73.91	76.62	77.01	77.89	80.58	79.64	
3	CA ACC	56.41	64.71	69.86	70.32	71.96	73.17	73.75	73.88	77.77	76.21	78.17	
4	CA ACC	54.92	62.36	64.80	64.70	66.56	67.18	68.44	69.63	71.91	73.68	74.91	
5	CA ACC	55.67	59.68	63.52	63.21	69.05	64.03	65.83	66.66	68.76	70.25	70.84	
		SUBSYSTEM											
1	CC ACC	0.00	12.34	20.01	27.29	31.94	35.63	40.11	44.14	45.85	47.06	49.87	
2	CC ACC	0.00	14.75	25.49	32.69	36.18	42.59	47.03	50.86	52.17	55.23	57.85	
3	CC ACC	0.00	15.66	25.62	33.22	39.05	43.69	46.87	50.03	52.73	55.08	56.98	
4	CC ACC	0.00	14.00	23.42	30.22	35.34	39.85	43.15	46.24	49.34	52.05	54.70	
5	CC ACC	0.00	13.17	22.27	28.68	34.33	37.61	41.30	44.08	46.47	49.39	51.99	
1	CA ACC	0.00	13.93	24.73	32.20	35.93	41.41	44.80	49.23	51.28	53.30	54.38	
2	CA ACC	0.00	15.91	27.03	35.21	41.06	45.69	50.51	52.64	56.26	58.38	59.74	
3	CA ACC	0.00	16.11	27.28	34.56	40.32	44.84	47.46	50.51	53.66	55.77	58.06	
4	CA ACC	0.00	14.78	23.90	30.31	35.53	39.65	43.00	46.13	49.58	52.18	54.05	
5	CA ACC	0.00	13.20	22.44	28.50	33.59	37.42	40.80	43.63	46.57	49.34	51.52	

TABLE 8-3



## HIGH TORQUE DC MOTOR

CC ACC			CW DEC		
SPEED	BIAS	S.F.	SPEED	BIAS	S.F.
0.	-1.19	9.95	0.	-0.17	10.13
250.	-1.50	10.21	250.	0.48	10.39
500.	-2.11	10.41	500.	0.98	10.45
750.	-2.11	10.41	750.	1.22	10.39
1000.	-2.71	10.71	1000.	1.22	10.39
1250.	-2.63	10.53	1250.	1.34	10.33
1500.	-2.85	10.60	1500.	0.95	10.36
1750.	-2.70	10.52	1750.	2.06	10.01
2000.	-3.23	10.65	2000.	2.27	9.97
2250.	-3.70	10.76	2250.	2.73	9.86
2500.	-3.86	10.72	2500.	2.97	9.78
INTERCEPT	-1.40	AVG 10.499	INTERCEPT	0.10	AVG 10.187
SLOPE	-0.000963	SD 0.233	SLOPE	0.001090	SD 0.233
CORR	-0.970		CORR	0.944	

CC ACC			CC DEC		
SPEED	BIAS	S.F.	SPEED	BIAS	S.F.
0.	0.65	-10.45	0.	-0.21	-10.68
250.	0.86	-10.72	250.	-1.09	-11.04
500.	1.05	-11.01	500.	-1.32	-11.21
750.	1.71	-11.25	750.	-1.68	-11.19
1000.	1.87	-11.33	1000.	-2.04	-11.07
1250.	1.87	-11.33	1250.	-1.88	-11.07
1500.	2.25	-11.41	1500.	-1.82	-11.07
1750.	2.45	-11.45	1750.	-2.22	-10.91
2000.	2.81	-11.57	2000.	-2.17	-10.88
2250.	3.13	-11.55	2250.	-2.84	-10.69
2500.	2.95	-11.27	2500.	-2.96	-10.59
INTERCEPT	0.70	AVG -11.212	INTERCEPT	-0.74	AVG -10.945
SLOPE	0.001008	SD 0.334	SLOPE	-0.000884	SD 0.202
CORR	0.983		CORR	-0.935	

## HIGH TORQUE DC MOTOR

## QUAD 1 CC ACC

	SPEED	0.	250.	500.	750.	1000.	1250.	1500.	1750.	2000.	2250.	2500.
TC												
1		2.5	4.5	6.5	8.5	9.5	11.0	13.0	15.0	16.5	18.0	19.5
2		2.5	1.0	-2.0	-4.0	-6.0	-8.5	-10.5	-11.5	-13.0	-15.0	-17.0
3		3.0	4.5	6.5	8.5	10.0	11.5	13.5	15.5	17.5	19.0	20.5
4		3.0	1.0	-2.0	-4.0	-6.0	-9.0	-11.0	-12.0	-13.5	-15.5	-17.5
5		5.5	9.0	13.5	17.0	20.5	24.0	28.0	31.5	35.0	39.0	42.5

## QUAD 2 CM DEC

	SPEED	0.	250.	500.	750.	1000.	1250.	1500.	1750.	2000.	2250.	2500.
TC												
1		5.5	9.0	13.5	17.0	20.5	24.0	28.0	31.5	35.0	39.0	42.5
2		5.5	1.0	-2.0	-5.5	-10.0	-14.5	-18.0	-21.5	-25.0	-29.5	-33.0
3		6.0	9.5	14.0	17.5	21.5	25.5	29.5	33.5	37.0	41.5	45.0
4		6.0	1.0	-1.5	-7.0	-11.0	-15.0	-18.5	-22.0	-26.0	-30.0	-34.0
5		10.5	16.5	23.0	28.5	34.0	40.0	46.0	52.0	57.0	63.0	68.5

## QUAD 3 CM ACC

	SPEED	0.	250.	500.	750.	1000.	1250.	1500.	1750.	2000.	2250.	2500.
TC												
1		10.5	16.5	23.0	28.5	34.0	40.0	46.0	52.0	57.0	63.0	68.5
2		10.5	5.0	-1.5	-7.5	-13.0	-19.0	-24.5	-30.0	-36.5	-41.5	-47.0
3		11.0	18.5	25.5	32.0	38.5	45.0	52.0	58.0	66.5	70.5	77.0
4		11.0	5.0	-1.0	-7.0	-13.0	-20.0	-26.5	-32.0	-38.0	-43.5	-49.5
5		20.0	28.0	37.0	45.0	53.0	61.0	69.0	78.0	86.0	93.0	99.5

## QUAD 4 CC DEC

	SPEED	0.	250.	500.	750.	1000.	1250.	1500.	1750.	2000.	2250.	2500.
TC												
1		20.0	28.0	37.0	45.0	53.0	61.0	69.0	78.0	86.0	93.0	99.5
2		20.0	11.5	2.5	-6.0	-14.5	-22.0	-29.5	-37.0	-45.0	-53.0	-60.0
3		19.5	30.5	40.5	49.5	59.0	67.5	77.0	86.0	96.0	105.0	112.0
4		19.5	12.5	4.0	-5.0	-13.5	-22.5	-31.0	-39.5	-48.0	-55.5	-64.0
5		26.0	36.0	47.0	56.5	66.0	76.0	85.5	95.5	106.0	125.5	123.5

## QUAD 1+2

## QUAD 3+4

TC	SLOPE	BIAS	SLOPE	BIAS
1	7.49	1.14	7.77	2.02
2	15.19	5.06	15.89	5.56
3	23.36	10.61	25.67	12.72
4	32.60	19.84	35.72	22.70
5	39.51	27.22	41.46	29.56

TORQUE CONSTANT

7.92

8.48 WATTS/VOLT/KRPM

10.71

11.47 OZ\*IN/VOLT

I SQUARED R CONSTANT

1.14

1.26 WATTS/VOLT SQRD

TABLE 8-5

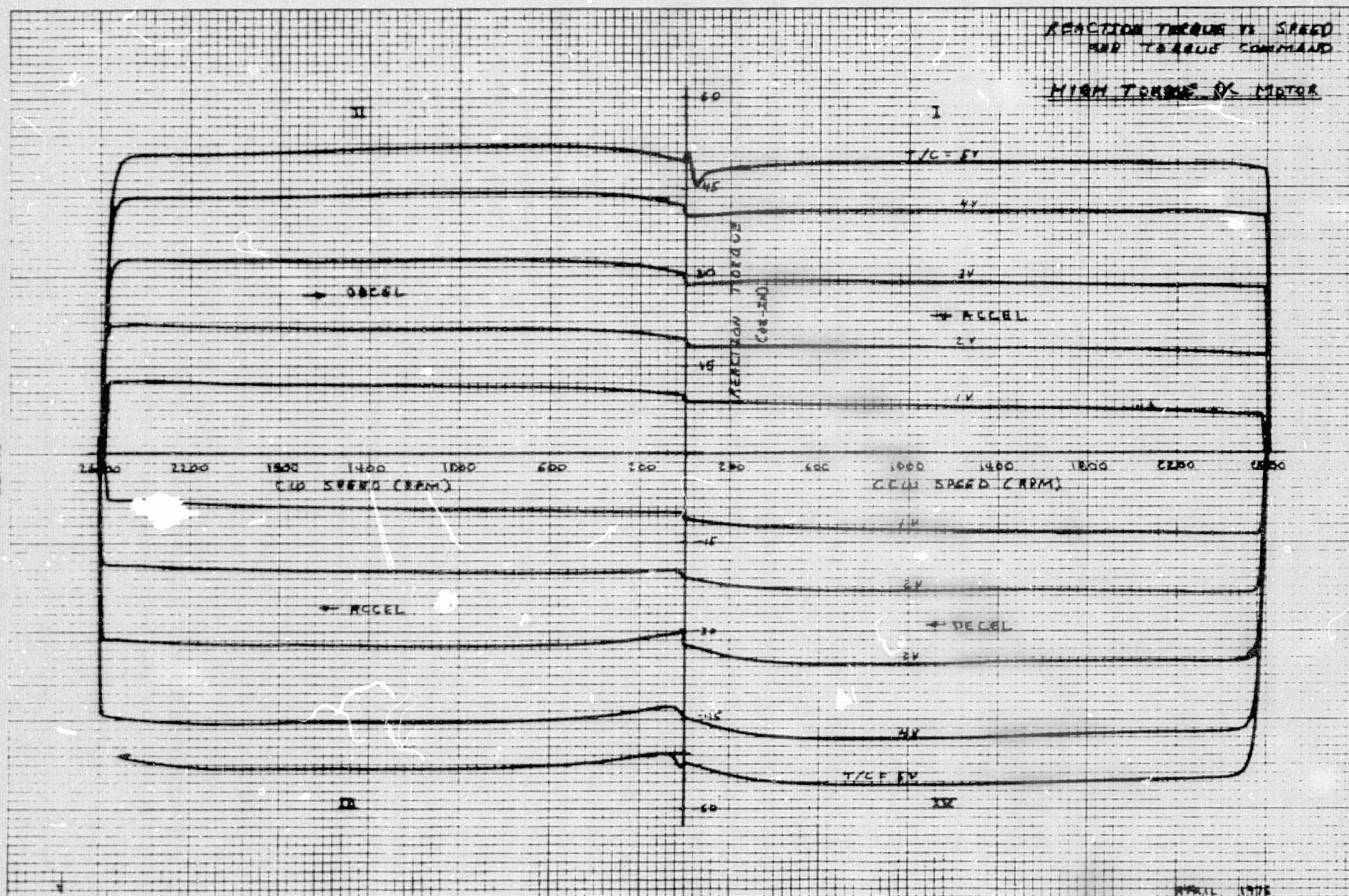
# HIGH TORQUE DC MOTOR STEADY STATE POWER

SUPPLY BUSS	24V	28V	32V	SPEED (RPM)
SYSTEM POWER	6.0	8.5	10.8	0
MOTOR OPEN	5.8	7.4	9.4	0
MOTOR POWER	0.3	0.6	0.9	0
SIN	0.1	0.2	0.3	0
COS	0.2	0.4	0.6	0
SYSTEM POWER	11.6	13.7	15.4	3000 CW
MOTOR POWER	6.5	6.5	6.8	"
SIN	3.1	3.1	3.2	"
COS	3.4	3.4	3.6	"
SYSTEM POWER	11.4	13.2	15.1	3000 CCW
MOTOR POWER	5.3	5.4	5.5	"
SIN	2.4	2.4	2.4	"
COS	2.9	3.0	3.1	"

POWER IN WATTS

FIGURE 8-1

FIGURE 8-2



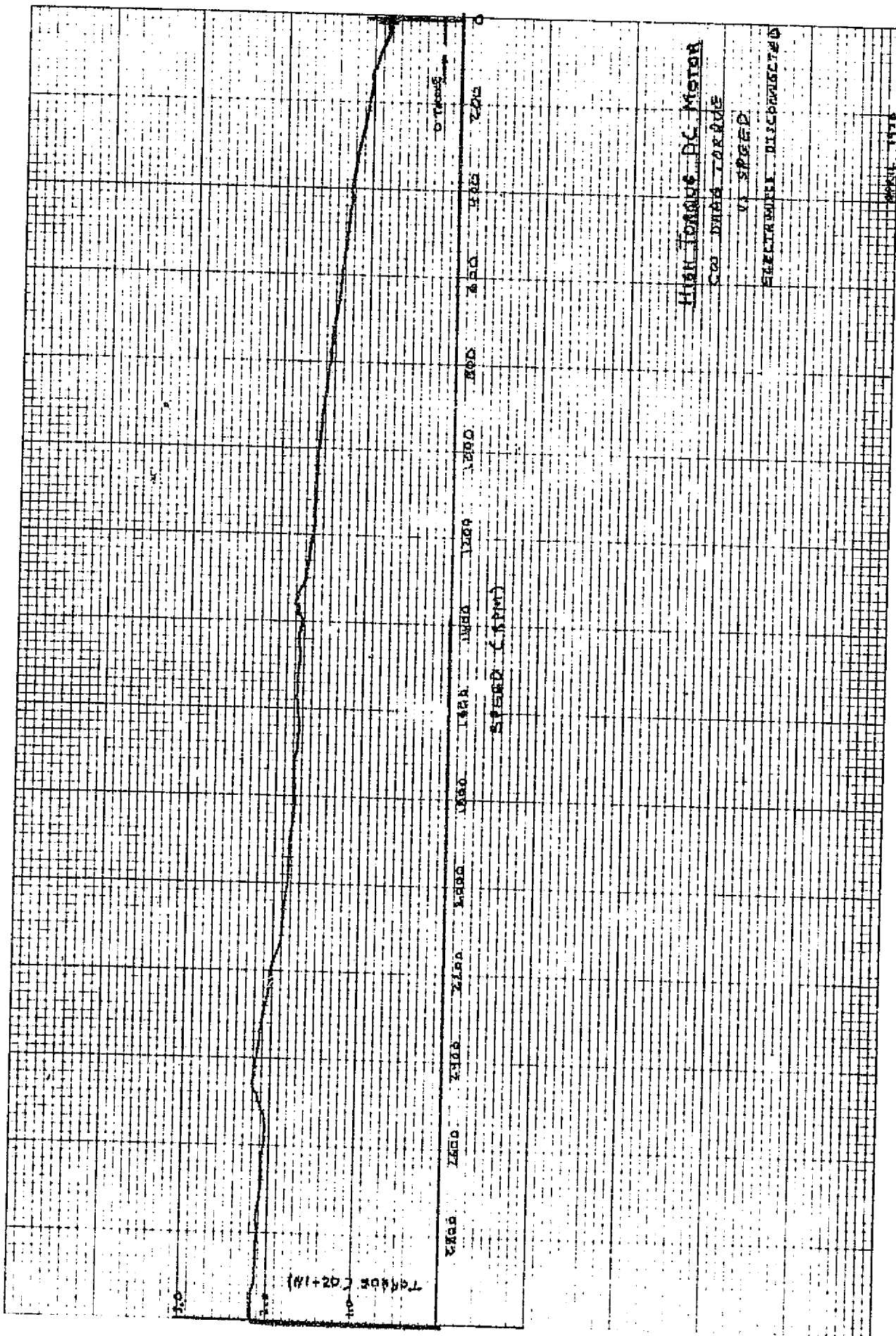


FIGURE 8-3  
8-12

47 0107

REPRODUCIBILITY OF THE  
ORIGINAL PAGE IS POOR



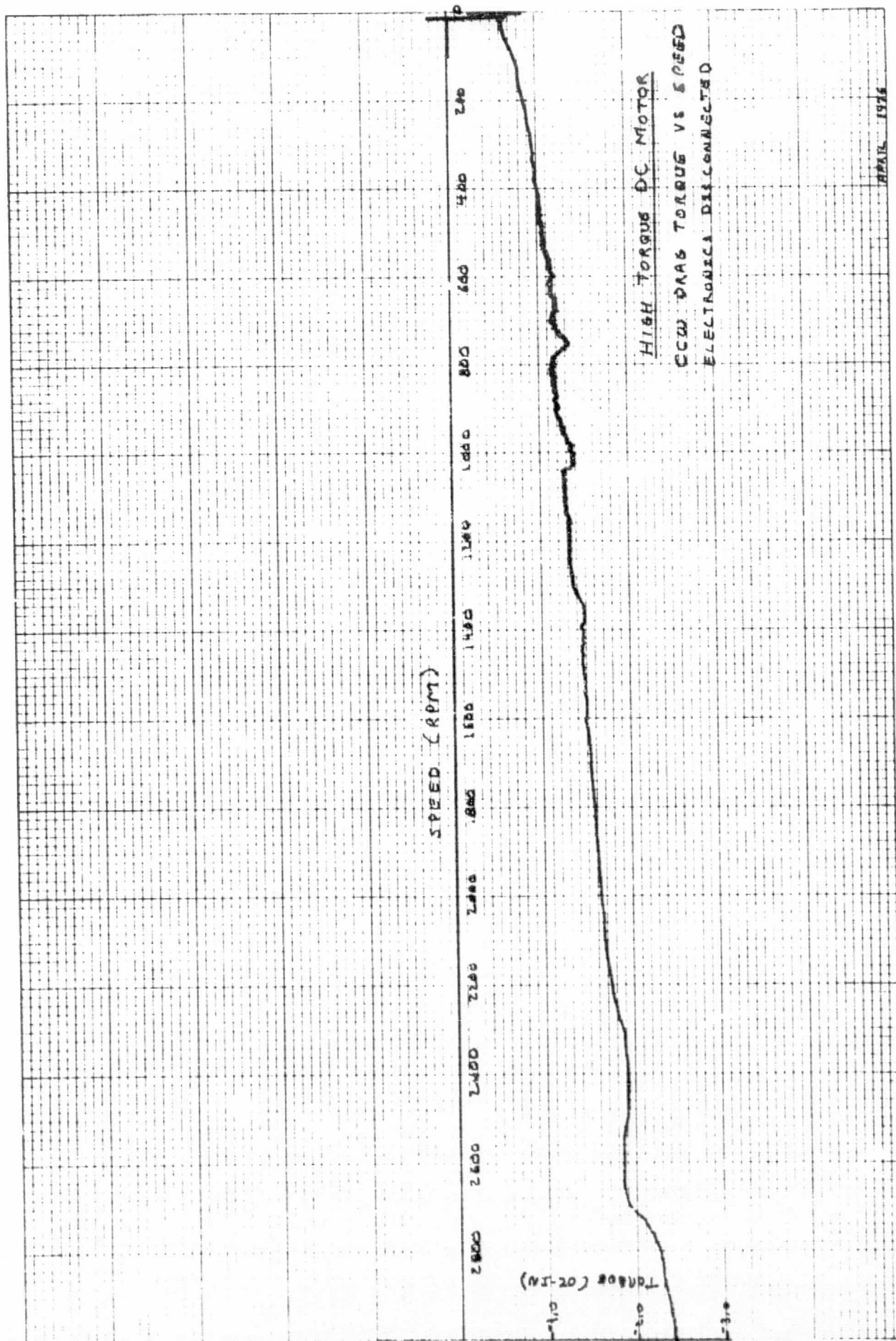


FIGURE B-4

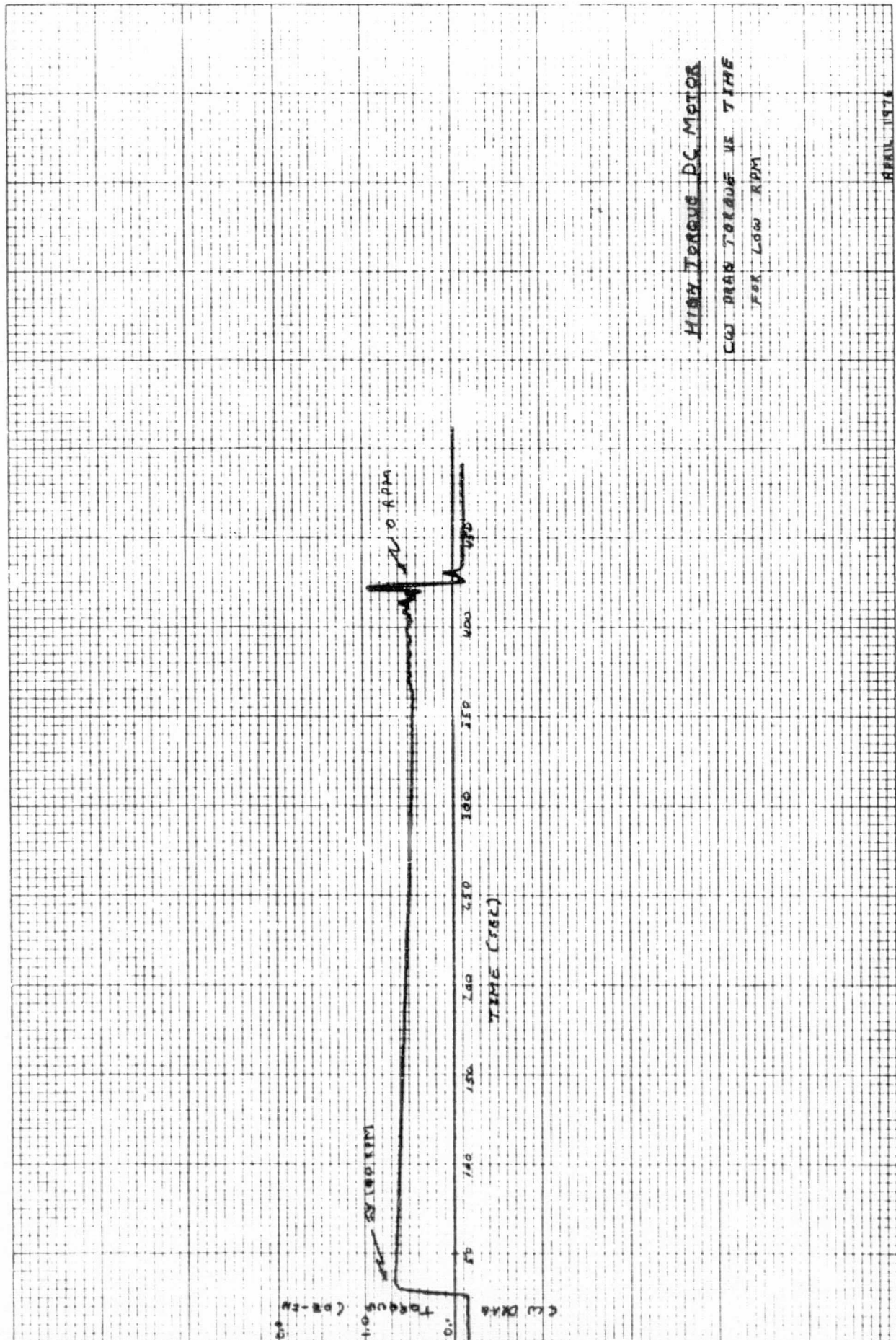


FIGURE 8-5  
8-14

HIGH TORQUE DC MOTOR

CW DRAW TORQUE VS TIME  
FOR LOW RPM

APRIL 1976

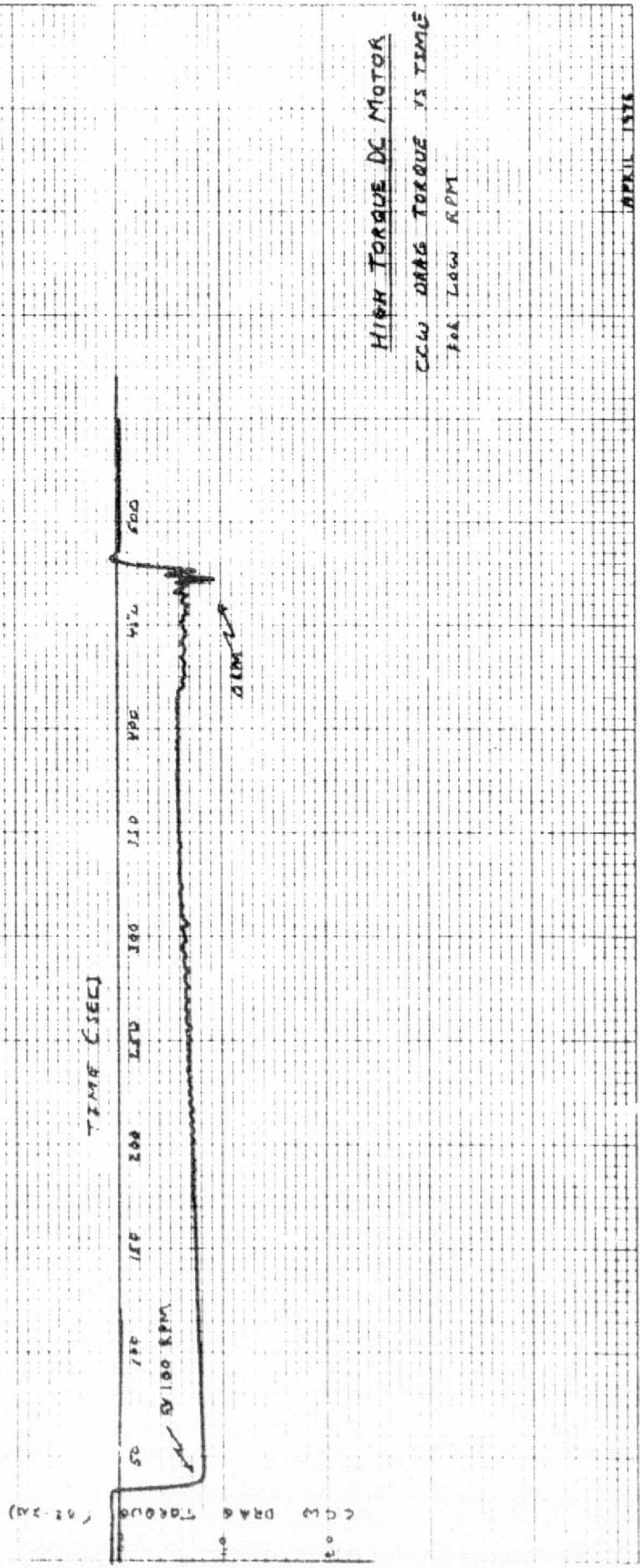
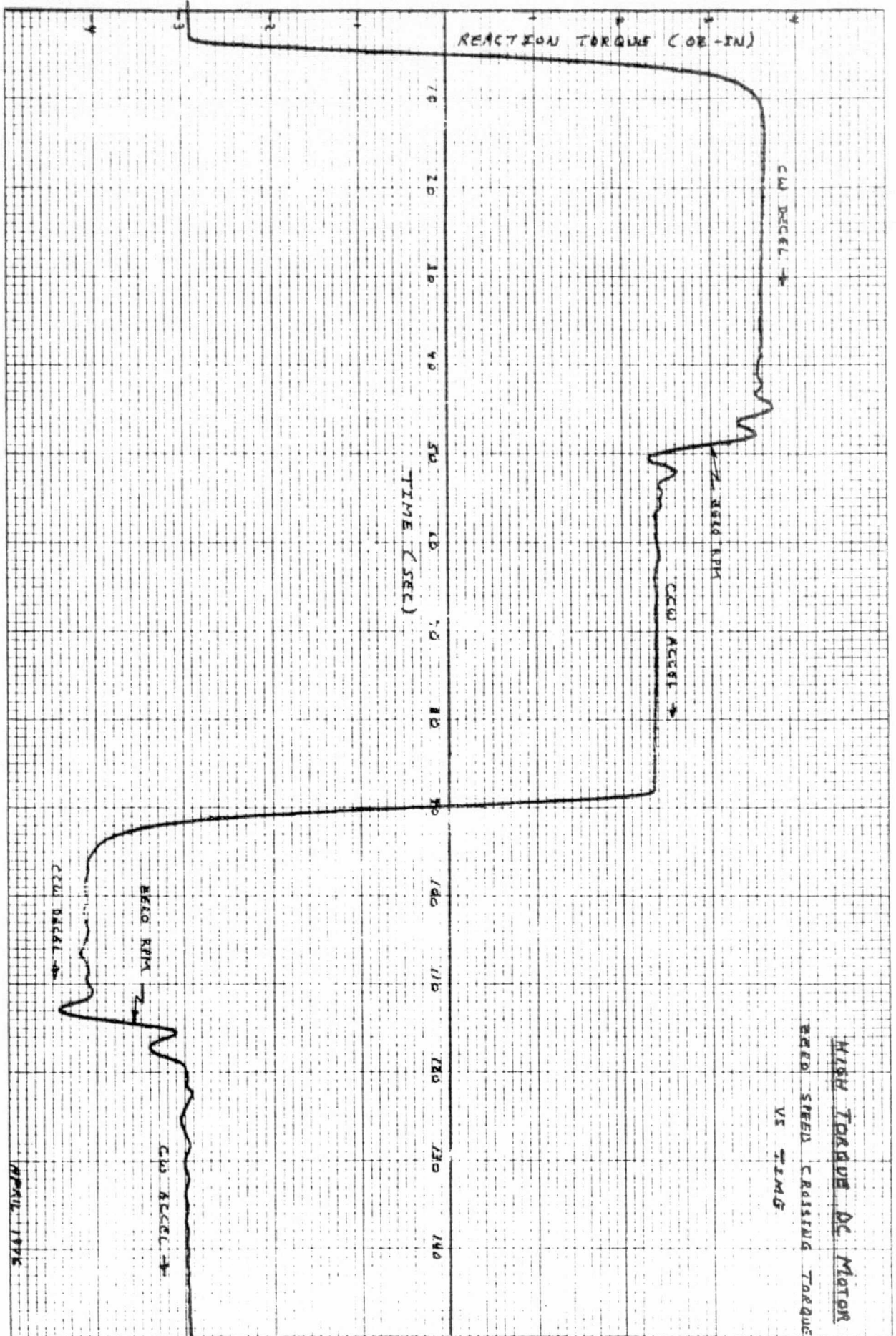


FIGURE 8-6





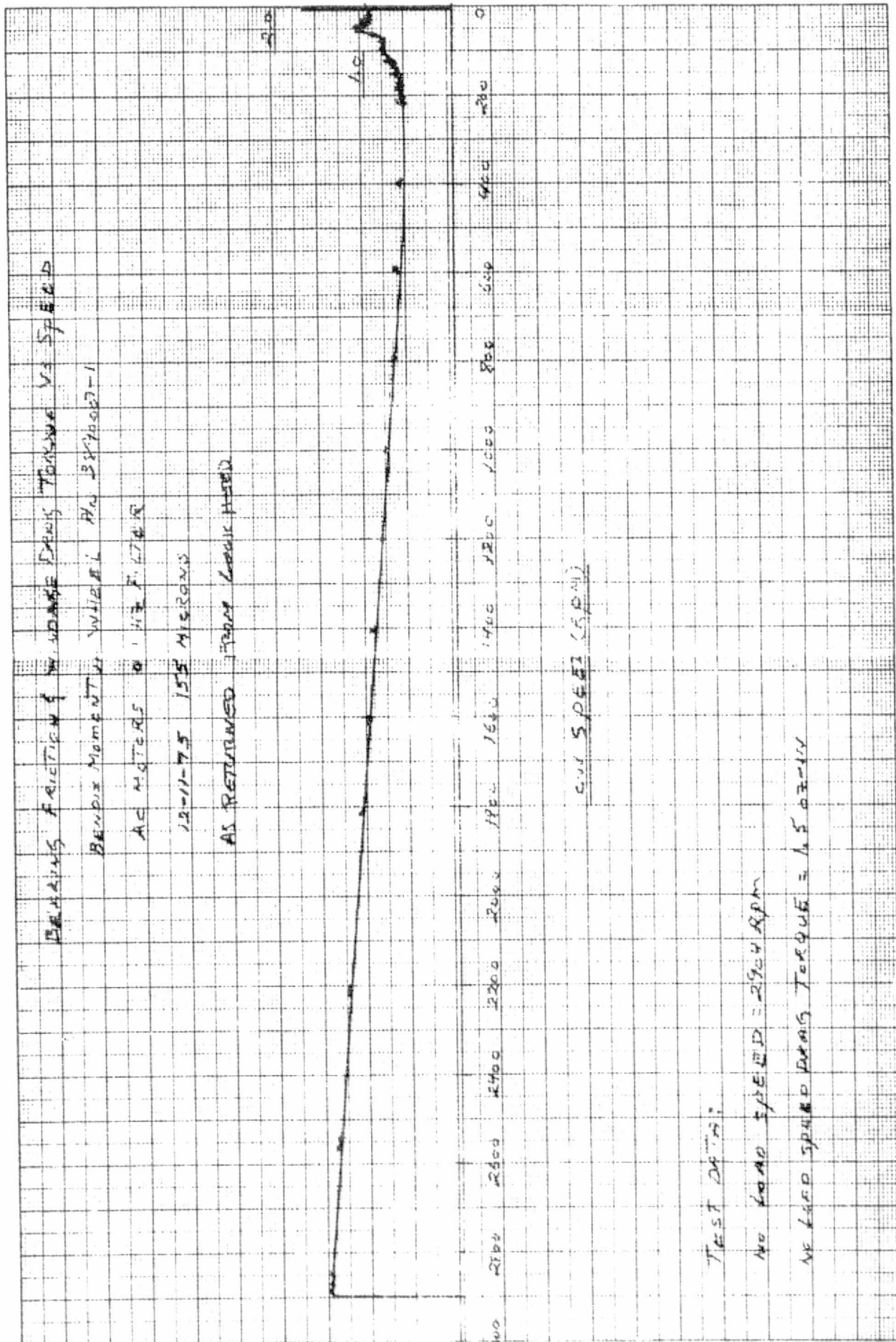
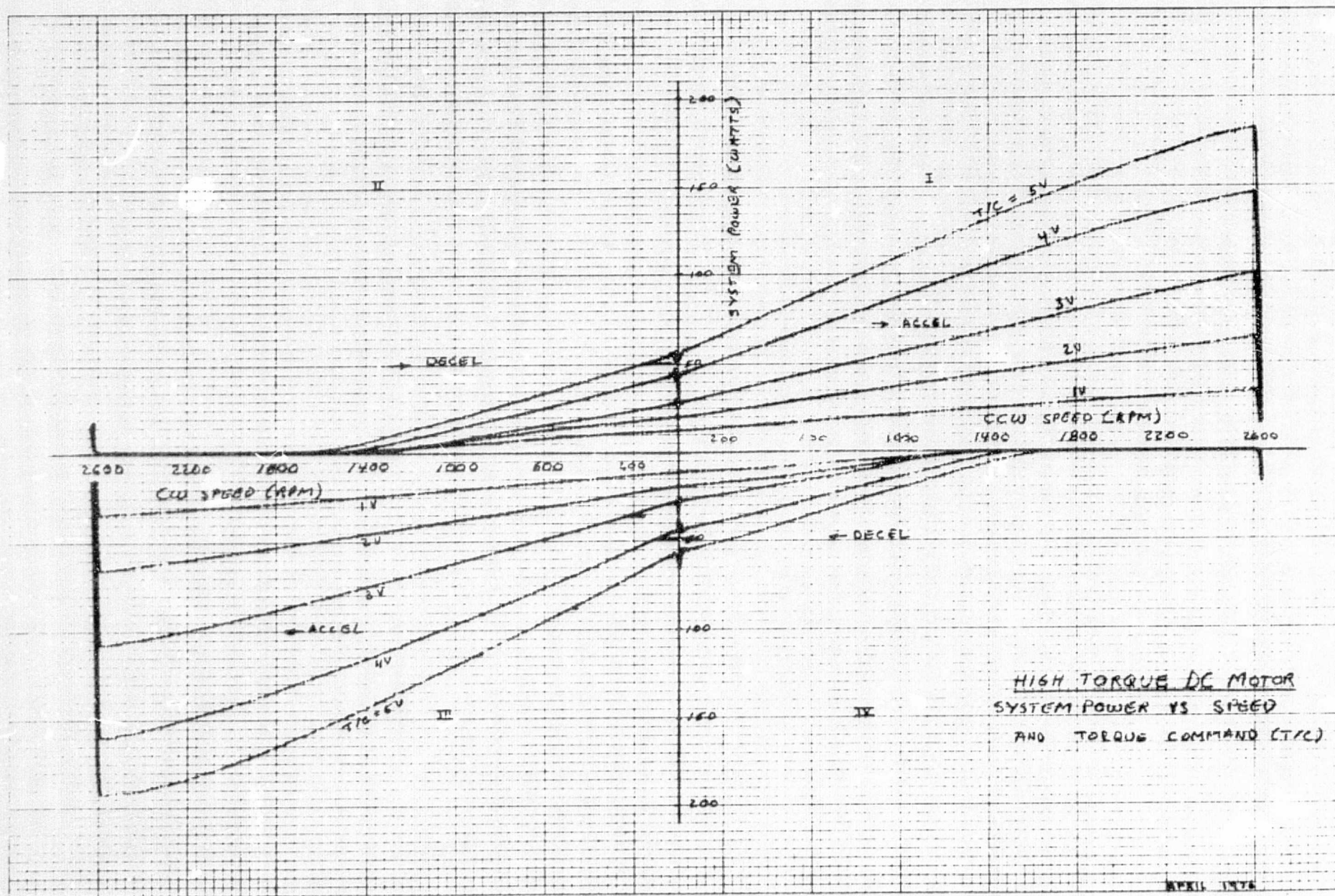


FIGURE 8-8



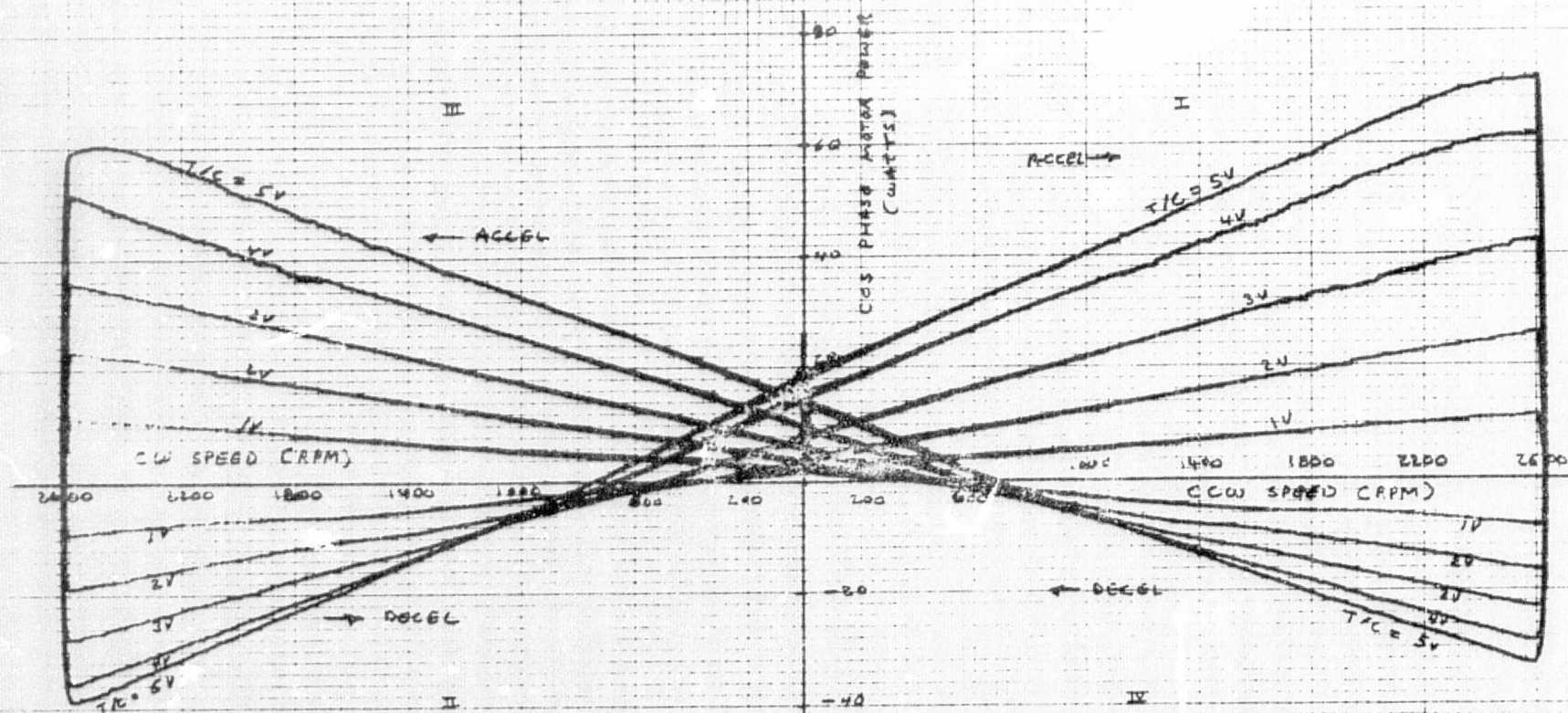


FIGURE 8-10  
8-19

APRIL 1974

FIGURE 8-11

N 210

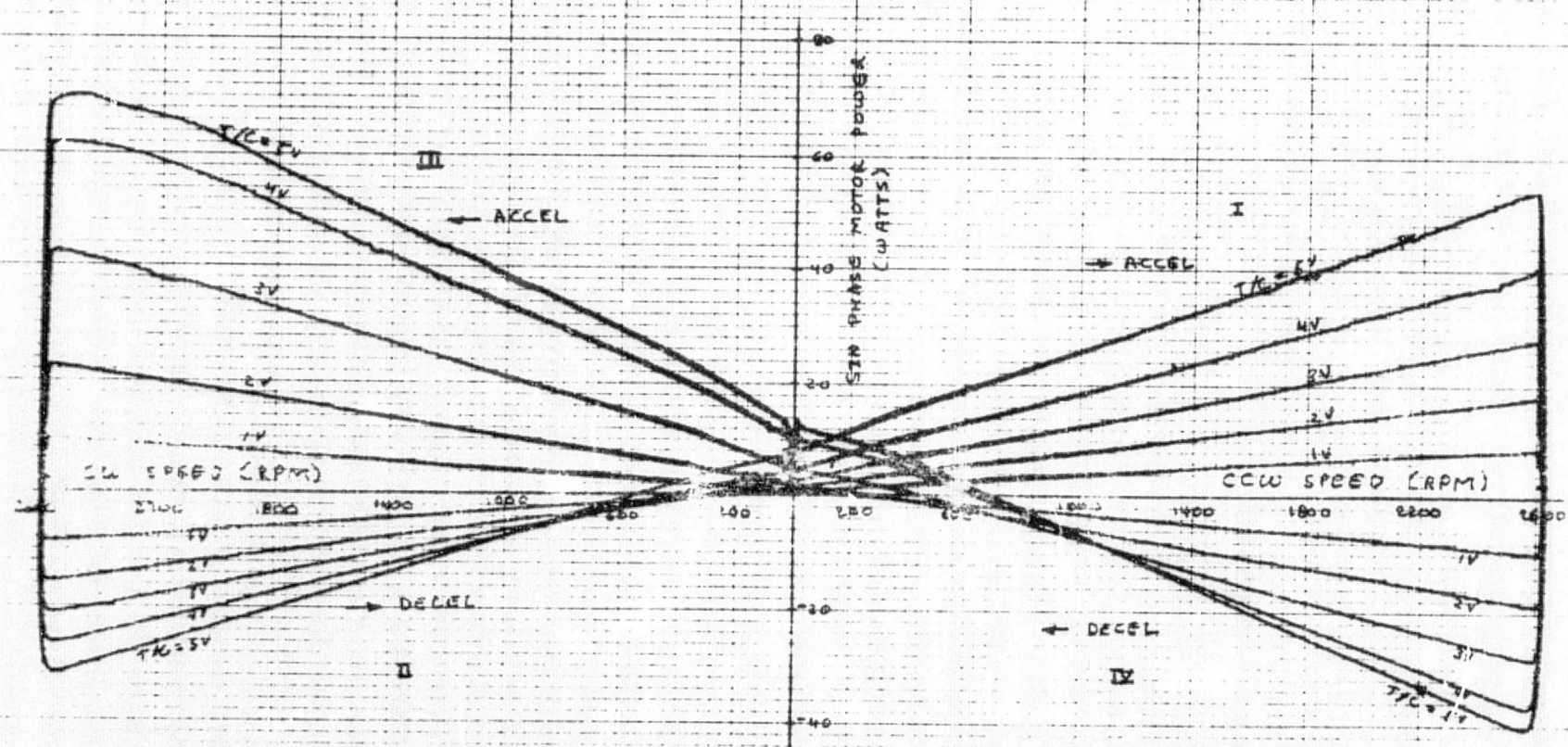


HIGH TORQUE DC MOTOR  
COS PHASE MOTOR POWER  
VS SPEED AND TORQUE COMMAND

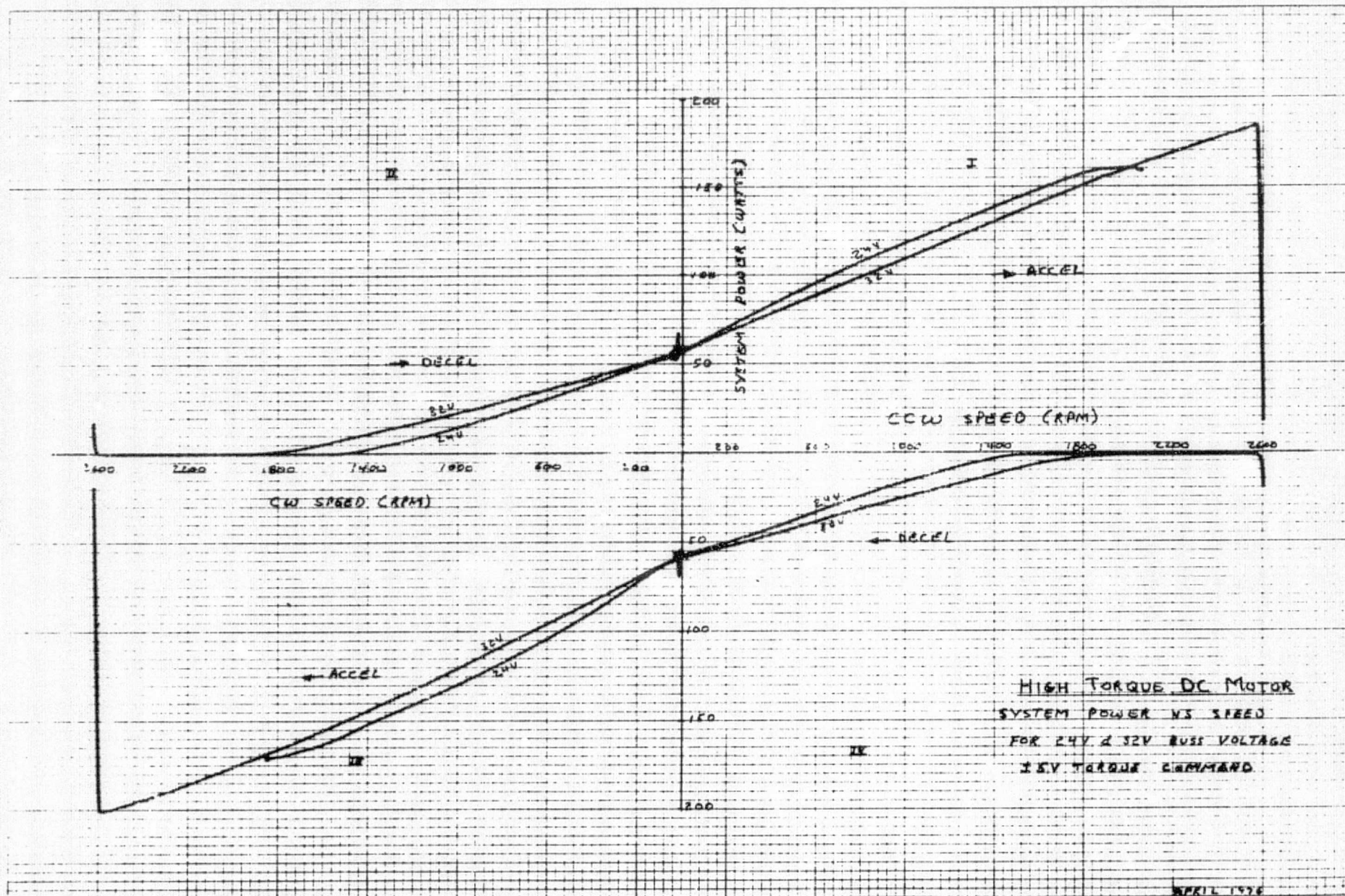
APRIL 1976



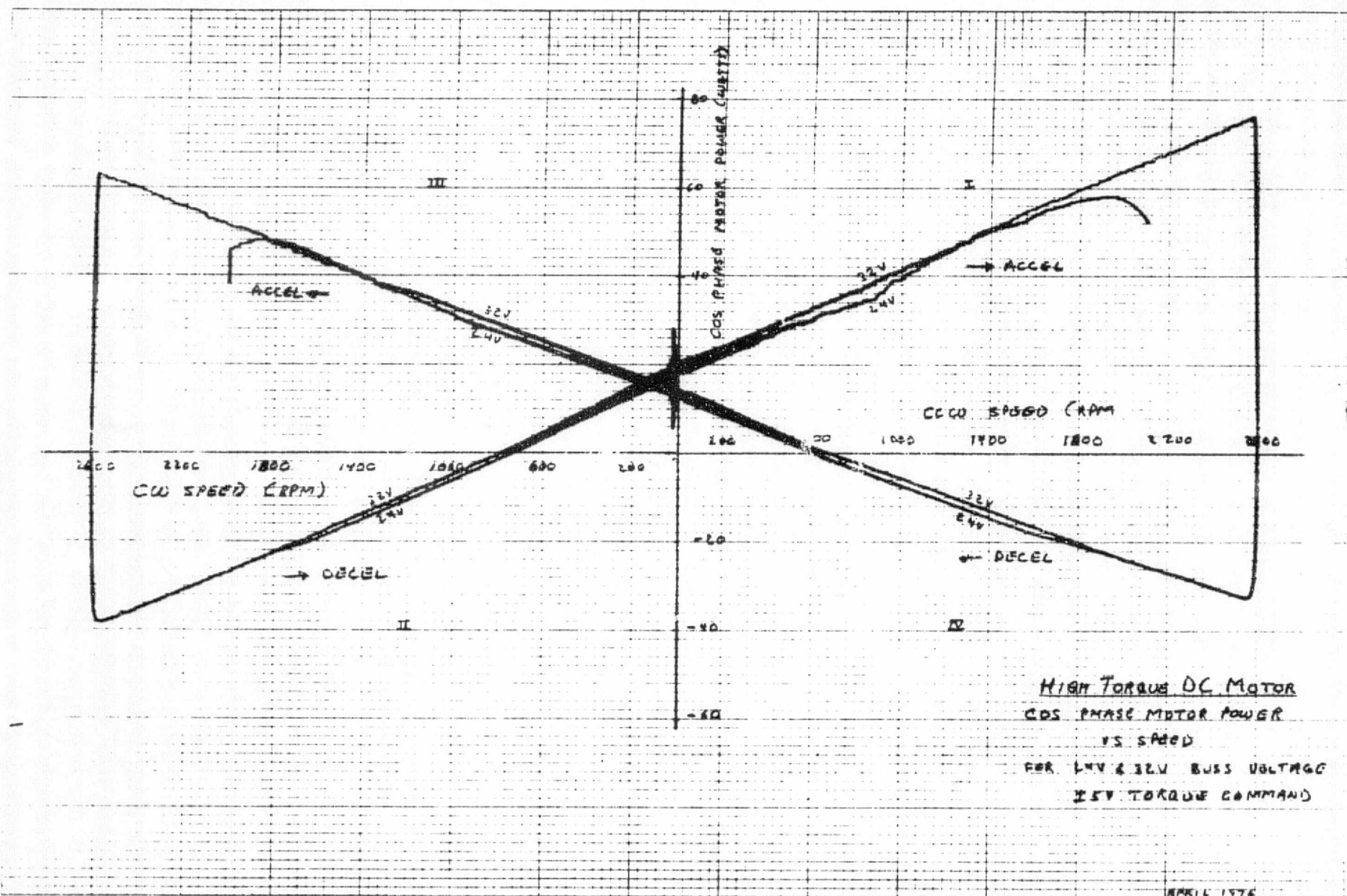
C-2



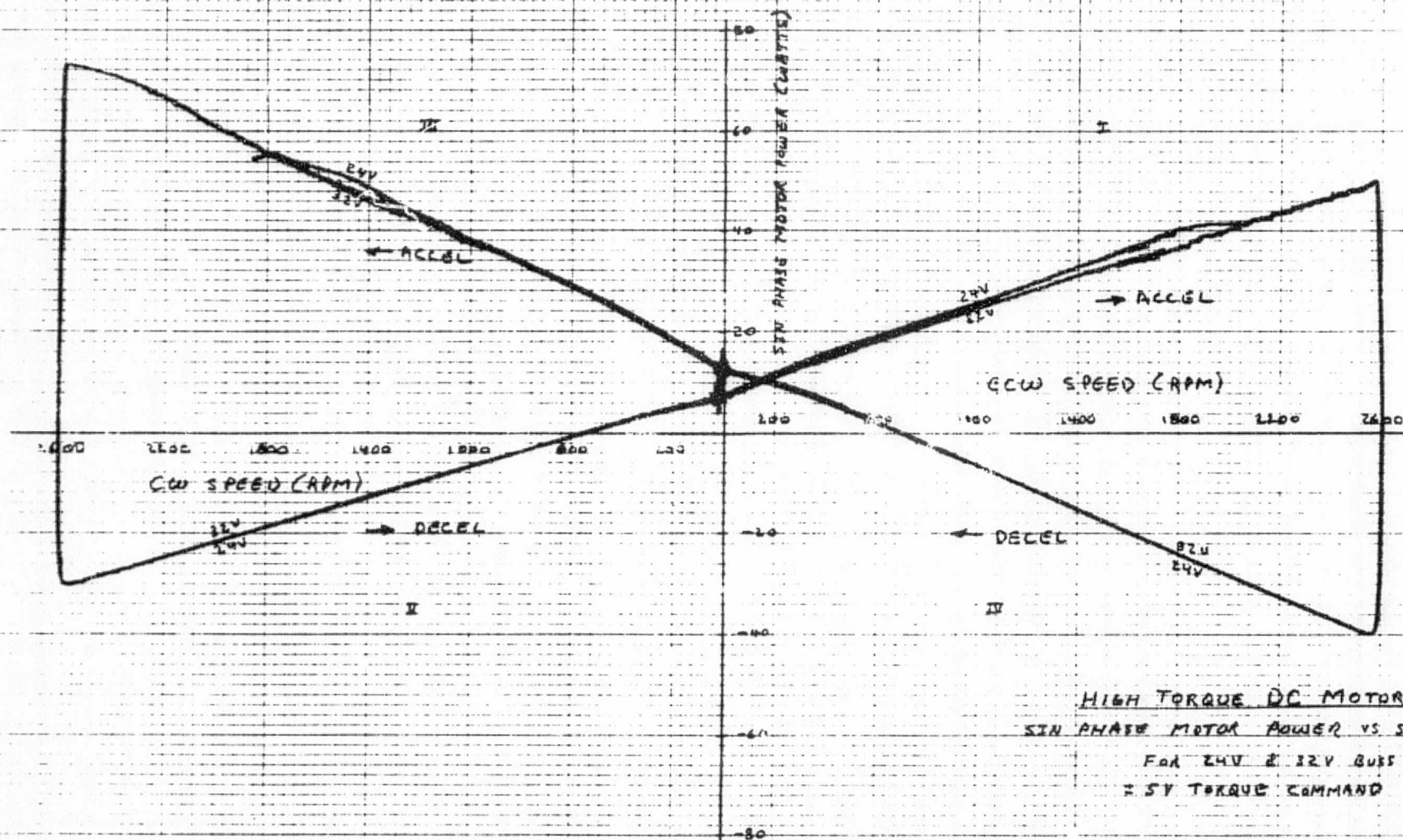
HIGH TORQUE DC MOTOR  
SIN PHASE MOTOR POWER  
VS SPEED AND TORQUE COMMAND

FIGURE 8-13  
R-22

APRIL 1976







### HIGH TORQUE DC MOTOR

SIN PHASE MOTOR POWER VS SPEED

FOR 24V & 32V BUS VOLTAGE  
= 5V TORQUE COMMAND

APRIL 1978

# HIGH TORQUE DC MOTOR

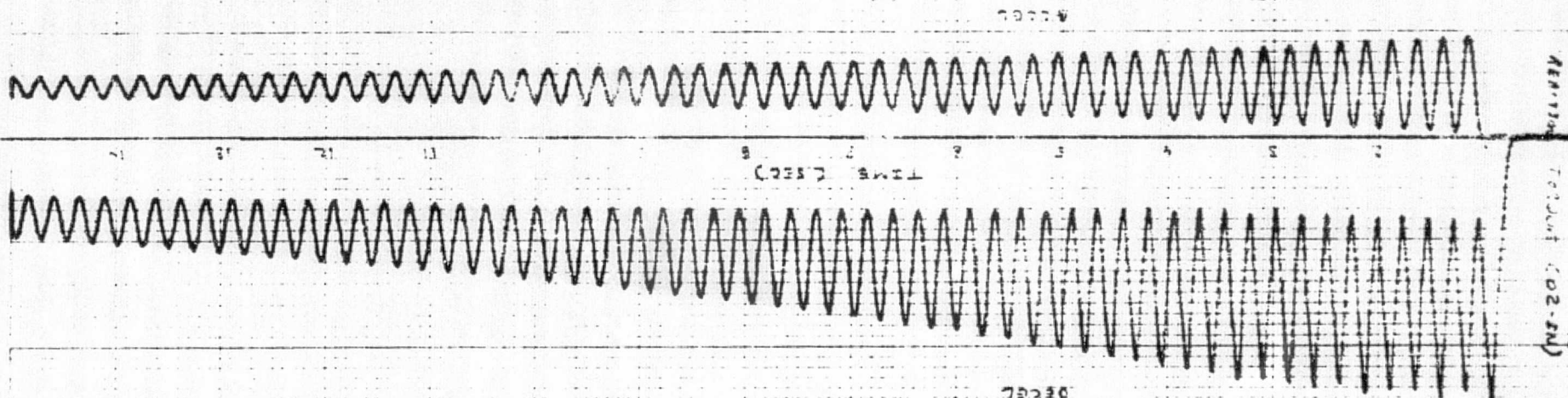
TRANSIENT RESPONSE

0.5V 1.000 COMMAND

1.000 2.000 RPM

TORQUE SIGNAL UNFILTERED

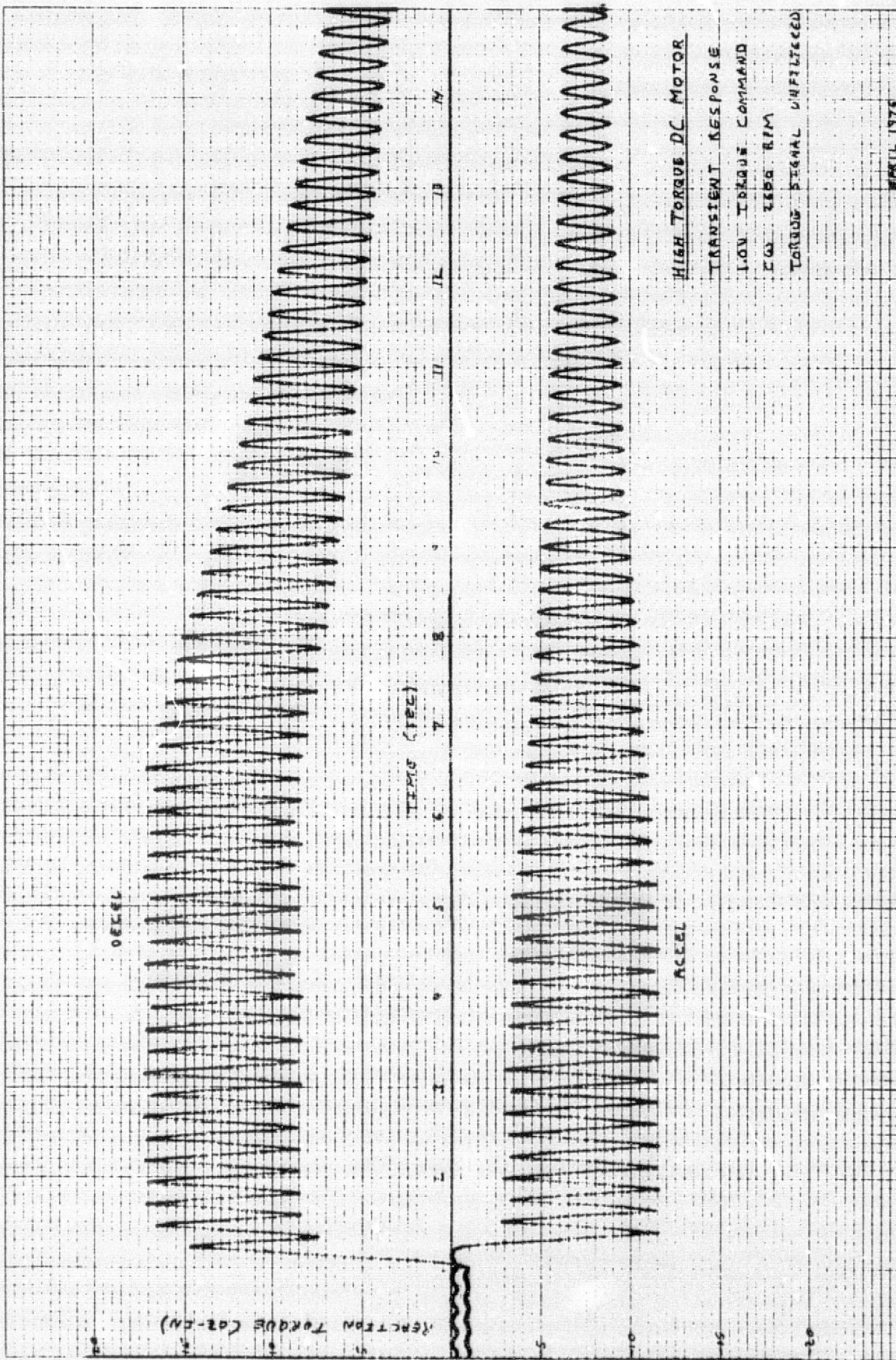
APRIL 1976

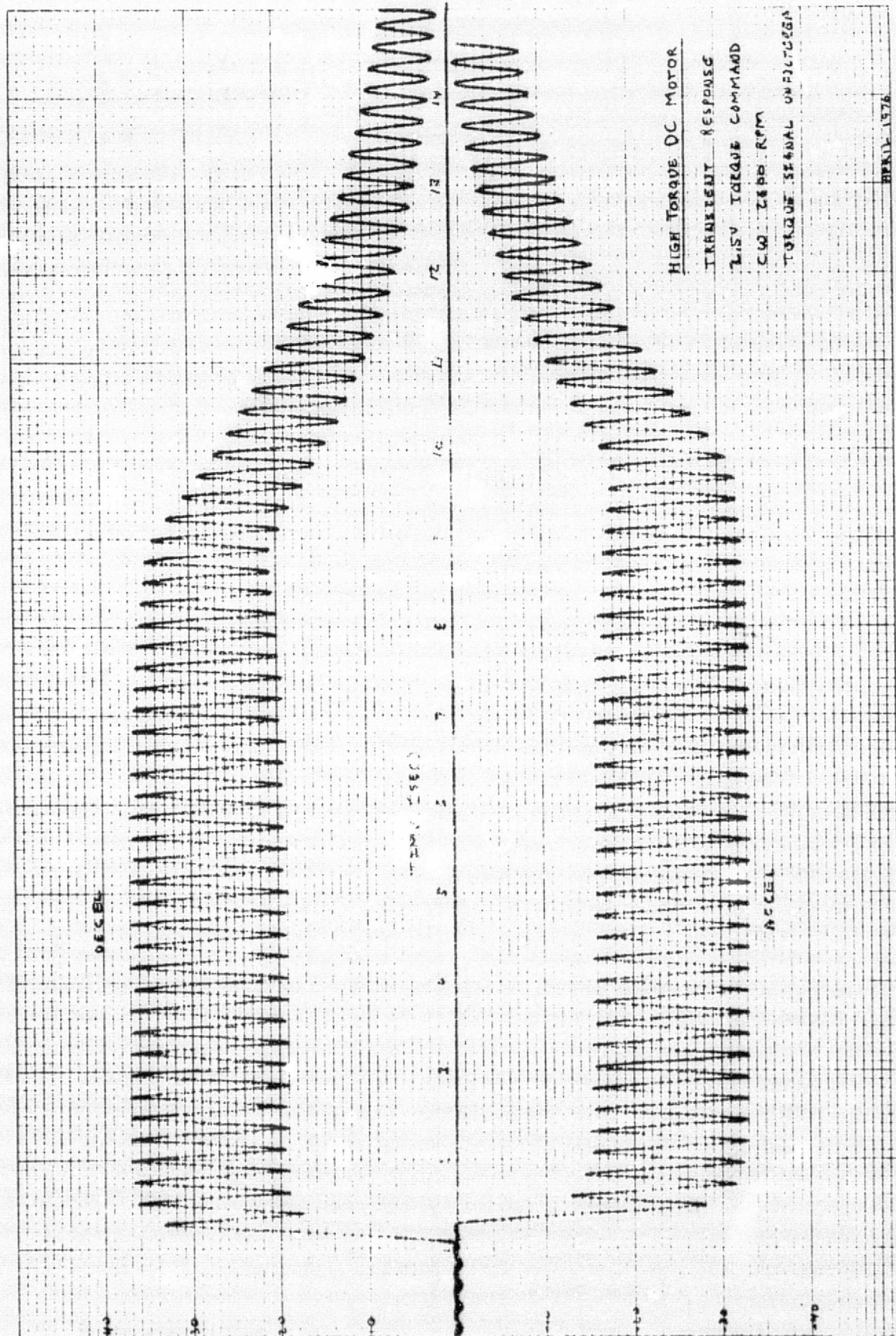


APRIL 1976

47 (1/02)







# HIGH TORQUE DC MOTOR

TRANSMITTANT RESPONSE

2.5V TORQUE COMMAND

CW 2600 R:PM

TELEPHONE SIGNAL UNIT

1976

FIGURE 8-18

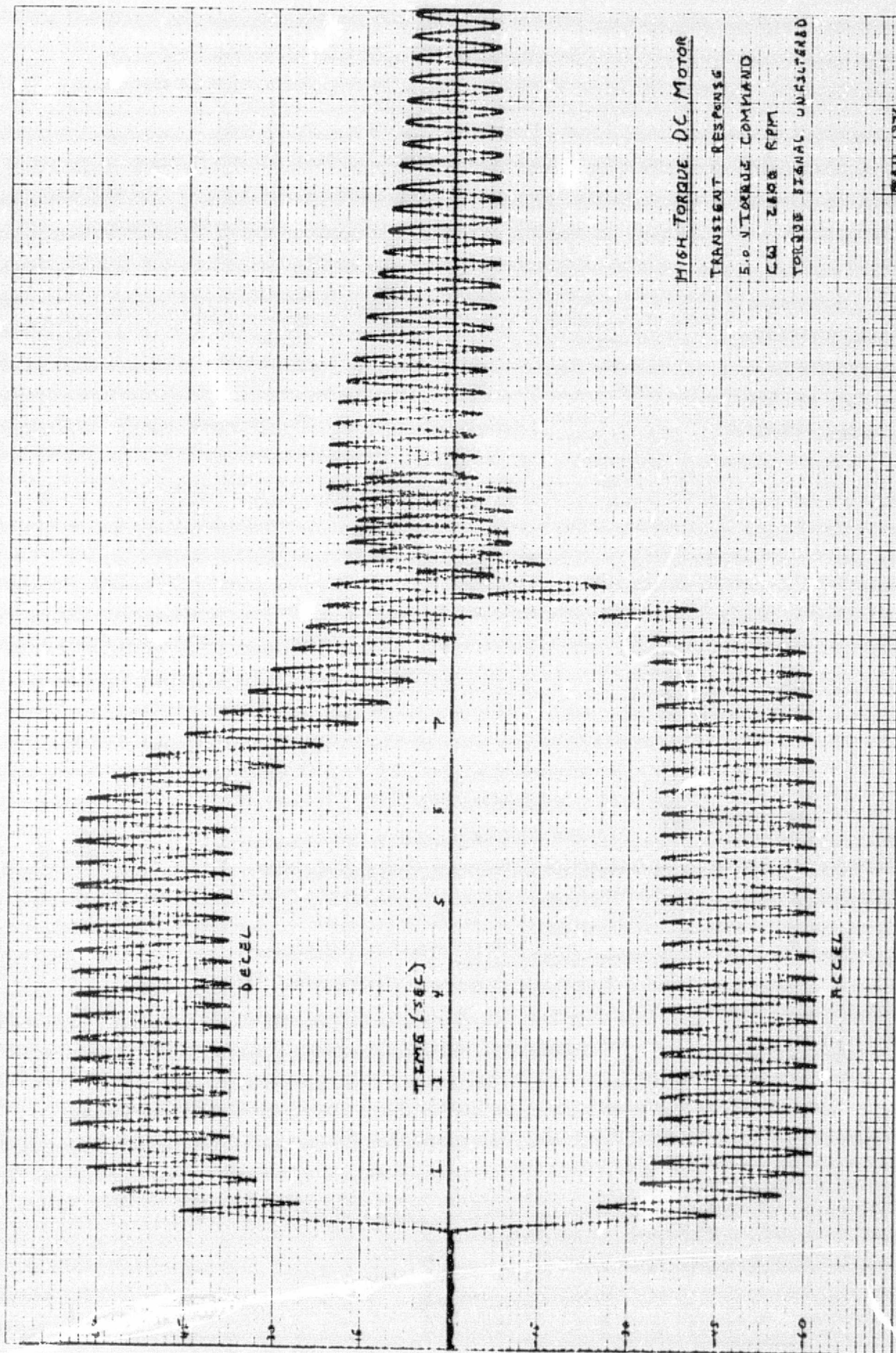
И-27

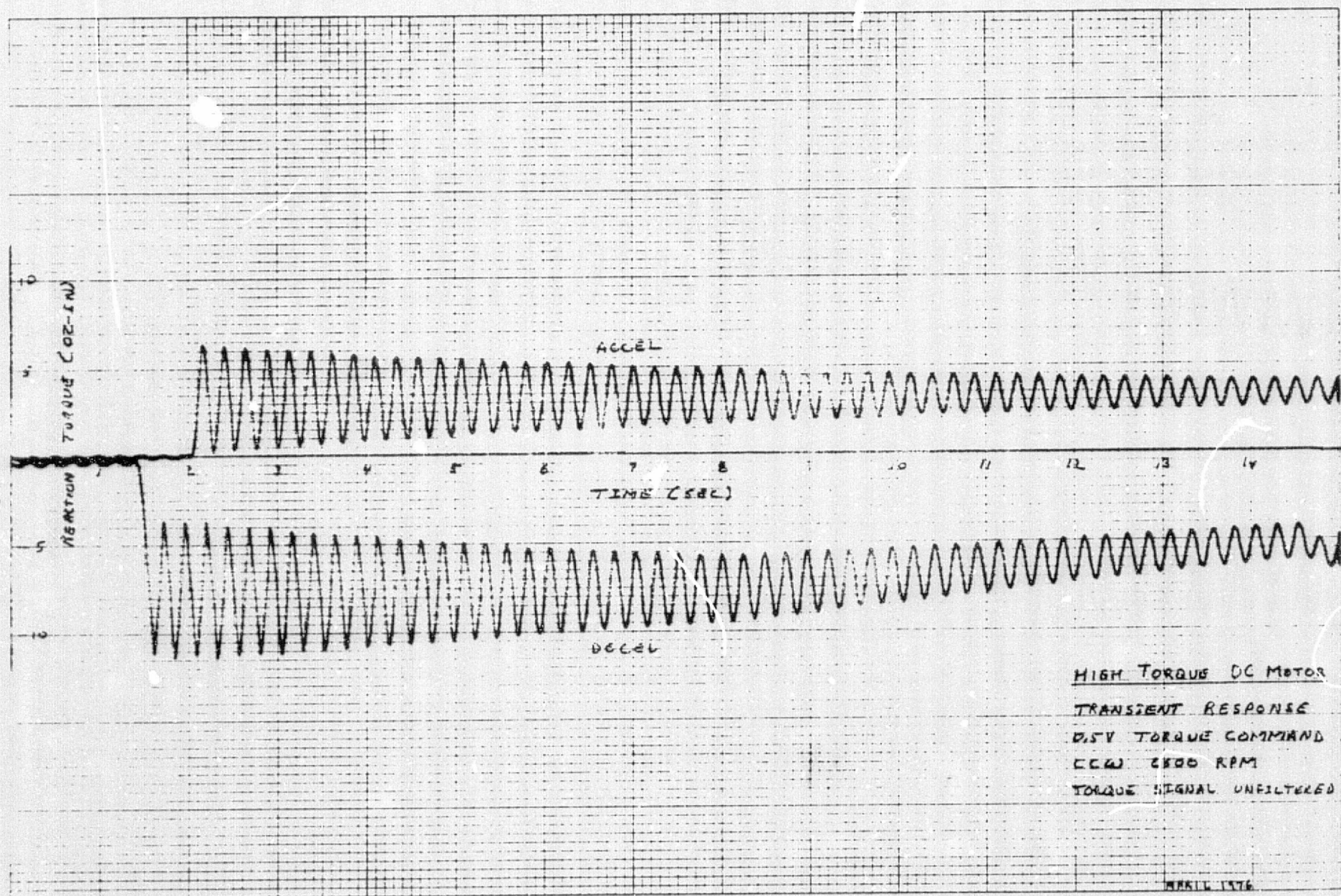
470707

3-11

REPRODUCIBILITY OF THE  
ORIGINAL PAGE IS POOR











8-30

REPRODUCIBILITY OF THE  
ORIGINAL PAGE IS POOR

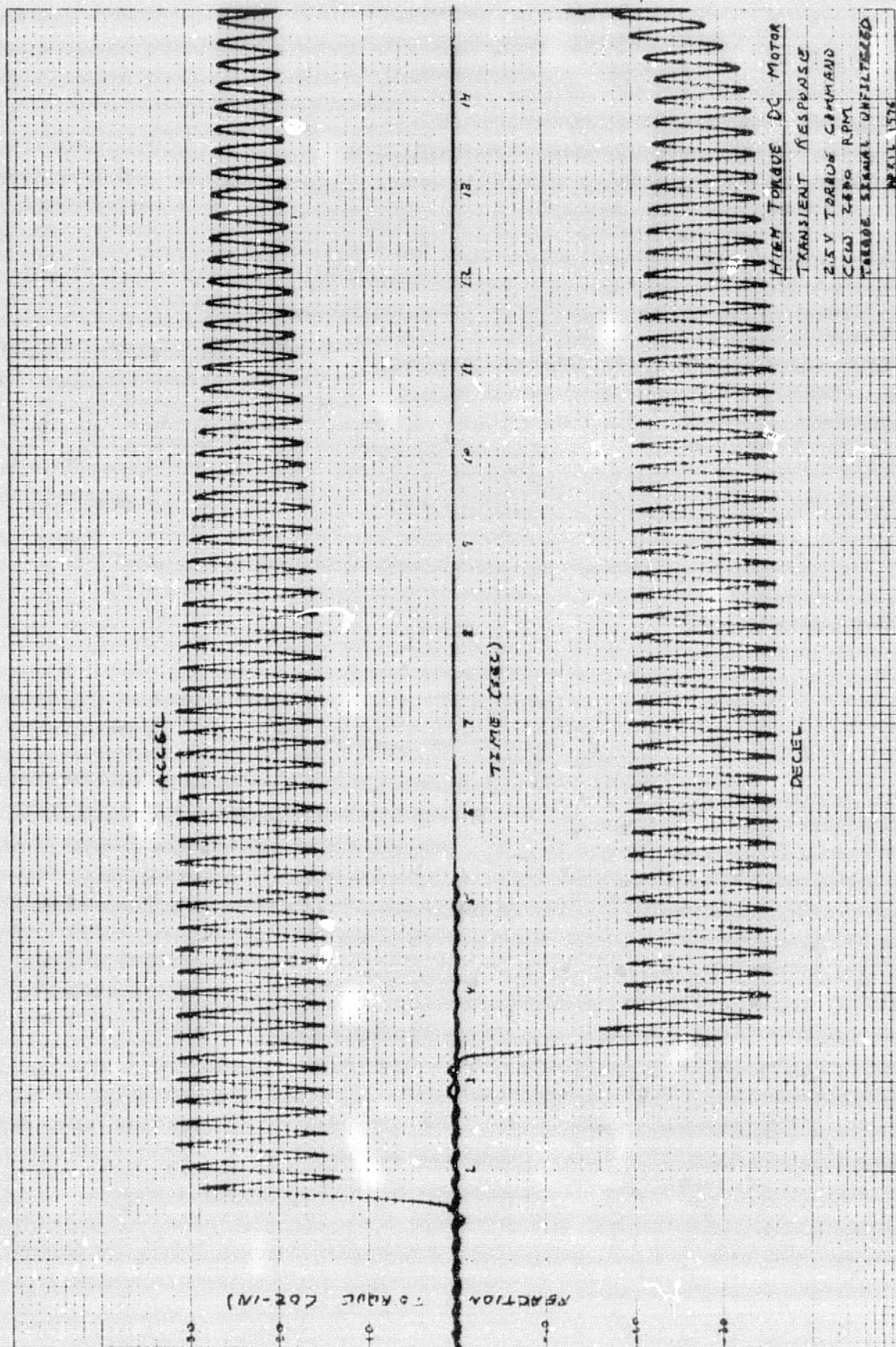


FIGURE 8-22

11



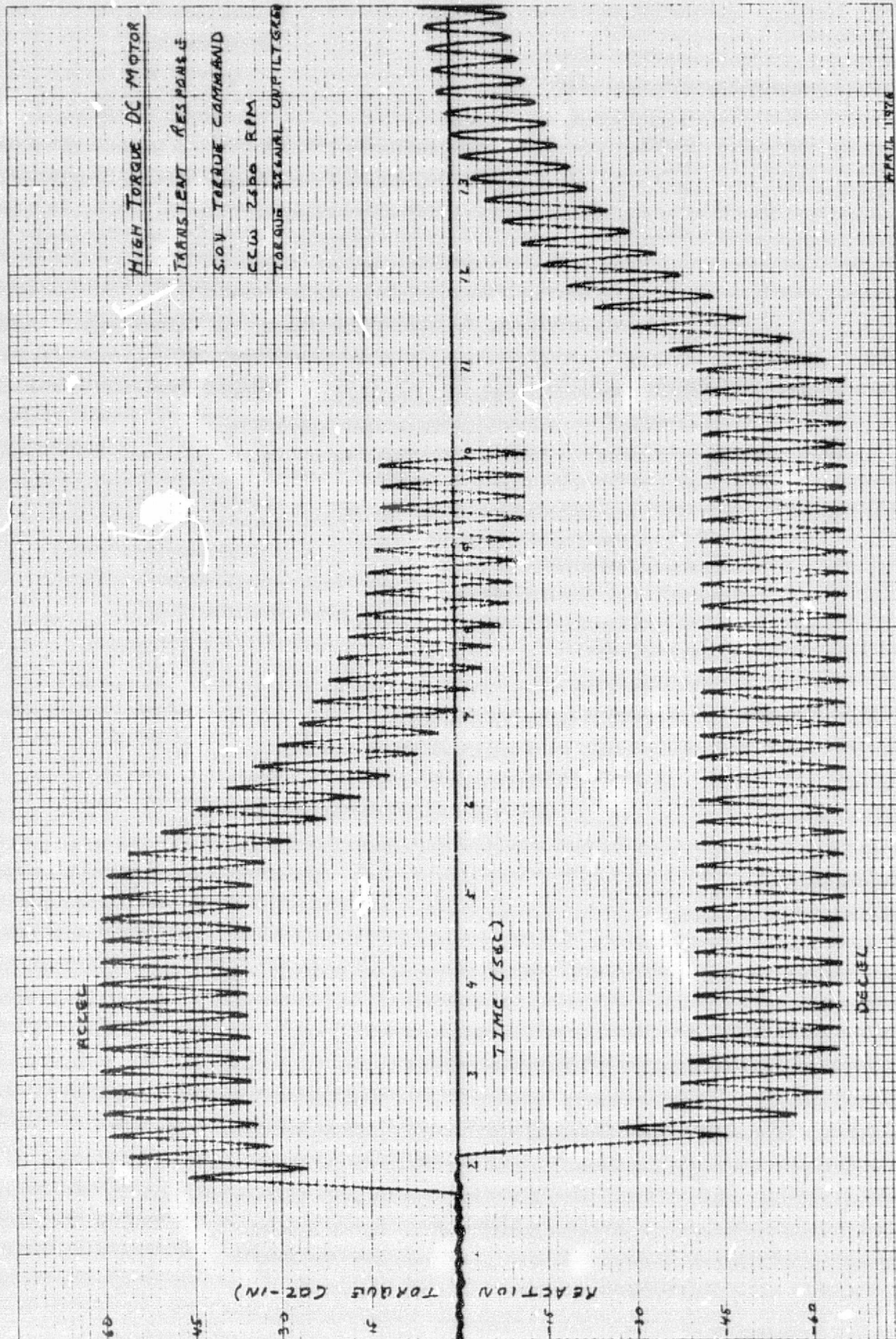
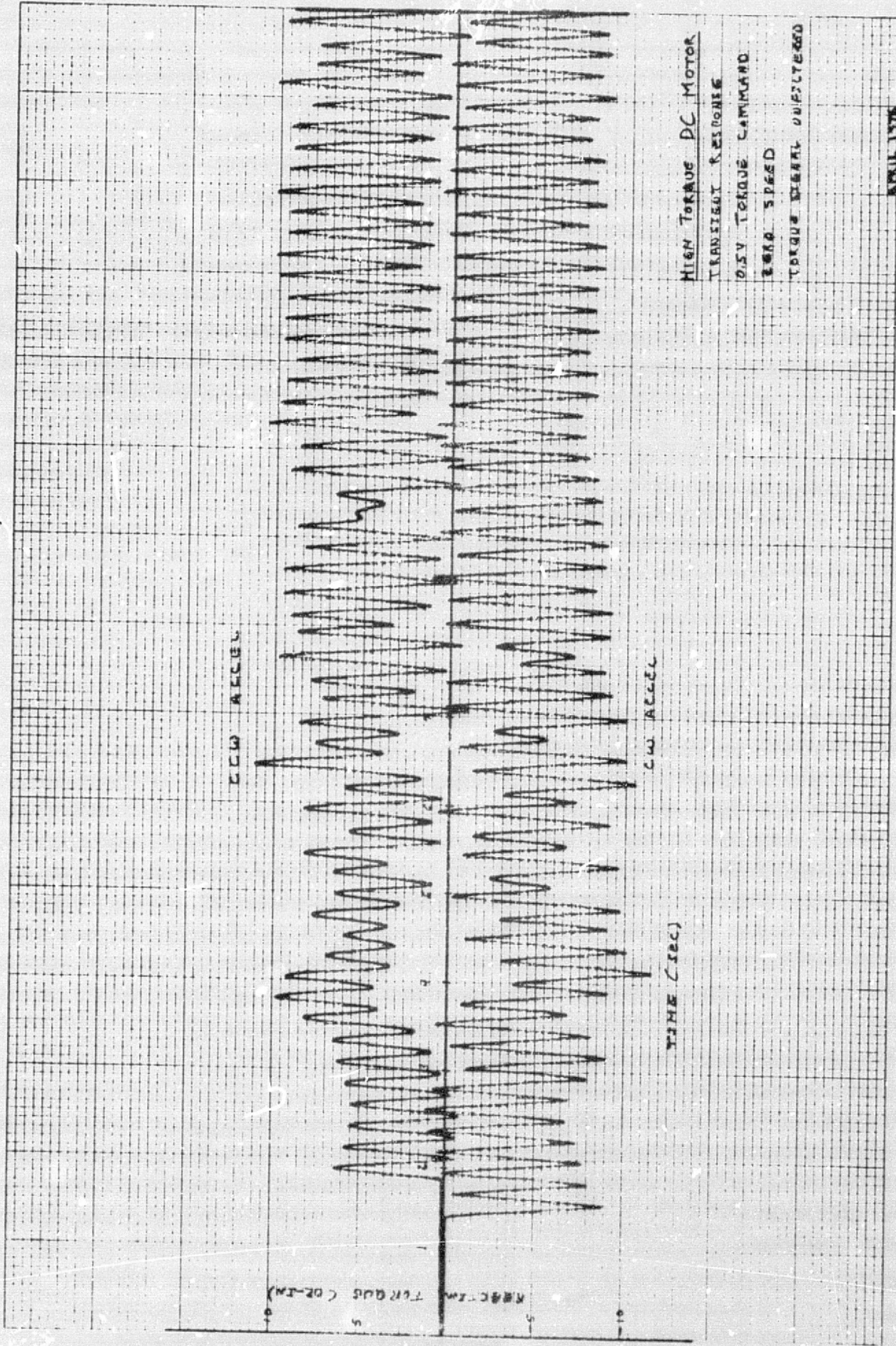


FIGURE 8-23  
N-32

REPRODUCIBILITY OF THE  
ORIGINAL PAGE IS POOR



HIGH TORQUE DC MOTOR  
 TRANSIENT RESPONSE  
 0.5V TORQUE COMMAND  
 2000 SPEED  
 TORQUE SIGNAL UNFILTERED

APRIL 1976

FIGURE 8-24

4707

REACT. TORQUE



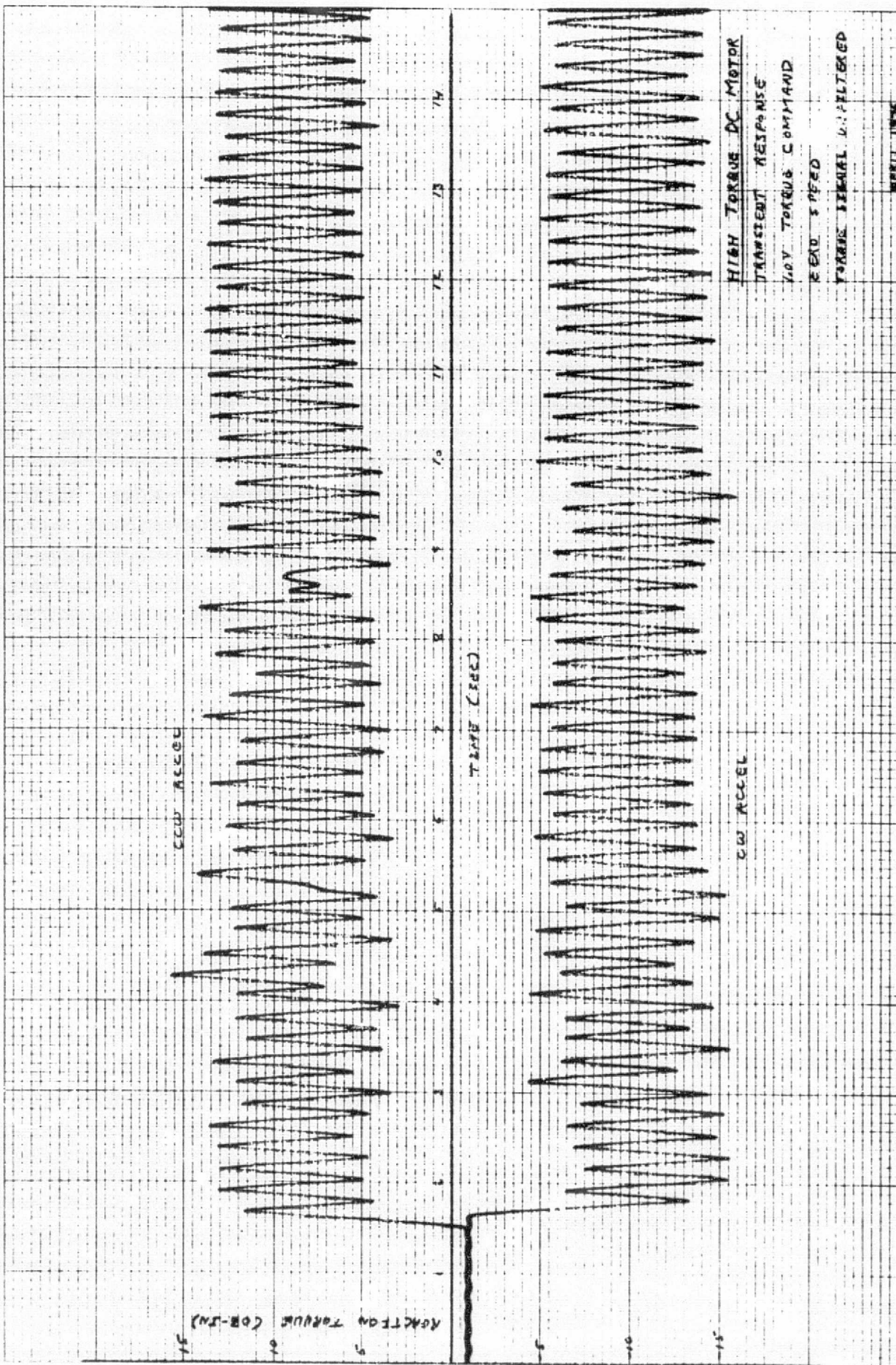


FIGURE 8-25

8-36

REPRODUCIBILITY OF THE  
ORIGINAL PAGE IS POOR

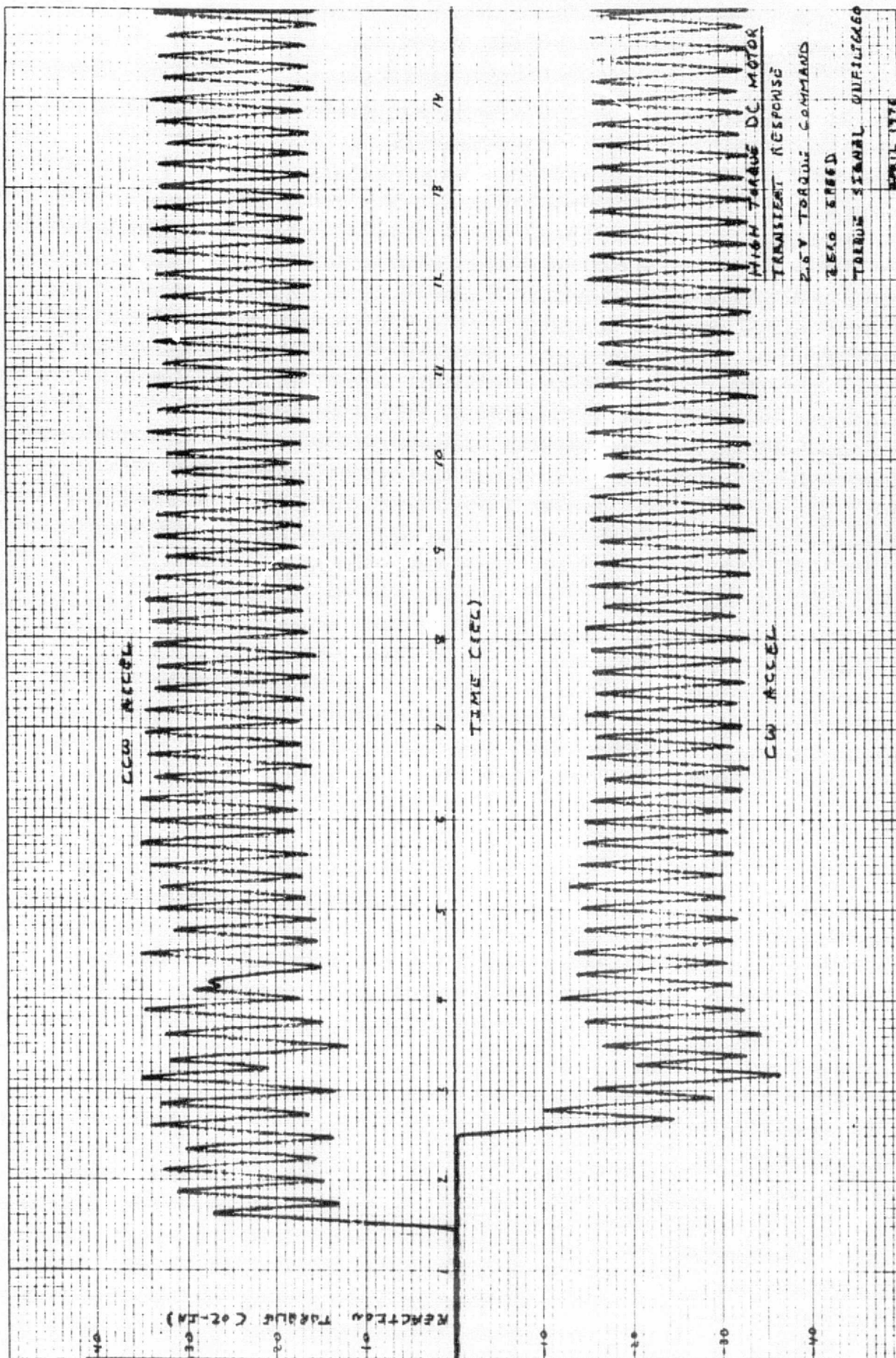


FIGURE 8-26

8-37



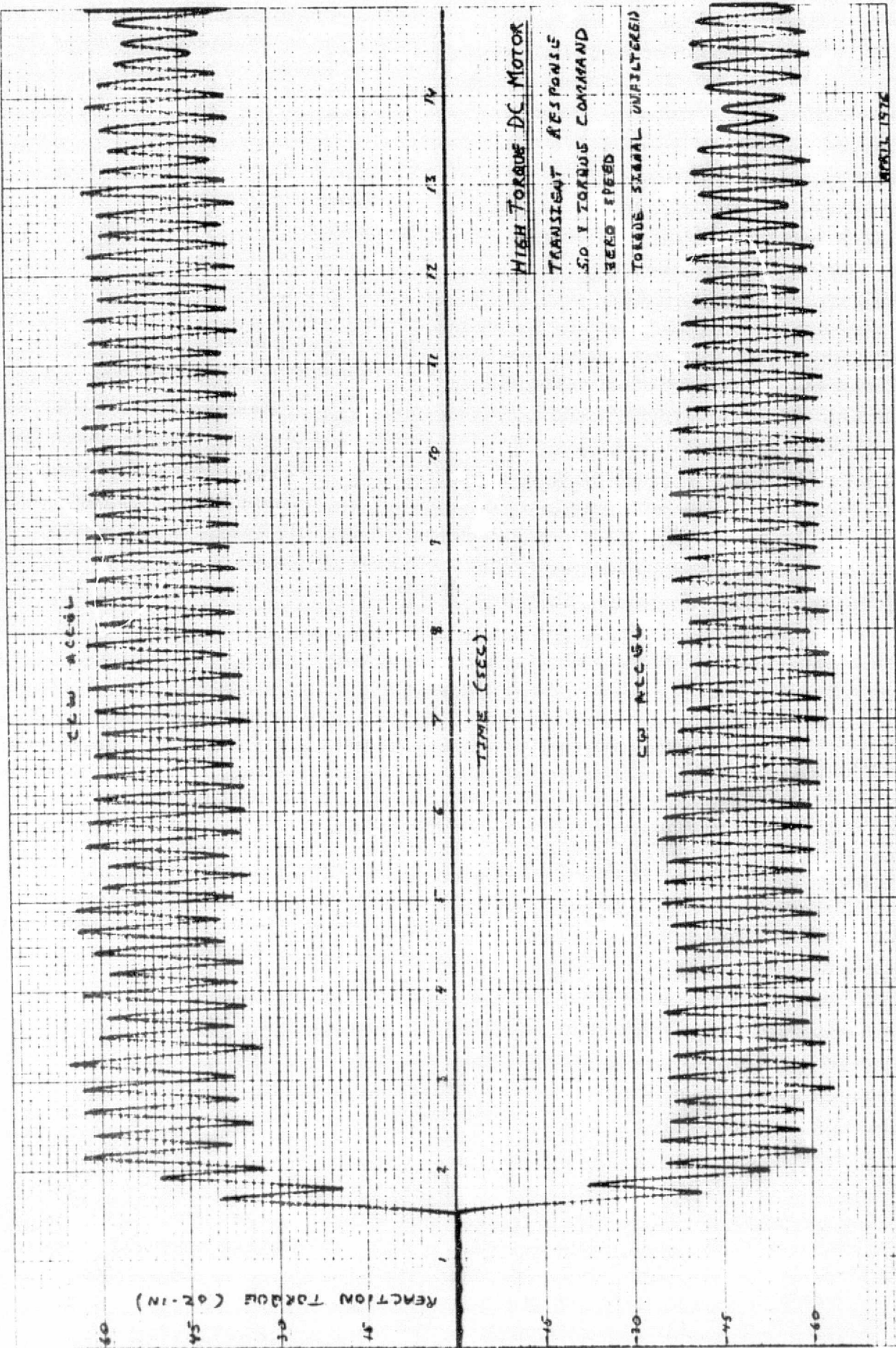


FIGURE 8-27

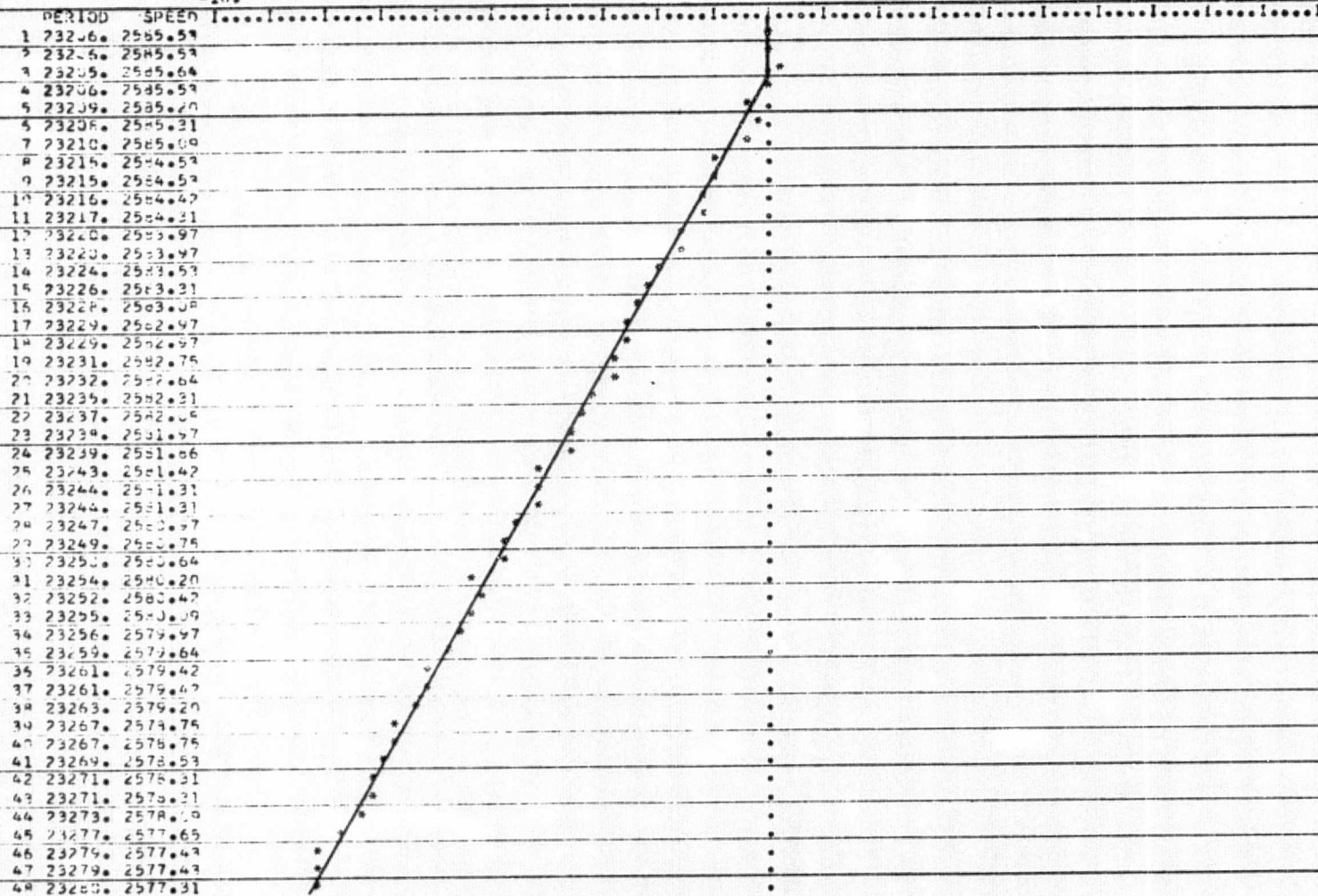
88-8

HIGH TORQUE DC MOTOR

CH. DECEL T/C=0.5V

-10.

10.



TORQUE = 0.55 02-11 (P.V.) 4 To 45 1

FIGURE 8-28  
8-39

HIGH TORQUE DC MOTOR

Cw ACCEL T/C=5V

-10.

10.

PERIOD	SPEED
1	23194. 2586.87
2	23194. 2586.87
3	23194. 2586.87
4	23193. 2586.88
5	23193. 2586.88
6	23191. 2587.21
7	23197. 2587.50
8	23195. 2587.37
9	23191. 2587.21
10	23159. 2587.43
11	23169. 2587.43
12	23184. 2587.54
13	23179. 2587.43
14	23157. 2587.65
15	23187. 2587.65
16	23136. 2587.76
17	23186. 2587.76
18	23185. 2587.80
19	23186. 2587.76
20	23145. 2587.80
21	23183. 2588.10
22	23184. 2587.80
23	23182. 2588.21
24	23182. 2588.21
25	23182. 2588.21
26	23181. 2588.37
27	23181. 2588.43
28	23180. 2588.43
29	23179. 2588.54
30	23180. 2588.43
31	23178. 2588.66
32	23174. 2588.66
33	23177. 2588.77
34	23177. 2588.77
35	23174. 2589.10
36	23176. 2588.80
37	23174. 2589.10
38	23175. 2588.90
39	23173. 2589.22
40	23174. 2589.10
41	23172. 2589.33
42	23173. 2589.22
43	23171. 2589.44
44	23172. 2589.33
45	23171. 2589.44
46	23171. 2589.44
47	23169. 2589.66

FIGURE 0-20  
8-40

TORQUE= 2.75 GZ-1 (FROM 5 TO 47)

## HIGH TORQUE DC MOTOR

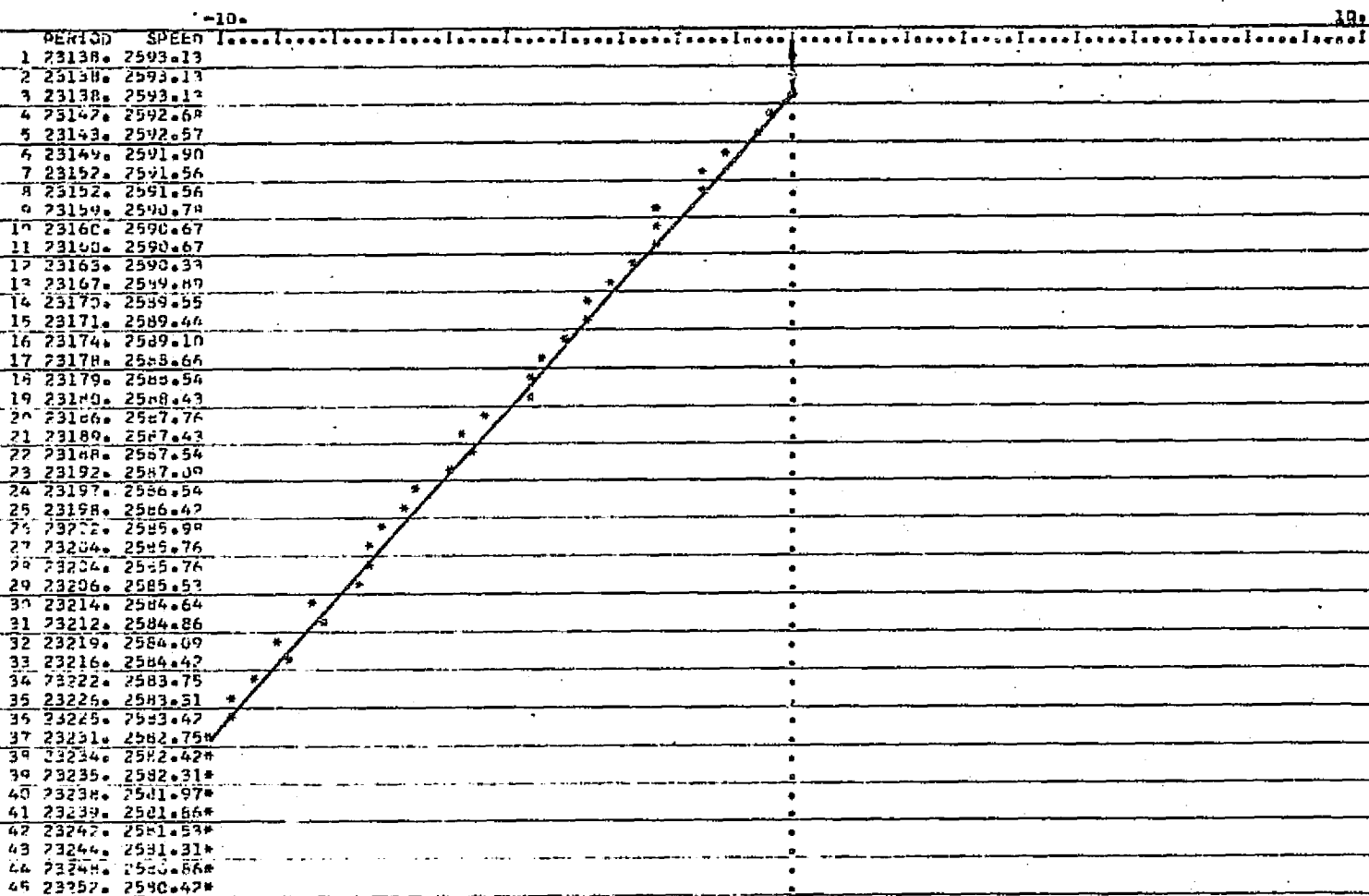
G<sub>2</sub> DECEL T/C=1V

FIGURE 8-30

8-41

TORQUE = -13.32 OZ-IN. (FOR 4 TO 45)

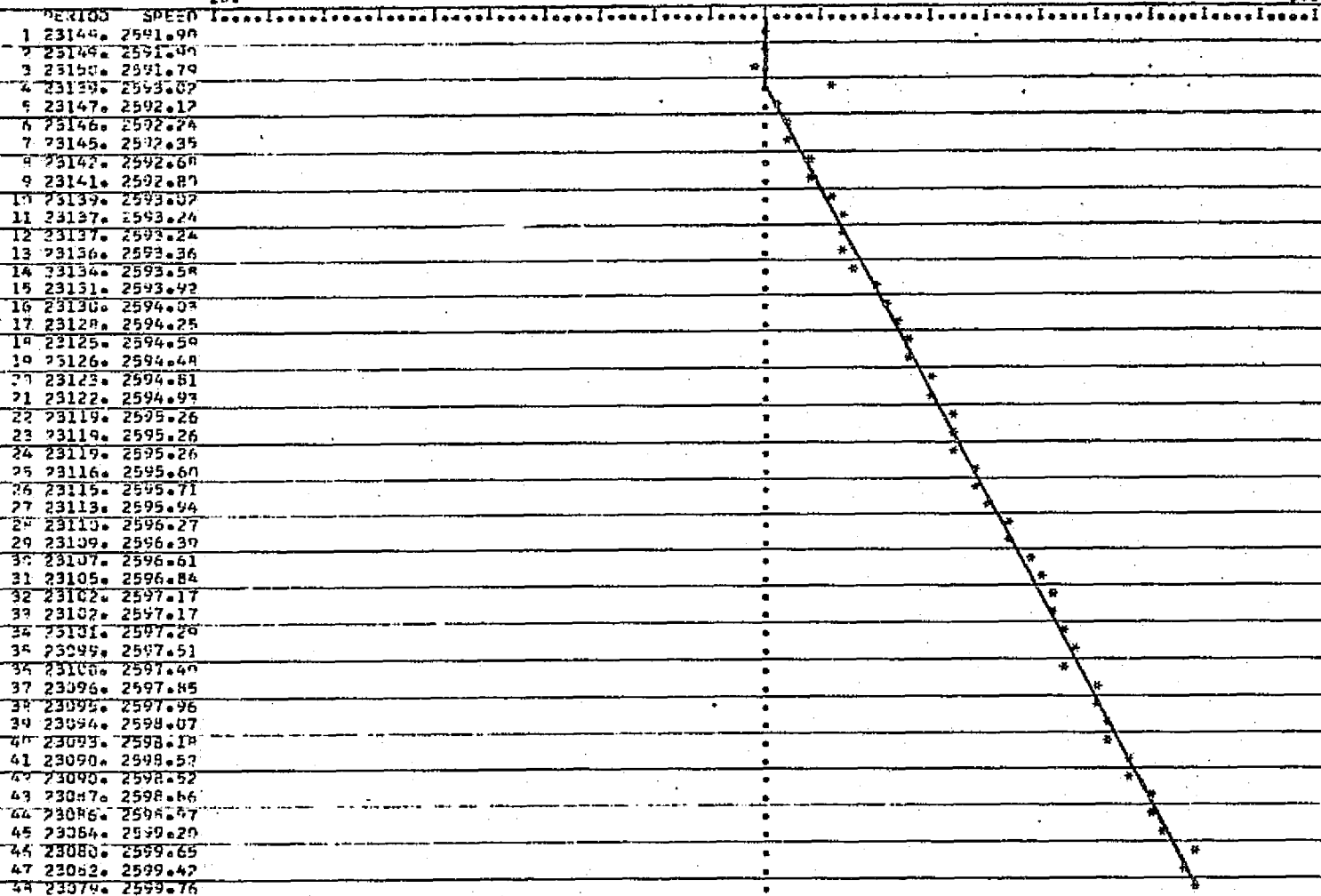


HIGH TORQUE DC MOTOR

CW ACCEL T/C=1V

-10.

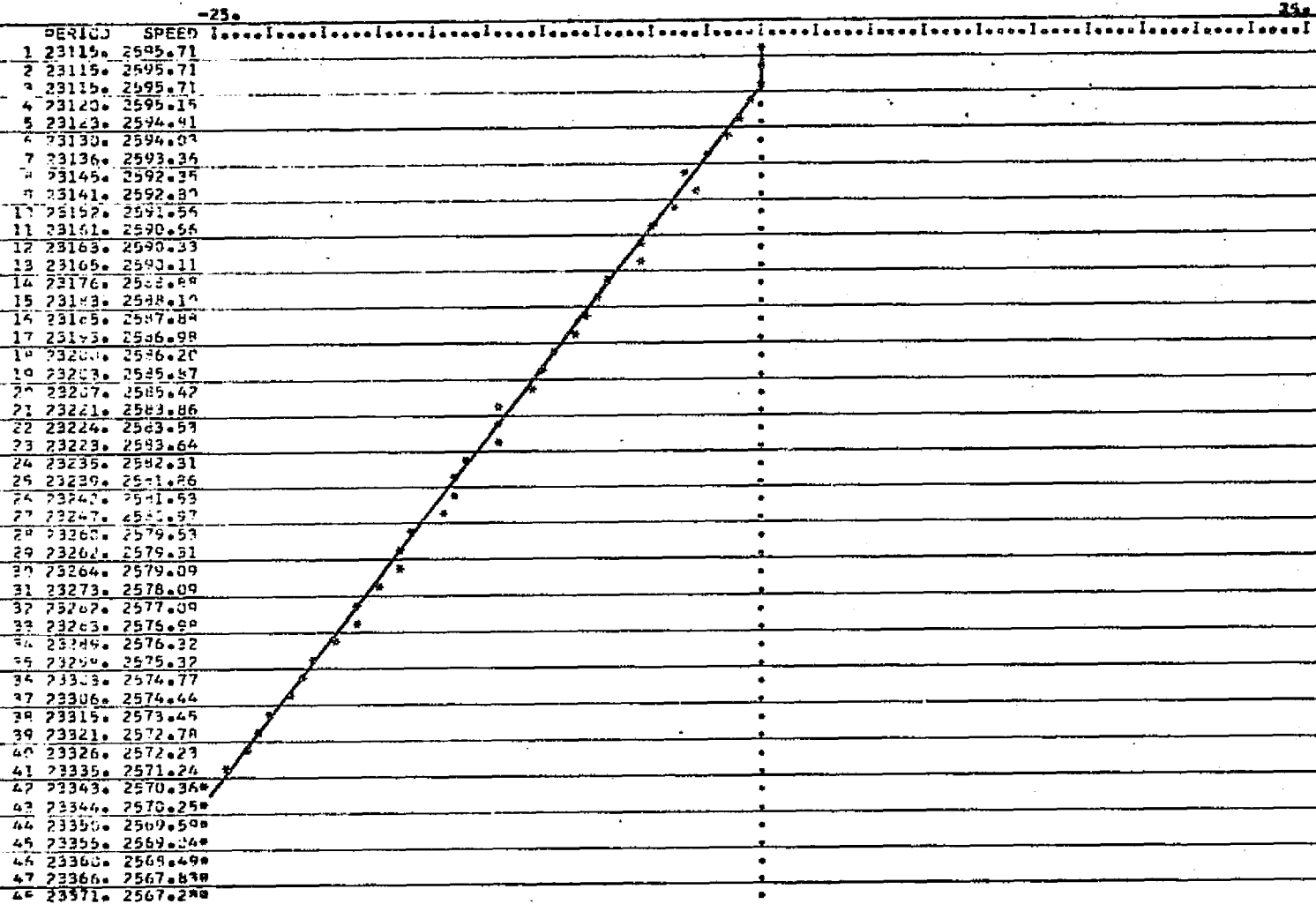
10.

FIGURE 8-31  
8-42

TORQUE = 8.10 OZ-IN (FRO 5 TO 45)

## HIGH TORQUE DC MOTOR

CR. DECEL 1/C=2.5W

FIGURE 8-33  
8-43

TORQUE = -29.10 02-1 (FNC. 4 TO 46)

HIGH TORQUE DC MOTOR

CA ACCEL T/C=2.5V

-25.

25.

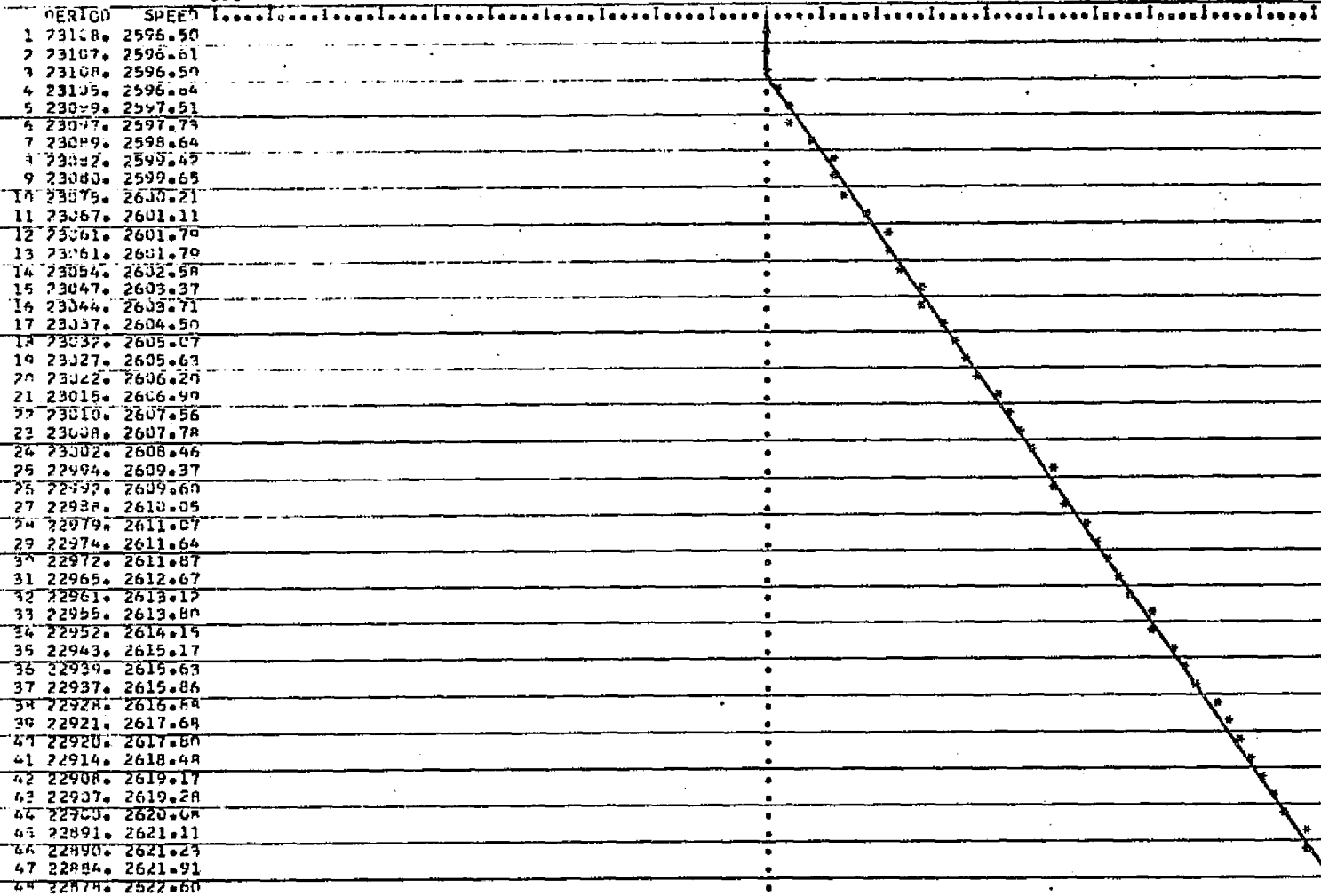


FIGURE 8-33

8-44

FIGURE 8-33 (CONT.)

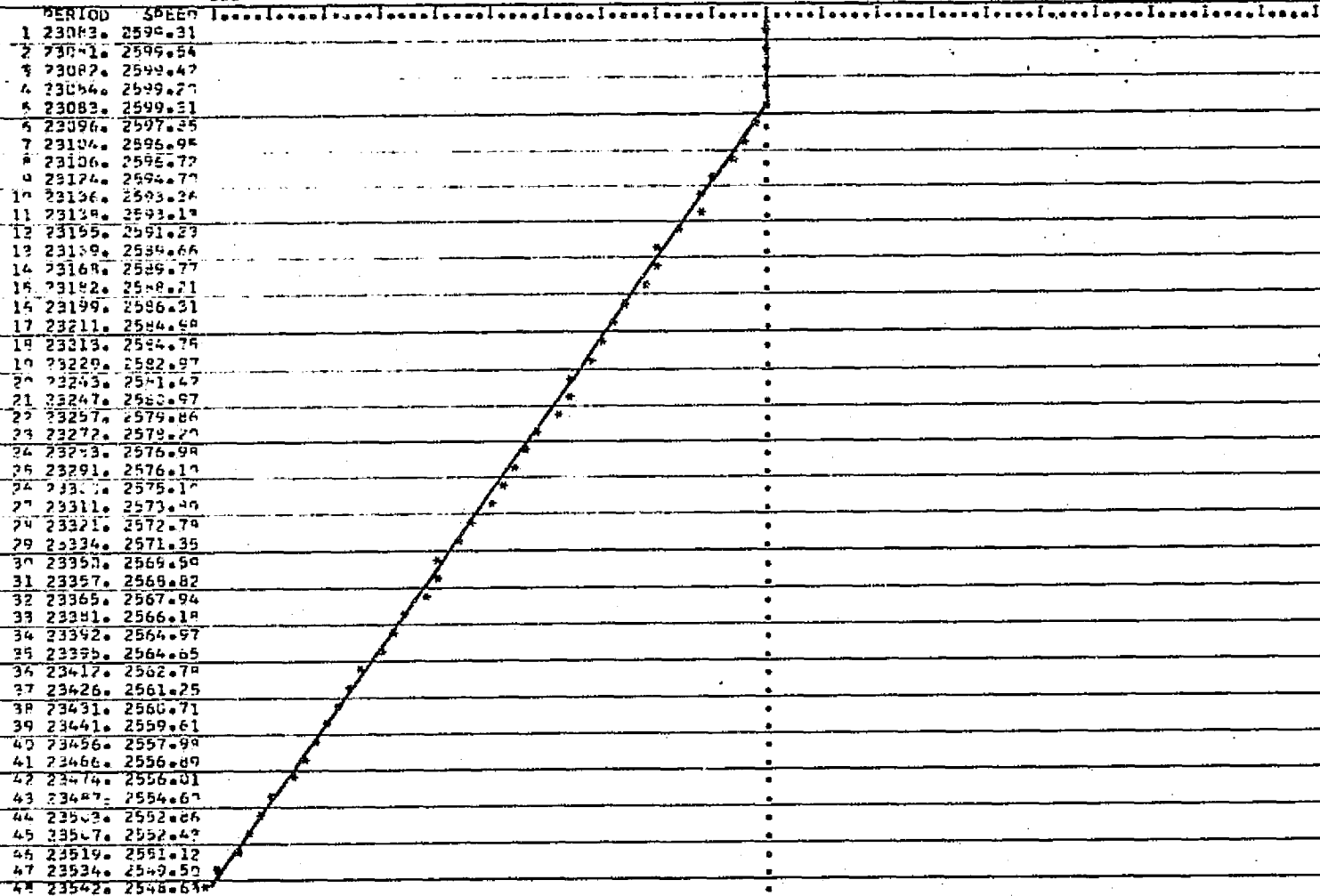
REPRODUCIBILITY OF THIS  
ORIGINAL PAGE IS POOR

## HIGH TORQUE DC MOTOR

C. DECEL 1/C=5V

-50.

50.



TQ=53.69 DZ=14 (PRT 6 TO 48)

-50.

50.

PERIOD	SPEED
1 23094.	2598.07
2 23094.	2598.07
3 23092.	2598.30
4 23094.	2598.07
5 23084.	2599.20
6 23054.	2599.20
7 23075.	2600.21
8 23075.	2600.78
9 23065.	2601.90
10 23043.	2603.92
11 23038.	2604.39
12 23023.	2606.08
13 23007.	2607.97
14 23002.	2608.46
15 22998.	2608.92
16 22976.	2611.42
17 22970.	2612.10
18 22965.	2612.57
19 22950.	2614.37
20 22933.	2616.51
21 22928.	2616.89
22 22920.	2617.80
23 22905.	2619.51
24 22895.	2620.65
25 22893.	2620.88
26 22878.	2622.60
27 22863.	2624.32
28 22859.	2624.78
29 22848.	2626.05
30 22831.	2628.00
31 22822.	2629.04
32 22819.	2629.38
33 22803.	2631.23
34 22790.	2632.73
35 22786.	2633.19
36 22779.	2634.30
37 22760.	2636.20
38 22751.	2637.24
39 22745.	2637.94
40 22727.	2640.03
41 22719.	2640.96
42 22713.	2641.65
43 22703.	2642.82
44 22690.	2644.33
45 22682.	2645.26
46 22680.	2645.59
47 22657.	2648.18
48 22648.	2649.74

FIGURE 8-35  
8-45

TORQUE= 54.46 OZ-IN (FROM 5 TO 48)

## HIGH TORQUE DC MOTOR

CCW DECEL T/C=5V

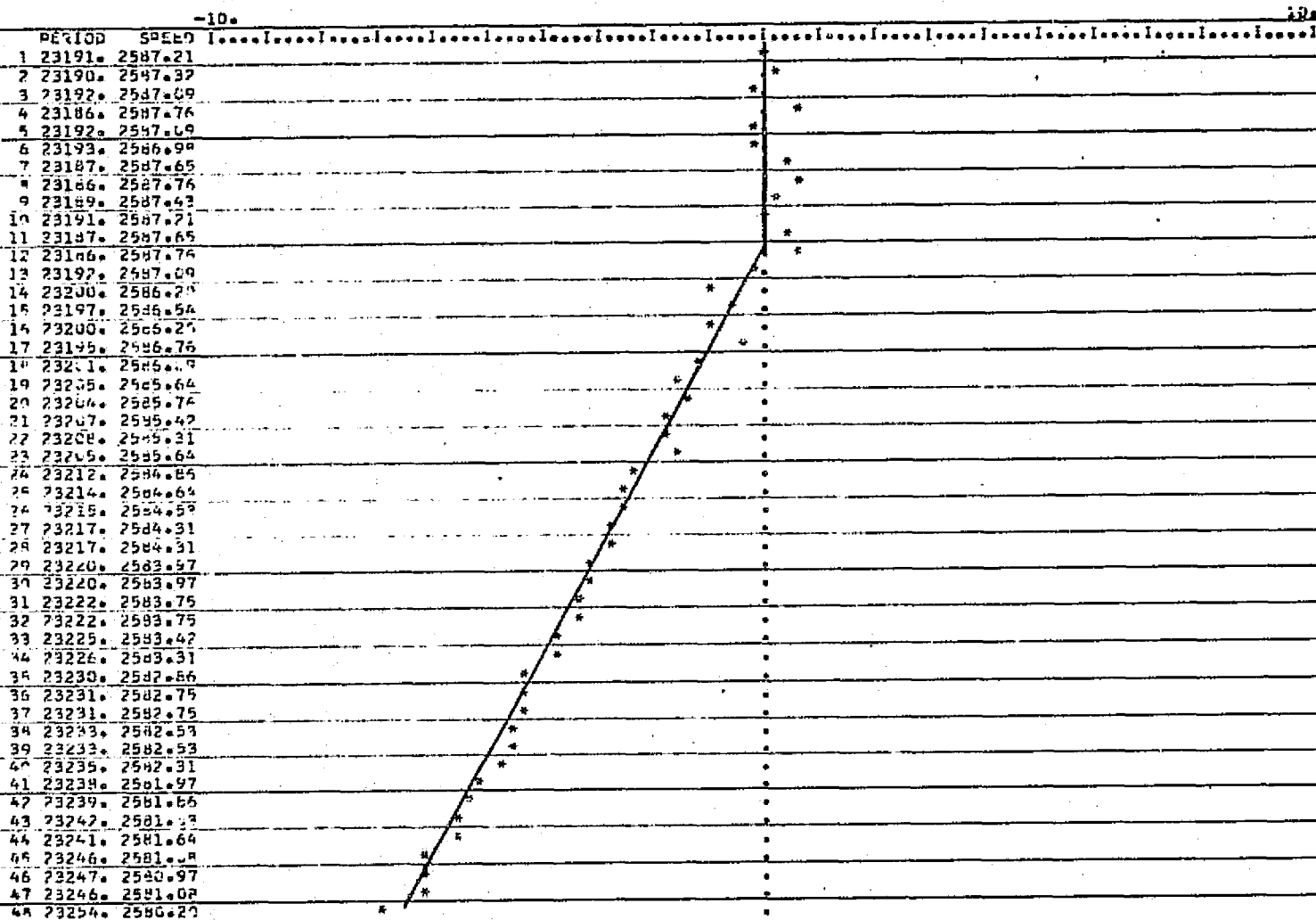


FIGURE 8-36  
8-47

TORQUE = -0.06 OZ-IN (FROM 13 TO 43)

## HIGH TORQUE DC MOTOR

CCW ACCEL T/C=5V

PERIOD	SPEED	
1	23154. 2591.34	
2	23154. 2591.34	
3	23154. 2591.34	
4	23153. 2591.45	
5	23153. 2591.45	
6	23151. 2591.68	*
7	23151. 2591.68	*
8	23154. 2591.34	*
9	23151. 2591.68	*
10	23149. 2591.90	*
11	23153. 2591.79	*
12	23150. 2591.79	*
13	23152. 2591.56	*
14	23147. 2592.12	*
15	23146. 2592.26	*
16	23150. 2591.79	*
17	23145. 2592.35	*
18	23144. 2592.46	*
19	23144. 2592.46	*
20	23142. 2592.68	*
21	23146. 2592.24	*
22	23143. 2592.57	*
23	23144. 2592.46	*
24	23142. 2592.68	*
25	23144. 2592.46	*
26	23141. 2592.80	*
27	23144. 2592.46	*
28	23142. 2592.68	*
29	23142. 2592.68	*
30	23143. 2592.57	*
31	23136. 2593.36	*
32	23143. 2592.57	*
33	23139. 2593.02	*
34	23137. 2593.24	*
35	23135. 2593.47	*
36	23139. 2593.02	*
37	23138. 2593.13	*
38	23134. 2593.58	*
39	23136. 2593.36	*
40	23135. 2593.47	*
41	23136. 2593.36	*
42	23134. 2593.58	*
43	23131. 2593.92	*
44	23133. 2593.60	*
45	23131. 2593.92	*
46	23130. 2594.03	*

TORQUE 4.62 OZ-IN (FROM 4 TO 46)

FIGURE 8-37  
8-48

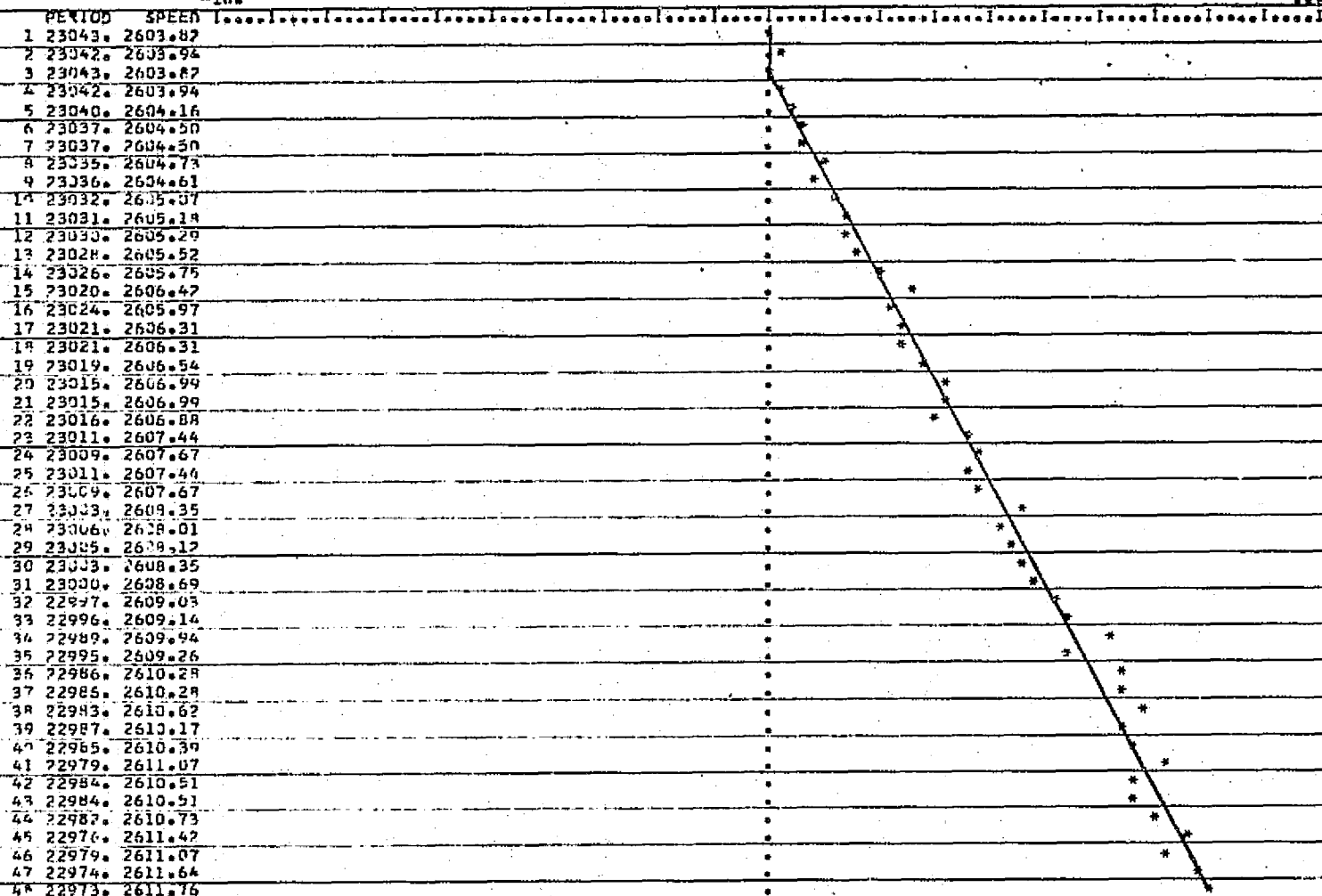
ORIGINAL DATA TO TOR

HIGH TORQUE DC MOTOR

CCs ACCEL T/C=1V

-10.

10.

FIGURE 8-38  
8-49

TORQUE\* 5.1 2-1. (FR 7 4 TO 48)

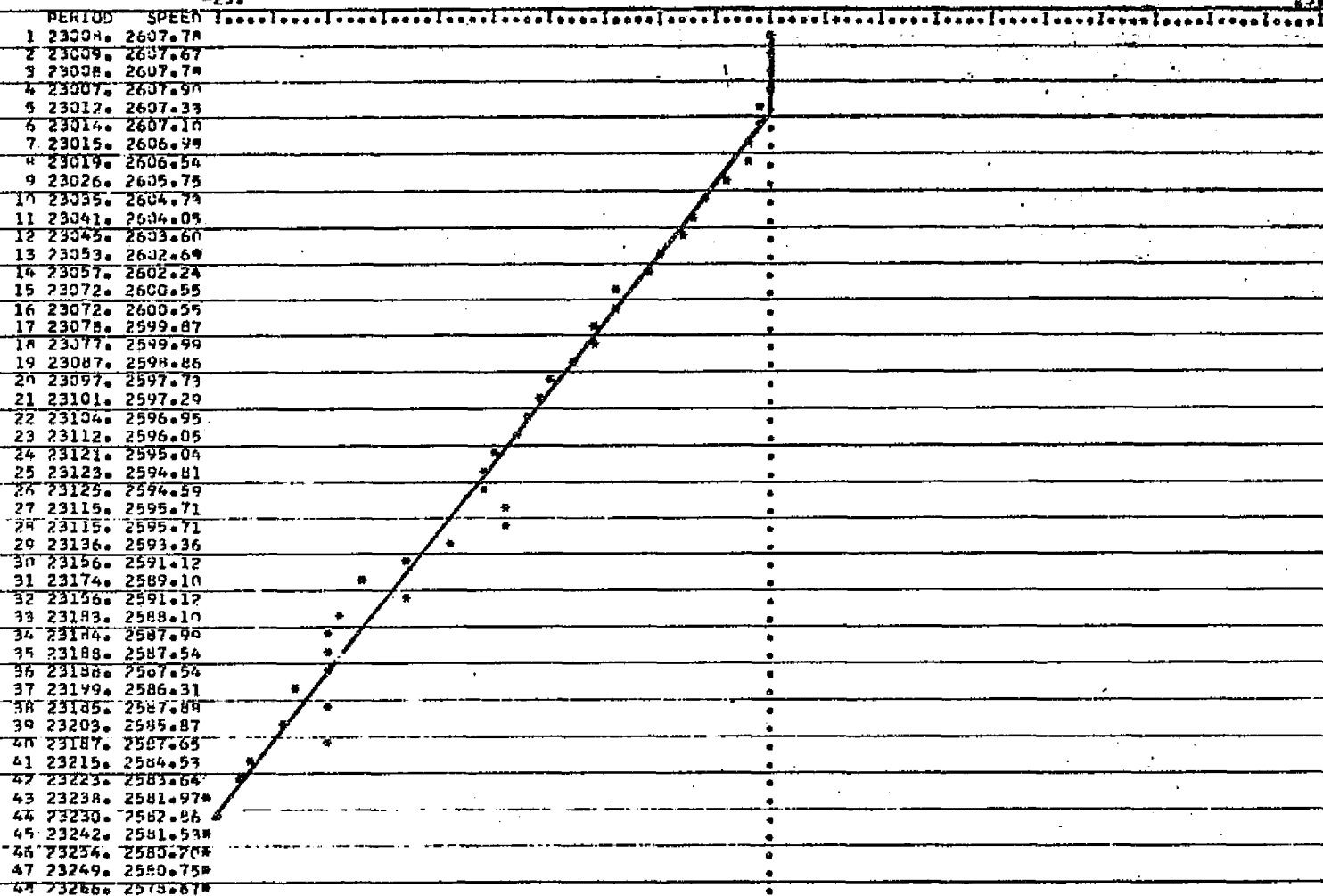


## HIGH TORQUE DC MOTOR

CC: DECEL T/C=2.8V

-25.

25.



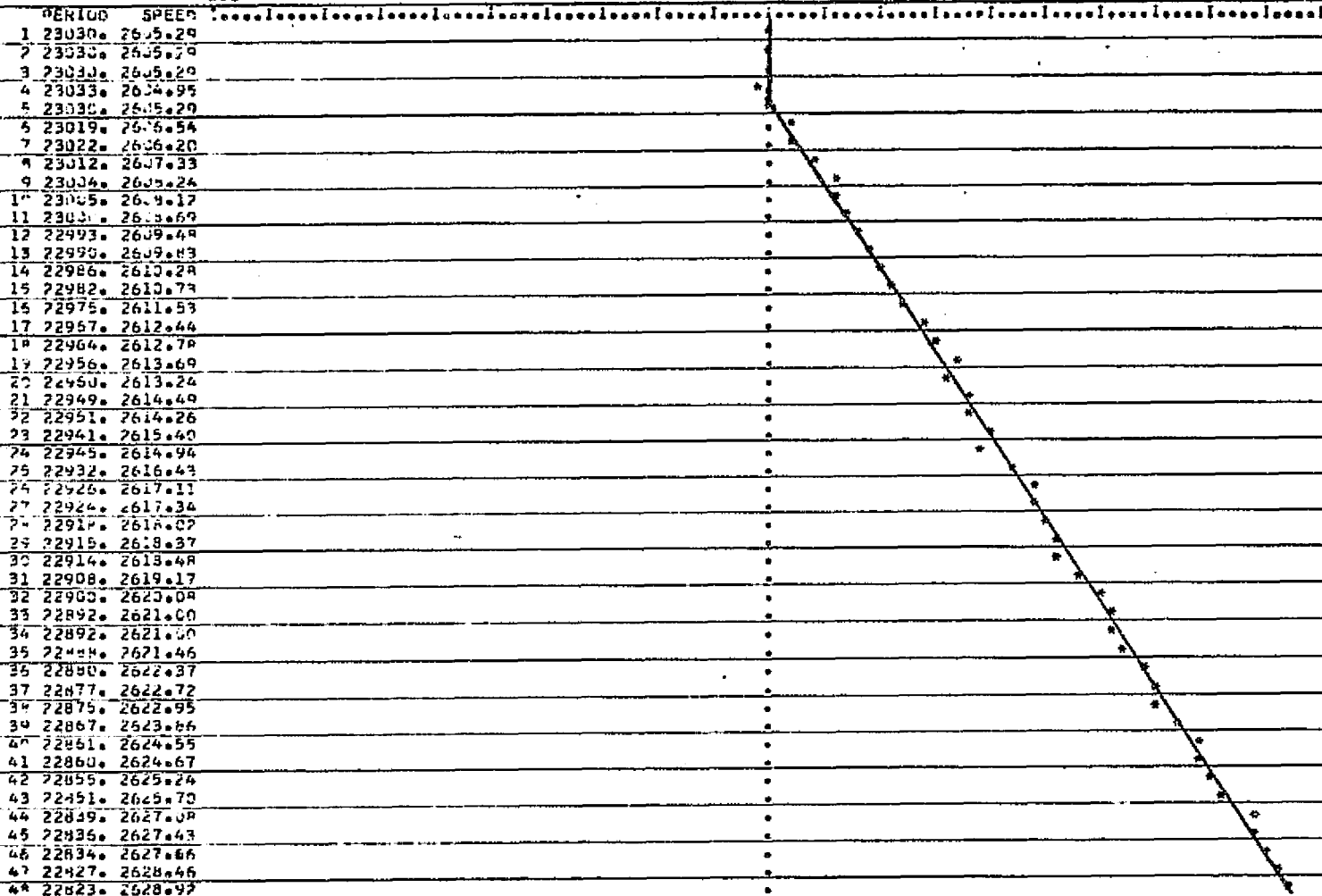
TORQUE= 29.57 OZ-IN (FROM 6 TO 48 T)

HIGH TORQUE DC MOTOR

50% ACCEL T/C=2.2V

-25.

25.

TQ-8  
OF-8  
TUB-12  
OF-40

TORQUE= 24.73 (2-T) (FROM 5 TO 48)

## HIGH TORQUE DC MOTOR

CC. DECEL T/C=5V

-90.

50.

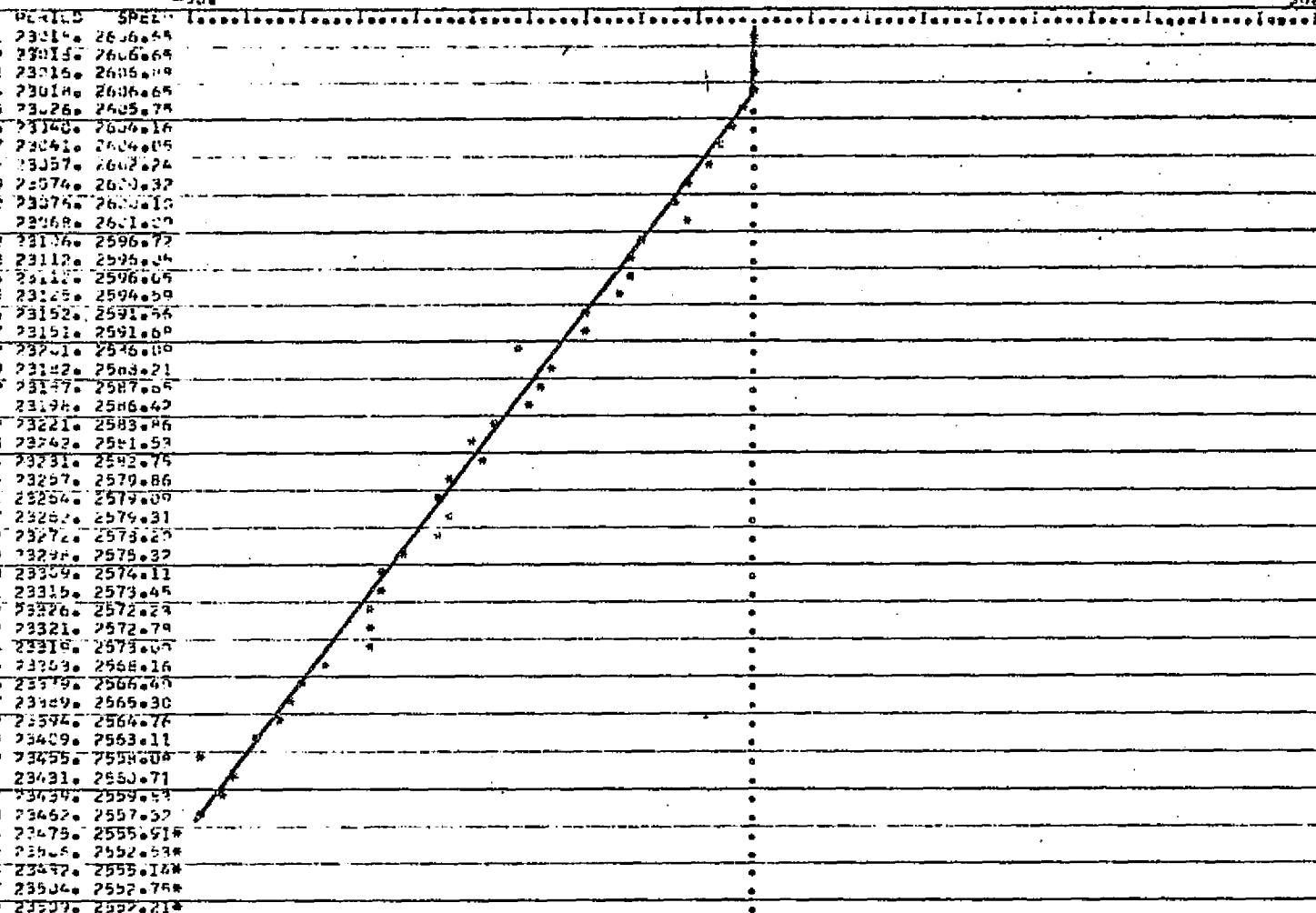


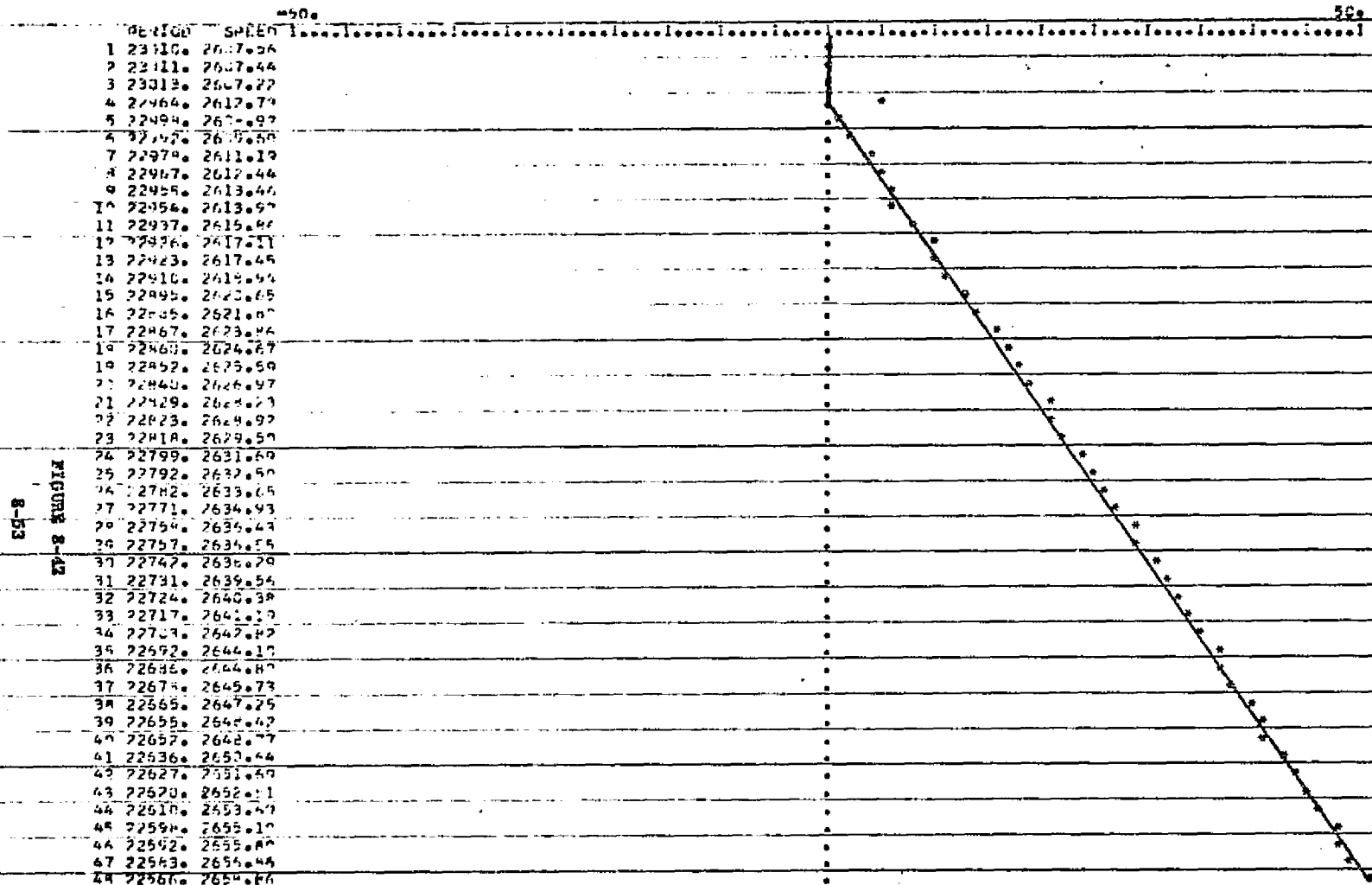
FIGURE 2-41

S-52

TORQUE = 457.63 OZ-IN (FROM 5 TO 45)

HIGH TORQUE DC MOTOR

CCW ACCEL T/C=2V

FIGURE 8-42  
8-53

# HIGH TORQUE DC MOTOR

SPEED\* C.RPM DRAG TORQUE= 0.00060 \* RPM + 0.6 QUIESCENT POWER= 8.5WATT

		PWR	MOTOR POWER			REAC	MOTOR	REQ	MOTOR	ELEC	HBRDGD	SYSTEM
TC	QUAD	TOT	SIN	COS	SUM	TRQ	TRQ	POWER	EFF	EFF	EFF	EFF
1	CC ACC	12.	0.5	2.0	2.5	8.6	9.1	0.0	0.0	20.8	71.4	0.0
2	CC ACC	20.	1.5	4.0	5.5	18.4	19.0	0.0	0.0	27.5	47.8	0.0
3	CC ACC	28.	2.5	8.0	10.5	28.5	29.1	0.0	0.0	37.5	53.8	0.0
4	CC ACC	45.	5.0	15.0	20.0	40.5	41.1	0.0	0.0	44.4	54.7	0.0
5	CC ACC	57.	8.0	18.0	26.0	47.3	47.9	0.0	0.0	45.6	53.6	0.0
BIAS						-1.19						
S.F.						9.95						
CORR						0.997						

1	CW DEC	12.	0.5	2.0	2.5	10.1	9.5	0.0				
2	CW DEC	20.	1.5	4.0	5.5	19.5	18.9	0.0				
3	CW DEC	28.	2.5	8.0	10.5	30.0	29.4	0.0				
4	CW DEC	45.	5.0	15.0	20.0	42.0	41.4	0.0				
5	CW DEC	57.	8.0	18.0	26.0	49.5	48.9	0.0				

BIAS -0.17  
S.F. 10.13  
CORR 0.998

1	CW ACC	12.	1.0	2.0	3.0	-9.8	-10.3	0.0	0.0	25.0	85.7	0.0
2	CW ACC	20.	2.0	4.0	6.0	-19.9	-20.5	0.0	0.0	30.0	52.1	0.0
3	CW ACC	28.	5.0	6.0	11.0	-30.4	-31.0	0.0	0.0	39.2	56.4	0.0
4	CW ACC	44.	10.5	9.0	19.5	-42.8	-43.4	0.0	0.0	44.3	54.9	0.0
5	CW ACC	57.	13.0	14.0	27.0	-50.6	-51.2	0.0	0.0	47.3	55.6	0.0

BIAS 0.65  
S.F. -10.45  
CORR -0.998

1	CC DEC	12.	1.0	2.0	3.0	-10.9	-10.3	0.0				
2	CC DEC	20.	2.0	4.0	6.0	-21.0	-20.4	0.0				
3	CC DEC	28.	5.0	6.0	11.0	-32.3	-31.7	0.0				
4	CC DEC	44.	10.5	9.0	19.5	-44.6	-44.0	0.0				
5	CC DEC	57.	13.0	14.0	27.0	-52.5	-51.9	0.0				

BIAS -0.21  
S.F. -10.69  
CORR -0.998

REPRODUCIBILITY OF THE  
ORIGINAL PAGE IS POOR

TABLE 8-6

# HIGH TORQUE DC MOTOR

SPEED = 250 RPM DRAG TORQUE = 0.00060 \* RPM + 0.6 QUIESCENT POWER = 8.5WATT

		PWR	MOTOR POWER			REAC	MOTOR	REQ	MOTOR	ELEC	HBRDGD	SYSTEM
TC	QUAD	TOT	SIN	COS	SUM	TRQ	TRQ	POWER	EFF	EFF	EFF	EFF
1	CC ACC	14.	1.5	3.0	4.5	8.6	9.3	1.7	38.4	32.1	81.8	12.3
2	CC ACC	24.	3.0	6.0	9.0	18.4	19.1	3.5	39.3	37.5	58.0	14.7
3	CC ACC	35.	5.0	11.5	16.5	28.9	29.6	5.4	33.2	47.1	62.2	15.6
4	CC ACC	55.	8.5	19.5	28.0	40.9	41.6	7.7	27.5	50.9	60.2	14.0
5	CC ACC	69.	12.5	23.5	36.0	48.4	49.1	9.0	25.2	52.1	59.5	13.1

RIAS -1.59  
S.F. 10.21  
CORR 0.998

1	CW DEC	11.	0.0	1.0	1.0	10.9	10.1	1.8				
2	CW DEC	17.	0.0	1.0	1.0	20.6	19.8	3.6				
3	CW DEC	23.	0.5	4.5	5.0	31.9	31.1	5.7				
4	CW DEC	37.	2.0	9.5	11.5	43.5	42.7	7.9				
5	CW DEC	47.	4.5	12.5	17.0	51.4	50.6	9.3				

RIAS 0.48  
S.F. 10.39  
CORR 0.998

1	CW ACC	14.	1.5	3.0	4.5	-9.8	-10.5	1.9	43.3	32.1	81.8	13.9
2	CW ACC	24.	4.0	5.5	9.5	-19.9	-20.6	3.8	40.1	39.5	61.2	15.9
3	CW ACC	37.	0.5	9.0	18.5	-31.5	-32.2	5.9	32.2	50.0	64.9	16.1
4	CW ACC	57.	17.0	13.5	30.5	-43.9	-44.6	8.2	27.0	53.5	62.8	14.4
5	CW ACC	73.	20.0	18.5	38.5	-51.4	-52.1	9.6	25.0	52.7	59.6	13.2

RIAS 0.86  
S.F. -10.72  
CORR -0.997

1	CC DEC	10.	0.0	1.0	1.0	-12.0	-11.2	2.0				
2	CC DEC	17.	0.0	1.0	1.0	-22.5	-21.7	4.0				
3	CC DEC	23.	2.5	2.5	5.0	-34.5	-33.7	6.2				
4	CC DEC	37.	7.0	5.5	12.5	-47.3	-46.5	8.6				
5	CC DEC	49.	9.0	9.0	18.0	-54.8	-54.0	9.9				

RIAS -1.09  
S.F. -11.04  
CORR -0.997

TABLE 8-7



# HIGH TORQUE DC MOTOR

SPEED= 500 RPM DRAG TORQUE= 0.00060 \* RPM + 0.6 QUIESCENT POWER= 8.5WATT

TC	QUAD	PWR TOT	MOTOR SIN	POWER COS	REAC SUM	MOTOR TRQ	REQ POWER	MOTOR EFF	ELEC EFF	MBRD G EFF	SYSTEM EFF
1	CC ACC	17.	2.5	4.0	6.5	8.3	9.2	3.4	52.3	38.2	20.0
2	CC ACC	28.	5.0	8.5	13.5	18.4	19.2	7.1	52.8	48.2	25.4
3	CC ACC	43.	8.0	15.0	23.0	28.9	29.7	11.0	47.9	53.4	25.6
4	CC ACC	66.	12.0	25.0	37.0	40.9	41.7	15.4	41.7	56.0	23.4
5	CC ACC	83.	17.5	29.5	47.0	49.1	50.0	18.4	39.3	56.6	22.2
BIAS						-2.11					
S.F.						10.41					
CORR						0.998					

1	CW DEC	9.	-1.5	-0.5	-2.0	11.3	10.4	3.8
2	CW DEC	14.	-1.5	-0.5	-2.0	21.4	20.5	7.5
3	CW DEC	17.	-1.5	0.0	-1.5	32.6	31.7	11.7
4	CW DEC	29.	-1.5	4.0	2.5	44.3	43.4	16.0
5	CW DEC	38.	0.5	6.0	6.5	52.1	51.2	18.9
BIAS						0.98		
S.F.						10.45		
CORR						0.998		

1	CW ACC	16.	2.5	4.0	6.5	-9.8	-10.7	3.9	60.8	40.6	86.6	24.7
2	CW ACC	29.	6.5	7.5	14.0	-20.3	-21.2	7.8	56.0	48.2	68.2	27.0
3	CW ACC	45.	13.5	12.0	25.5	-32.3	-33.2	12.2	48.1	56.6	69.8	27.2
4	CW ACC	71.	23.0	17.5	40.5	-45.0	-45.9	16.9	41.9	57.0	54.8	23.9
5	CW ACC	88.	27.0	23.5	50.5	-52.5	-53.4	19.7	39.1	57.3	63.5	22.4
BIAS						1.05						
S.F.						-11.01						
CORR						-0.997						

1	CC DEC	8.	-1.5	-0.5	-2.0	-12.4	-11.5	4.2
2	CC DEC	13.	-1.0	-0.5	-1.5	-22.9	-22.0	8.1
3	CC DEC	17.	-0.5	-0.5	-1.0	-35.6	-34.7	12.8
4	CC DEC	30.	2.5	1.5	4.0	-48.0	-47.1	17.4
5	CC DEC	39.	4.5	4.0	8.5	-55.0	-55.0	20.3
BIAS					-1.32			
S.F.					-11.21			
CORR					-0.997			

TABLE 8-8

# HIGH TORQUE DC MOTOR

SPEED= 750RPM DRAG TORQUE= 0.00060 \* RPM + 0.6 QUIESCENT POWER= 8.5WATT

TC	QUAD	PWR TOT	MOTOR SIN	POWER COS	REAC SUM	MOTOR TRQ	REQ TRQ	MOTOR POWER	ELEC EFF	MOTOR EFF	SYST EFF
1	CC ACC	19.	3.5	5.0	8.5	8.3	9.3	5.1	61.0	44.7	27.2
2	CC ACC	33.	6.5	10.5	17.0	18.4	19.4	10.7	63.4	51.5	32.6
3	CC ACC	50.	10.0	18.5	28.5	28.9	29.9	16.6	58.2	57.0	33.2
4	CC ACC	77.	15.0	30.0	45.0	40.9	41.9	23.2	51.7	58.4	30.2
5	CC ACC	97.	21.5	35.0	56.5	49.1	50.1	27.8	49.2	58.2	28.6

BIAS -2.11  
S.F. 10.41  
CORR 0.998

1	CW DEC	7.	-2.0	-2.0	-4.0	11.6	10.5	5.8
2	CW DEC	10.	-3.5	-3.0	-6.5	21.4	20.3	11.2
3	CW DEC	13.	-4.0	-3.5	-7.5	32.6	31.5	17.5
4	CW DEC	21.	-4.5	-1.5	-6.0	44.3	43.2	23.9
5	CW DEC	28.	-3.5	0.0	-3.5	52.1	51.0	28.3

BIAS 1.22  
S.F. 10.39  
CORR 0.998

1	CA ACC	18.	3.5	5.0	8.5	-9.4	-10.4	5.7	68.1	47.2	32.2
2	CA ACC	33.	6.5	9.0	17.5	-19.9	-20.9	11.6	66.4	53.0	35.2
3	CA ACC	54.	17.5	14.5	32.0	-32.6	-33.6	18.6	58.3	59.2	34.5
4	CA ACC	85.	28.5	21.0	49.5	-45.4	-46.4	25.7	52.0	58.2	30.4
5	CA ACC	105.	33.0	28.0	61.0	-52.9	-53.9	29.9	49.0	58.0	28.5

BIAS 1.71  
S.F. -11.25  
CORR -0.996

1	CC DEC	6.	-2.0	-2.0	-4.0	-12.8	-11.7	6.5
2	CC DEC	10.	-4.0	-3.0	-7.0	-23.3	-22.2	12.3
3	CC DEC	13.	-4.0	-3.0	-7.0	-35.6	-34.5	19.1
4	CC DEC	22.	-2.0	-3.0	-5.0	-48.4	-47.3	26.2
5	CC DEC	30.	-1.0	-2.0	-3.0	-56.2	-55.1	30.5

BIAS -1.68  
S.F. -11.19  
CORR -0.997

TABLE 8-9

# HIGH TORQUE DC MOTOR

SPEED= 1000.RPM DRAG TORQUE= 0.00060 \* RPM + 0.6 QUIESCENT POWER= 8.5WATT

ATC	QUAD	P/R	TOT	MOTOR SIN	POWER COS	REAC SUM	MOTOR TRQ	REQ TRQ	MOTOR POWER	ELEC EFF	HBRDG EFF	SYSTM EFF
1	CC	ACC	22.	4.0	5.5	9.5	8.3	9.5	7.0	73.9	43.1	31.9
2	CC	ACC	37.	8.0	12.5	20.5	18.4	19.6	14.4	70.7	55.4	39.1
3	CC	ACC	57.	12.5	21.5	34.0	28.9	30.1	22.2	65.4	59.6	39.0
4	CC	ACC	88.	18.5	34.5	53.0	40.9	42.0	31.1	58.7	60.2	35.3
5	CC	ACC	110.	25.5	40.5	66.0	50.6	51.8	38.3	58.0	60.0	34.8

RIAS -2.71  
S.F. 10.71  
CORR 0.999

1	CW	DEC	5.	-3.0	-3.0	-6.0	11.6	10.4	7.6			
2	CW	DEC	6.	-5.0	-5.5	-10.5	21.4	20.2	14.9			
3	CW	DEC	7.	-6.5	-6.5	-13.0	32.6	31.4	23.2			
4	CW	DEC	14.	-8.0	-6.5	-14.5	44.3	43.1	31.8			
5	CW	DEC	19.	-8.0	-6.5	-14.5	52.1	50.9	37.6			

RIAS 1.22  
S.F. 10.39  
CORR 0.998

1	CW	ACC	22.	4.5	9.5	10.0	-9.4	-10.6	7.8	78.4	45.4	35.6
2	CW	ACC	38.	10.5	11.0	21.5	-19.9	-21.1	15.6	72.5	56.5	41.0
3	CW	ACC	62.	21.0	17.5	38.5	-32.6	-33.8	25.0	64.9	62.0	40.3
4	CW	ACC	97.	33.5	25.5	59.0	-45.4	-46.5	34.4	58.4	60.8	35.5
5	CW	ACC	120.	44.0	33.0	77.0	-53.3	-54.5	40.3	52.3	64.1	33.5

RIAS 1.87  
S.F. -11.33  
CORR -0.997

1	CC	DEC	8.	-3.0	-3.0	-6.0	-13.1	-11.9	8.8			
2	CC	DEC	13.	-6.0	-5.0	-11.0	-23.3	-22.1	16.3			
3	CC	DEC	18.	-7.0	-6.0	-13.0	-35.6	-34.4	25.4			
4	CC	DEC	30.	-7.0	-6.5	-13.5	-48.4	-47.2	34.9			
5	CC	DEC	39.	-7.0	-6.5	-13.5	-55.9	-54.7	40.4			

RIAS -2.04  
S.F. -11.07  
CORR -0.996

TABLE 8-10

# HIGH TORQUE DC MOTOR

SPEED= 1250.RPM DRAG TORQUE= 0.00060 \* RPM + 0.6 QUIESCENT POWER= 8.5WATT

		PWR	MOTOR	POWER	REAC	MOTOR	REQ	MOTOR	ELEC	IBRDG	SYSTEM	
TC	QUAD	TOT	SIN	COS	SUM	TRQ	TRQ	POWER	EFF	EFF	EFF	
1	CC ACC	24.	4.5	6.5	11.0	7.9	9.2	8.5	77.7	45.8	70.9	35.6
2	CC ACC	42.	9.5	14.5	24.0	18.0	19.3	17.8	74.5	57.1	71.6	42.5
3	CC ACC	64.	15.0	25.0	40.0	28.9	30.2	27.9	69.9	62.5	72.0	43.6
4	CC ACC	98.	22.0	39.0	61.0	40.9	42.2	39.0	64.0	62.2	68.1	39.8
5	CC ACC	124.	30.0	46.0	76.0	49.1	50.4	46.6	61.3	61.2	65.8	37.6

RIAS -2.63  
S.F. 10.53  
CORR 0.998

1	CW DEC	2.	-4.0	-4.5	-8.5	11.6	10.2	9.4				
2	CW DEC	2.	-6.5	-8.0	-14.5	21.4	20.0	18.5				
3	CW DEC	3.	-8.5	-10.5	-19.0	32.6	31.2	28.8				
4	CW DEC	7.	-10.5	-11.5	-22.0	44.3	42.9	39.7				
5	CW DEC	12.	-11.5	-11.5	-23.0	51.8	50.4	46.6				

RIAS 1.34  
S.F. 10.33  
CORR 0.997

1	CW ACC	24.	5.0	6.5	11.5	-9.4	-10.7	9.9	86.4	47.9	74.1	41.4
2	CW ACC	43.	12.5	13.0	25.5	-19.9	-21.2	19.6	77.0	59.3	73.9	45.6
3	CW ACC	70.	25.0	20.0	45.0	-32.6	-33.9	31.3	69.7	64.2	75.1	44.8
4	CW ACC	109.	38.5	29.0	67.5	-45.4	-46.7	43.2	64.0	61.9	67.1	39.6
5	CW ACC	135.	44.0	37.0	81.0	-53.3	-54.6	50.5	62.3	60.0	64.0	37.4

RIAS 1.87  
S.F. -11.33  
CORR -0.997

1	CC DEC	1.	-4.0	-4.0	-8.0	-13.1	-11.7	10.8				
2	CC DEC	1.	-8.0	-7.0	-15.0	-22.7	-21.5	19.9				
3	CC DEC	2.	-11.0	-9.0	-20.0	-35.6	-34.2	31.6				
4	CC DEC	7.	-12.0	-10.5	-22.5	-48.0	-46.6	43.1				
5	CC DEC	12.	-12.0	-10.5	-22.5	-55.9	-54.5	50.4				

RIAS -1.88  
S.F. -11.07  
CORR -0.997

TABLE 8-11

# HIGH TORQUE DC MOTOR

SPEED= 1500 RPM DRAG TORQUE= 0.00063 \* RPM + 0.6 QUIESCENT POWER= 8.5WATT

TC	QUAD	PWR TOT	MOTOR SIN	POWER COS	REAC SUM	MOTOR TRQ	REQ TRQ	MOTOR POWER	ELEC EFF	MOTOR EFF	SYSTX EFF
1	CC ACC	26.	5.5	7.5	13.0	7.9	9.3	10.4	80.2	50.0	40.1
2	CC ACC	46.	11.0	17.0	28.0	18.0	19.5	21.6	77.2	60.8	47.0
3	CC ACC	71.	17.5	28.5	46.0	28.5	30.0	33.2	72.3	64.7	46.8
4	CC ACC	109.	25.0	44.0	69.0	40.9	42.3	47.0	68.1	63.3	43.1
5	CC ACC	137.	34.0	51.5	85.5	49.5	51.0	56.5	66.1	62.4	41.2

RIAS -2.86  
S.F. 10.60  
CORR 0.998

1	CW DEC	0.	-5.0	-5.5	-10.5	12.0	10.5	11.6			
2	CW DEC	0.	-8.5	-9.5	-18.0	19.9	18.4	20.4			
3	CW DEC	0.	-11.0	-13.5	-24.5	32.6	31.1	34.5			
4	CW DEC	0.	-13.5	-16.0	-29.5	43.9	42.4	47.0			
5	CW DEC	3.	-15.5	-16.5	-32.0	51.8	50.3	55.8			

RIAS 0.95  
S.F. 10.36  
CORR 0.996

1	CW ACC	26.	6.0	7.5	13.5	-9.0	-10.5	11.6	86.2	51.8	44.8
2	CW ACC	47.	14.5	15.0	29.5	-19.9	-21.3	23.7	80.4	62.7	50.5
3	CW ACC	79.	28.5	23.5	52.0	-32.3	-33.7	37.4	72.1	65.8	47.4
4	CW ACC	121.	44.0	33.0	77.0	-45.4	-46.8	52.0	67.5	63.6	43.0
5	CW ACC	149.	50.0	42.5	92.5	-53.3	-54.7	60.7	65.7	62.0	40.8

RIAS 2.25  
S.F. -11.41  
CORR -0.997

1	CC DEC	0.	-5.5	-5.5	-11.0	-13.1	-11.6	12.8			
2	CC DEC	0.	-10.0	-8.5	-18.5	-22.9	-21.4	23.7			
3	CC DEC	0.	-14.5	-12.0	-26.5	-35.3	-33.8	37.5			
4	CC DEC	0.	-17.0	-14.0	-31.0	-48.0	-46.5	51.5			
5	CC DEC	4.	-18.0	-15.5	-33.5	-55.9	-54.4	60.3			

RIAS -1.82  
S.F. -11.07  
CORR -0.997

TABLE 8-12

# HIGH TORQUE DC MOTOR

SPEED= 1750.RPM DRAG TORQUE= 0.00060 \* RPM + 0.6 QUIESCENT POWER= 8.5WATT

		P&R	MOTOR POWER			REAC	MOTOR	REQ	MOTOR	ELEC	HBRDGD	SYSTEM
TC	LOAD	TOT	SIN	COS	SUM	TRQ	TRQ	POWER	EFF	EFF	EFF	EFF
1	CC ACC	28.	6.5	8.5	15.0	7.9	9.5	12.3	82.4	53.5	76.9	44.1
2	CC ACC	50.	12.5	19.0	31.5	18.0	19.6	25.4	80.7	63.0	75.9	50.8
3	CC ACC	78.	20.0	32.0	52.0	28.5	30.1	39.0	75.0	66.6	74.8	50.0
4	CC ACC	119.	28.5	49.5	78.0	40.9	42.5	55.0	70.6	65.5	70.5	46.2
5	CC ACC	149.	38.5	57.0	95.5	49.1	50.7	65.6	68.7	64.0	67.9	44.0

RIAS -2.70  
S.F. 10.52  
CORR 0.998

1	CC DEC	0.	-5.5	-6.0	-11.5	12.0	10.3	13.3				
2	CC DEC	0.	-10.0	-11.5	-21.5	21.4	19.7	25.6				
3	CC DEC	0.	-13.5	-16.5	-30.0	32.6	30.9	40.0				
4	CC DEC	0.	-16.5	-20.5	-37.0	43.5	41.8	54.1				
5	CC DEC	0.	-19.5	-22.0	-41.5	51.0	49.3	63.8				

RIAS 2.06  
S.F. 10.01  
CORR 0.998

1	CC ACC	28.	7.0	8.5	15.5	-9.0	-10.6	13.7	84.9	55.3	79.4	49.2
2	CC ACC	52.	16.5	17.0	33.5	-19.5	-21.1	27.3	81.7	64.4	77.0	52.6
3	CC ACC	87.	32.0	26.0	58.0	-32.3	-33.9	43.9	75.7	66.6	73.8	50.5
4	CC ACC	132.	49.5	36.5	86.0	-45.4	-47.0	60.9	70.8	65.1	69.6	46.1
5	CC ACC	163.	55.0	47.0	103.0	-53.3	-54.9	71.1	69.0	63.1	66.6	43.6

RIAS 2.45  
S.F. -11.45  
CORR -0.997

1	CC DEC	0.	-6.0	-6.0	-12.0	-13.1	-11.4	14.8				
2	CC DEC	0.	-12.0	-10.0	-22.0	-23.3	-21.6	28.0				
3	CC DEC	0.	-18.0	-14.0	-32.0	-35.3	-33.6	43.5				
4	CC DEC	0.	-22.0	-17.5	-39.5	-47.6	-45.9	59.4				
5	CC DEC	0.	-24.0	-19.5	-43.5	-55.5	-53.8	69.7				

RIAS -2.22  
S.F. -10.91  
CORR -0.997

TABLE 8-13



# HIGH TORQUE DC MOTOR

SPEED= 2000 RPM DRAG TORQUE= 0.00060 \* RPM + 0.6 QUIESCENT POWER= 8.5WATT

TC	QUAD	PWR TOT	MOTOR SIN	POWER COS	REAC SUM	MOTOR TRQ	REQ TRQ	MOTOR POWER	ELEC EFF	HBRDG EFF	SYSTEM EFF
1	CC ACC	30.	7.0	9.5	16.5	7.5	9.3	13.7	83.3	55.0	45.8
2	CC ACC	55.	14.0	21.0	35.0	17.6	19.4	28.6	81.9	63.6	52.1
3	CC ACC	85.	22.5	34.5	57.0	28.5	30.3	44.8	78.6	67.0	52.7
4	CC ACC	128.	31.5	54.5	86.0	40.9	42.7	63.1	73.4	67.1	49.3
5	CC ACC	162.	43.0	63.0	106.0	49.1	50.9	75.2	71.0	65.4	46.4
BIAS						-3.23					
S.F.						10.65					
CORR						0.998					

1	CW DEC	0.	-6.5	-6.5	-13.0	12.0	10.2	15.0			
2	CW DEC	0.	-11.5	-13.5	-25.0	21.8	20.0	29.5			
3	CW DEC	0.	-16.0	-20.5	-36.5	32.6	30.8	45.5			
4	CW DEC	0.	-20.0	-25.0	-45.0	43.5	41.7	61.6			
5	CW DEC	0.	-23.5	-27.5	-51.0	51.0	49.2	72.7			

BIAS 2.27  
S.F. 9.97  
CORR 0.998

1	CA ACC	30.	8.0	9.5	17.5	-8.6	-10.3	15.3	87.9	58.3	51.2
2	CA ACC	56.	19.5	18.5	37.0	-19.5	-21.3	31.5	85.1	66.0	54.2
3	CA ACC	94.	37.5	29.0	66.5	-32.3	-34.0	50.4	75.8	70.7	53.6
4	CA ACC	142.	55.0	41.0	96.0	-45.8	-47.5	70.4	73.3	67.6	49.9
5	CA ACC	175.	62.5	52.0	114.5	-53.3	-55.0	81.5	71.1	65.4	46.5

BIAS 2.81  
S.F. -11.57  
CORR -0.996

1	CC DEC	0.	-7.5	-6.0	-13.5	-13.1	-11.3	16.7			
2	CC DEC	0.	-14.0	-12.0	-26.0	-23.3	-21.5	31.8			
3	CC DEC	0.	-21.0	-17.0	-38.0	-34.9	-33.1	48.9			
4	CC DEC	0.	-26.5	-21.5	-48.0	-47.3	-45.5	67.3			
5	CC DEC	0.	-29.0	-24.0	-53.0	-55.5	-53.7	79.4			

BIAS -2.17  
S.F. -10.88  
CORR -0.998

TABLE 8-14

# HIGH TORQUE DC MOTOR

SPEED= 2250.RPM DRAG TORQUE= 0.00060 \* RPM + 0.6 QUIESCENT POWER= 8.5WATT

TC	PWR		MOTOR POWER			REAC MOTOR		REQ	MOTOR	ELEC	HBRDGD	SYSTEM
	QUAD	TOT	SIN	COS	SUM	TRQ	TRQ	POWER	EFF	EFF	EFF	EFF
1	CC ACC	32.	8.0	10.0	18.0	7.1	9.0	15.0	83.6	56.2	76.5	47.0
2	CC ACC	58.	16.0	23.0	39.0	17.3	19.2	32.0	82.1	67.2	78.7	55.2
3	CC ACC	92.	24.5	38.5	63.0	28.5	30.4	50.6	80.4	68.4	75.4	55.0
4	CC ACC	137.	34.5	58.5	93.0	40.9	42.8	71.3	76.6	67.8	72.3	52.0
5	CC ACC	172.	57.5	68.0	125.5	49.1	51.0	84.9	67.6	72.9	76.7	49.3
RIAS						-3.70						
S.F.						10.76						
CORR						0.998						

1	CW DEC	0.	-7.5	-7.5	-15.0	12.4	10.4	17.3
2	CW DEC	0.	-13.5	-16.0	-29.5	22.1	20.1	33.5
3	CW DEC	0.	-18.0	-23.5	-41.5	32.6	30.6	51.0
4	CW DEC	0.	-23.0	-30.0	-53.0	43.5	41.5	69.1
5	CW DEC	0.	-27.0	-32.5	-59.5	51.0	49.0	81.6

RIAS						2.73						
S.F.						9.66						
CORR						0.998						

1	CW ACC	32.	8.5	10.5	19.0	-8.3	-10.2	17.0	89.7	59.3	80.8	53.3
2	CW ACC	60.	20.5	21.0	41.5	-19.1	-21.0	35.0	84.4	69.1	80.5	58.3
3	CW ACC	101.	38.5	32.0	70.5	-31.9	-33.8	56.3	79.9	69.8	76.2	55.7
4	CW ACC	151.	59.5	45.5	105.0	-45.4	-47.3	78.7	75.0	69.5	73.6	52.1
5	CW ACC	185.	67.0	57.0	124.0	-52.9	-54.8	91.2	73.6	67.0	70.2	49.3

RIAS						3.13						
S.F.						-11.55						
CORR						-0.996						

1	CC DEC	0.	-8.5	-7.0	-15.5	-13.5	-11.5	19.2
2	CC DEC	0.	-16.0	-14.0	-30.0	-23.6	-21.6	36.0
3	CC DEC	0.	-24.0	-19.5	-43.5	-35.3	-33.3	55.5
4	CC DEC	0.	-31.0	-24.5	-55.5	-47.3	-45.3	75.4
5	CC DEC	0.	-34.0	-28.0	-62.0	-55.1	-53.1	88.4

RIAS						-2.88						
S.F.						-10.69						
CORR						-0.997						

TABLE 8-15

# HIGH TORQUE DC MOTOR

SPEED= 2500.RPM DRAG TORQUE= 0.00060 \* RPM + 0.6 QUIESCENT POWER= 8.5WATT

PC	QUAD	PWR TOT	MOTOR SIN	POWER COS	REAC SUM	MOTOR TRQ	REQ TRQ	MOTOR POWER	ELEC EFF	MBRDG EFF	SYSTEM EFF
1	CC ACC	33.	8.5	11.0	19.5	6.8	8.8	16.4	84.3	59.0	49.8
2	CC ACC	62.	17.5	25.0	42.5	17.3	19.4	35.8	84.4	68.5	57.8
3	CC ACC	98.	27.0	41.5	68.5	28.1	30.2	55.8	81.5	69.8	56.9
4	CC ACC	144.	38.0	61.5	99.5	40.5	42.6	78.7	79.1	69.0	54.7
5	CC ACC	181.	52.5	71.0	123.5	48.8	50.9	94.1	76.2	68.2	51.9
BIAS						-3.86					
S.F.						10.72					
CORR						0.998					

1	CW DEC	0.	-8.5	-8.5	-17.0	12.4	10.3	19.0			
2	CW DEC	0.	-15.0	-18.0	-33.0	22.1	20.0	36.9			
3	CW DEC	0.	-20.5	-27.0	-47.5	33.0	30.9	57.1			
4	CW DEC	0.	-26.0	-34.0	-60.0	43.5	41.4	76.5			
5	CW DEC	0.	-31.0	-38.0	-69.0	50.6	48.5	89.6			
BIAS						2.97					
S.F.						9.78					
CORR						0.997					

1	CW ACC	34.	9.5	11.0	20.5	-7.9	-10.0	18.4	90.2	60.2	54.3
2	CW ACC	65.	22.5	22.5	45.0	-18.9	-21.0	38.8	86.2	69.2	59.7
3	CW ACC	107.	42.0	35.0	77.0	-31.5	-33.6	62.1	80.6	71.9	58.0
4	CW ACC	158.	62.0	50.0	112.0	-44.6	-46.7	86.3	77.1	70.8	54.6
5	CW ACC	192.	70.0	60.0	130.0	-51.4	-53.5	98.9	76.0	67.7	51.5
BIAS						2.95					
S.F.						-11.27					
CORR						-0.995					

1	CC DEC	0.	-9.5	-8.0	-17.5	-13.5	-11.4	21.0			
2	CC DEC	0.	-18.0	-16.0	-34.0	-23.6	-21.5	39.7			
3	CC DEC	0.	-27.5	-22.0	-49.5	-34.9	-32.8	60.6			
4	CC DEC	0.	-36.0	-28.0	-64.0	-46.9	-44.8	82.8			
5	CC DEC	0.	-39.5	-31.5	-71.0	-54.8	-52.7	97.4			
BIAS						-2.96					
S.F.						-10.59					
CORR						-0.998					

TABLE 8-16